

For Reference

NOT TO BE TAKEN FROM THIS ROOM

Ex libris
UNIVERSITATIS
ALBERTAENSIS





Digitized by the Internet Archive
in 2019 with funding from
University of Alberta Libraries

<https://archive.org/details/Haverslew1976>

T H E U N I V E R S I T Y O F A L B E R T A

RELEASE FORM

NAME OF AUTHOR Rodèrick E. Haverslew
TITLE OF THESIS Geology and Genesis of the Ruttan
 Lake Deposit, Manitoba
DEGREE FOR WHICH THESIS WAS PRESENTED M.Sc.
YEAR THIS DEGREE GRANTED 1976

Permission is hereby granted to THE UNIVERSITY
OF ALBERTA LIBRARY to reproduce single copies of
this thesis and to lend or sell such copies for
private, scholarly or scientific research purposes
only.

The author reserves other publication rights,
and neither the thesis nor extensive extracts from
it may be printed or otherwise reproduced without
the author's written permission.

THE UNIVERSITY OF ALBERTA
GEOLOGY AND GENESIS OF THE
RUTTAN LAKE DEPOSIT, MANITOBA

by



RODERICK E. HAVERSLEW

A THESIS

SUBMITTED TO THE FACULTY OF GRADUATE STUDIES AND RESEARCH
IN PARTIAL FULFILMENT OF THE REQUIREMENTS FOR THE DEGREE
OF MASTER OF SCIENCE

DEPARTMENT OF GEOLOGY

EDMONTON, ALBERTA

SPRING 1976

THE UNIVERSITY OF ALBERTA
FACULTY OF GRADUATE STUDIES AND RESEARCH

The undersigned certify that they have read,
and recommend to the Faculty of Graduate Studies
and Research, for acceptance, a thesis entitled
"Geology and Genesis of the Ruttan Lake Deposit,
Manitoba" submitted by Roderick E. Haverslew in
partial fulfilment of the requirements for the degree
of Master of Science.

ABSTRACT

The greenstone belt comprising the Ruttan Lake Mine consists of an intimately interlayered sequence of basalt and andesite followed by acid volcanic rocks ranging from rhyolite to dacite and intercalated with minor sedimentary rocks. The presence of pillow structures suggest that the volcanic rocks were extruded in a subaerial to shallow marine environment. Their tholeiitic trend is characteristic of island arc systems.

The Ruttan Lake Cu-Zn deposit consists of two main ore types within the Wasekwan volcanic rocks of the Precambrian Shield. Massive ore occurs in a complex sequence of mainly rhyolite, dacite and tuffs which are overlain with a layer of andesite and basalt. The disseminated ores occur in andesites below the massive ores. Pyrite and pyrrhotite are the predominant sulphides. There is an enrichment of barium and of sphalerite relative to chalcopyrite and of Fe/Mn ratios toward the stratigraphic hanging wall. This trend appears to be consistent with marine basin deposition and supports the general hypothesis of volcanic-sedimentary deposition for massive sulphides.

During the Hudsonian Orogeny, the Wasekwan volcanic rocks underwent upper greenschist and lower amphibolite facies metamorphism. Widespread metamorphic features in

the ore deposit suggest that the ores are premetamorphic in age.

Iron content of sphalerite, which is resistant to post mineral changes, indicates equilibrium deposition for pyrite, pyrrhotite and sphalerite. The established pressure of deposition is about 6 Kb using the Fe content in sphalerite as a geobarometer. A probable temperature of deposition determined from the mole % FeS in sphalerite and from the variation in sulphur isotope fractionation between co-existing sulphides is between 200° and 250°C. The narrow range of sulphur isotopic composition (with a near magmatic mean value) indicates a magmatic source of sulphur.

The lead isotope data support a three or higher stage development of the ore leads, with mineralization occurring sometime between 1900 m.y. and 1140 m.y. ago. The lead probably was derived from a deep-seated source and was well-mixed subsequently to ore deposition. The intercept with the growth curve at 2850 m.y. suggests an Archean parentage.

ACKNOWLEDGEMENTS

The writer wishes to express his gratitude to his supervisor, Dr. R.E. Folinsbee, whose suggestions and vast knowledge of ore deposits were very helpful.

Dr. H. Baadsgaard's interest and invaluable suggestions in interpreting the isotopic data are much appreciated.

Dr. John Gray of the Department of Physics, for allowing the writer to use the Mass Spectrometry facilities and giving assistance whenever it was needed and to Dr. D.G.W. Smith for his supervision and assistance in using the electron microprobe.

Say-Lee Kuo whose friendship and help in doing the experimental work and suggestions in interpreting the data was greatly appreciated and encouraging.

Dr. D. Herrick for his assistance in doing the sulphur isotope experimental work.

Mr. G.D. Ruttan, A. de Carle and D. Speakman of Sherritt Gordon Mines Ltd. for allowing me permission to obtain the thesis material, their friendly cooperation and assistance with sample collection and geological information.

The assistance of Ms. Val Stephansson and Mr. Z. Widtman in typing, editing and drafting is much appreciated.

TABLE OF CONTENTS

CHAPTER	PAGE
I. REGIONAL GEOLOGY	4
Previous Work	4
Structural Geology	13
Metamorphism	14
Chemistry of the Volcanic Igneous Rocks .	15
Introduction	15
Results	16
Discussion	27
II. GEOLOGY OF THE RUTTAN LAKE ORE DEPOSIT . . .	30
A. The Host Rocks	30
B. The Sulphide Deposit	36
Description of the ore minerals . . .	43
Textures	45
Genesis	46
III. TECHNIQUES OF GEOCHEMISTRY STUDY	48
A. Sulphur Isotopes	48
Introduction	48
Sample Selection and Preparation . . .	50
Preparation of SO ₂ for Mass Spectrometer Analysis	51
Isotope Analysis	51
Results	56

TABLE OF CONTENTS (cont'd)

CHAPTER		PAGE
III.	B. Fe-Content in Sphalerite	58
	Introduction	58
	Experimental Procedure	69
	Results	72
	C. Pb Isotopes	72
	Introduction	72
	Theoretical Considerations and Ore Genesis	82
	(i) Single-stage leads	83
	(ii) Two-stage or anomalous leads	83
	(iii) Multi-stage systems	84
	Experimental Procedures	85
	Analytical Methods and Instrumenta- tion	86
	Accuracy of Results	87
	Results	88
	D. Trace Elements in Ores	93
	Introduction	93
	Experimental Procedures	93
	Results	93

TABLE OF CONTENTS (cont'd)

CHAPTER	PAGE
IV. INTERPRETATIONS - DISCUSSION	104
A. Sulphur Isotopes	104
B. Fe-content in Sphalerite	115
C. Isotopic Data of Ore Lead	119
D. Trace Elements	125
V. SUMMARY AND CONCLUSIONS	130

LITERATURE CITED	134
APPENDIX A. RECIPE FOR MAGNETIC COLLOID	141
APPENDIX B. EXTRACTION PROCEDURE OF LEAD FROM SULPHIDE MINERALS	142
APPENDIX C. SILICA GEL LOADING PROCEDURE	144
APPENDIX D. LEAD ISOTOPE REGRESSION FORMULA	145
PHOTOGRAPHIC PLATES AND THEIR EXPLANATION	146

LIST OF FIGURES

Figure	Page
1. Location Map of the Ruttan Lake Deposit	2
2. Geology of the Ruttan Lake area	6
3. Location of chemically analyzed samples	17
4. Magnesium-Iron-Alkali Ternary Oxide Diagram for Volcanic Rocks in the Rusty Lake Greenstone Belt	23
5. Changes in SiO ₂ content with increasing FeO/MgO Ratios	25
6. Variation of TiO ₂ content	25
7. Alkali-Silica Diagram	26
8. TiO ₂ -K ₂ O-P ₂ O ₅ Plot of Volcanic Rocks from the Rusty Lake Greenstone Belt	28
9. Plan View and Cross Section of the Ruttan Lake Mine	33
10. Plan view and Cross Section showing shape of the Ruttan Lake Ore Body	38
11. Cu/Zn Ratios between the Footwall and Hanging Wall	42
12. Cross section showing Location of samples for sulphur isotope study	66
13. Distribution of Isotope Results between Footwall and Hanging Wall	67
14. Frequency Distribution of $\delta^{34}\text{S}$ Values	68
15. Cross section showing location of samples analyzed for Fe content in sphalerite	70
16. Frequency Distribution of FeS mole % from Fe content in sphalerite	81

LIST OF FIGURES (cont'd)

Figure		Page
17.	Cross section showing location of samples for Pb-Isotope Study	91
18.	Cross section showing sample distribution for Trace Element Study	101
19.	Geothermometric Plot by Kajiwara and Krouse (1971)	107
20.	Sulphur Isotope Equilibrium Line for Pyrite-Chalcopyrite Pairs	108
21.	Sulphur Isotope Equilibrium Line for Pyrite-Sphalerite and Pyrite-Pyrrhotite Pairs	108
22.	Sulphur Isotope Fractionation between co-existing pyrite-sphalerite and pyrite-pyrrhotite	110
23.	Sulphur Isotope Fractionation between co-existing pyrite-chalcopyrite and pyrite-pyrrhotite	110
24.	Influence of fO_2 and pH on Mole Fractions of Aqueous Sulphur Species	113
25.	FeS - ZnS - S System at Low Temperatures	117
26.	Temperature - fS_2 Diagram	118
27.	Isobars for the FeS - ZnS - S System	118
28.	Anomalous Lead Lines for $^{207}Pb/^{204}Pb$ vs $^{206}Pb/^{204}Pb$ for the Ruttan Lake Ore Leads	120
29.	Anomalous Lead Lines for $^{208}Pb/^{204}Pb$ vs $^{206}Pb/^{204}Pb$ for the Ruttan Lake Ore Leads	121
30.	Trend of Fe/Mn Ratios between Hanging Wall and Footwall	126
31.	Trend of Barium between Hanging Wall and Footwall	127

LIST OF TABLES

Table	Description	Page
1.	Table of Formations	7
2.	Chemical Composition and CIPW Norms for Volcanic Rocks from the Ruttan Lake Area	18
3.	Possible Metamorphic Equivalents of Primary Rock Types commonly associated with Precambrian Massive Sulphide Deposits	32
4.	Cu/Zn Ratios	41
5.	SO ₂ Yields for Sulphur Isotope Analysis	52
6.	Calibration of SO ₂ Line Standard (1974)	57
7.	Description and Location of Samples used for Sulphur Isotope Study	59
8.	Results of Sulphur Isotope Analysis	62
9.	$\Delta \delta^{34}\text{S}$ in co-existing Sulphides from Ruttan Lake	64
10.	Composition of Standards used in Microprobe Analysis	71
11.	Results of Microprobe Study showing composition of Sphalerite in Weight Percent and Metal:Non-metal Ratios	73
12.	Calibrated FeS mole % from Microprobe Results	80
13.	Interlaboratory Comparison of Broken Hill Galena Standards used in Pb-Isotope Study	89
14.	Pb-Growth Curve Parameters	90
15.	Lead Isotope Data of the Ruttan Lake Ores	92

LIST OF TABLES (cont'd)

Table	Description	Page
16.	Location and Description of Samples Analyzed for Trace Elements	94
17.	Trace Element Results	102

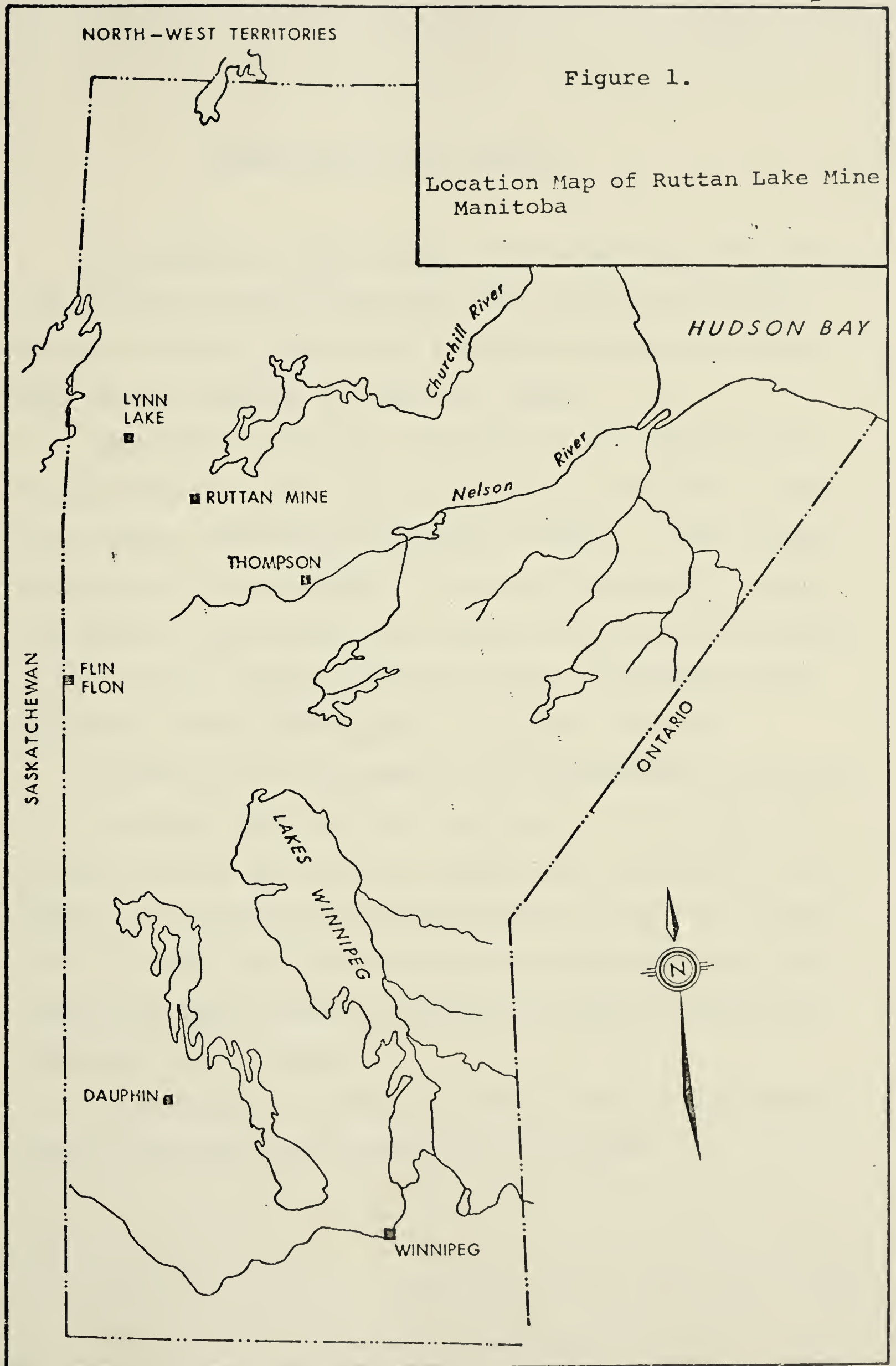
INTRODUCTION

The Ruttan Lake deposit is located approximately 510 miles north of Winnipeg, Manitoba and is owned and operated by Sherritt Gordon Mines Ltd. The property is situated fifteen miles from the Provincial Highway 391, which now connects Lynn Lake and Thompson (see Figure 1).

The ore body was discovered through an airborne geophysical survey flown in July, 1968. Ground magnetic and electromagnetic surveys were conducted that same summer and by April, 1969 the area was staked and diamond drilling was started. The mine was brought into production by open pit method in the spring of 1973.

Primary diamond drilling (202,000 feet) outlined an ore body of 51,000,000 tons at a grade of 1.47% copper and 1.61% zinc between the surface and the 2000 foot level. Initial open pit diluted reserves were calculated to be 21,000,000 tons of ore at a grade of 1.34% copper and 2.12% zinc (Sherritt Gordon Mines Ltd. Annual Report - 1972).

The topography of the Ruttan Lake area is typical of the Precambrian Shield. Topographic relief is almost nonexistent, with a maximum difference in elevation of about 100 feet. Numerous lakes and muskeg occur and permafrost conditions exist in most parts of this area.



OBJECTIVES OF THE THESIS

The purpose of this thesis is to study the geological and chemical factors that would have influenced ore deposition and hence reconstruct a possible geological environment at the time the ore body was formed.

Laboratory techniques conducted on the samples from Ruttan Lake included: optical, electron microprobe, mass spectrometer and atomic absorption analyses. Using these techniques, it was possible to obtain information concerning mineral associations and textural relations, Fe-content in sphalerite, sulphur isotope ratios, Pb isotope ratios and minor element distribution in the ore minerals.

Objectives of the present work are outlined as follows:

- (1) to relate the local mine geology to the regional geological setting and hence to provide some fundamental knowledge on the nature and characteristics of the ore deposit.
- (2) to reveal the possible processes responsible for ore deposition from a study of isotope and minor element geochemistry of the deposit.
- (3) to postulate a geological and geochemical environment which influenced the formation of the deposit.

CHAPTER I REGIONAL GEOLOGY

The Ruttan Lake area belongs to the Churchill Structural Province and is characterized by a thick Archean complex of metavolcanic and metasedimentary rocks (see Figure 2). Reconnaissance mapping in the Granville Lake, Rusty Lake, Lynn Lake and Ruttan Lake areas by Henderson, Norman and Downie (1936), Bateman (1945), Milligan (1960), Burwash (1962), Pearce (1964), Milligan (1964), Bristol (1966) and more recently in 1972 by M.A. Steeves and C.F. Lamb established the Precambrian rocks into five stratigraphic units: (1) Wasekwan series of volcanic and sedimentary rocks, (2) Pre-Sickle intrusives, (3) Sickle sediments, (4) Opachuanau gneisses, and (5) Post-Sickle intrusives (see Table of Formations in Table 1).

The oldest rocks are the Wasekwan series which comprise the Rusty Lake greenstone belt of interbedded tightly and intricately folded volcanic and sedimentary rocks. The volcanic rocks include broadly differentiated suites ranging from basalts to rhyolites in composition, while the intercalated sedimentary rocks include cherts, siliceous fragmental tuffs, and argillites. These rocks have been metamorphosed to hornblende schists, amphibolites and quartz-biotite schists. The amphibolitic rocks are probably the metamorphosed equivalents of volcanoclastic rocks while the

Legend for Figure 2

Precambrian

Post Sickle Intrusive Rocks



Pink Granite and Quartz Monzonite



Granodiorite

Pre Sickle Intrusive Rocks



Hornblende Diorite and Gabbro

Wasekwan Group



Meta-basalt; meta-andesite



Meta-arkose, feldspathic quartzite, minor
arkosic conglomerate

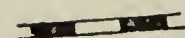


Dacite, minor rhyolite and rhyodacite,
acid tuff, agglomerate, volcanic
breccia



Meta-argillite, acid and intermediate
pyroclastic rocks

Symbols



Road



Ruttan Lake Mine

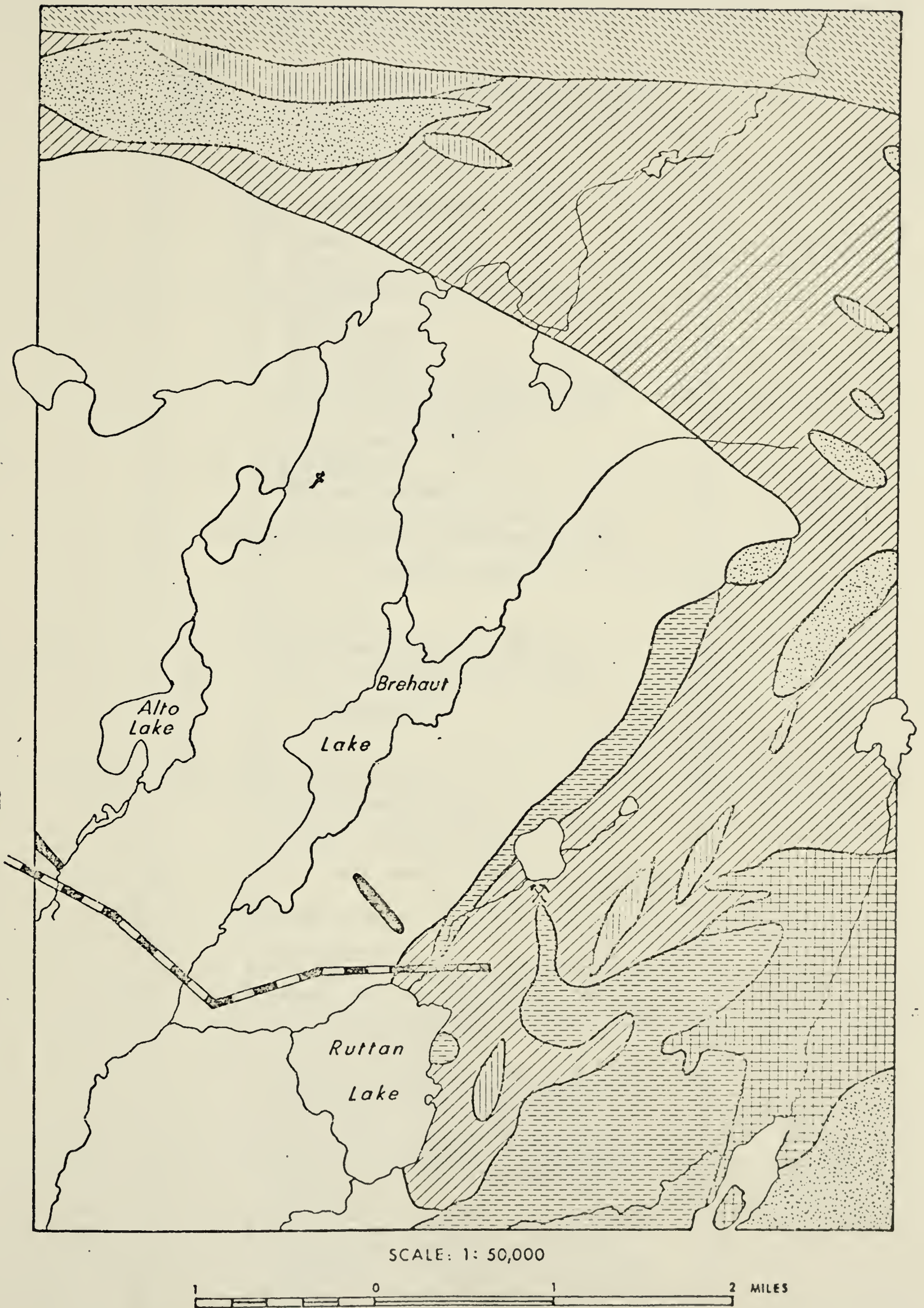


Figure 2. Geology of the Ruttan Lake Area
(Steeves and Lamb, 1972)

TABLE 1 TABLE OF FORMATIONS
(Steeves and Lamb, 1972)

PLEISTOCENE

AND
RECENT

Till: lacustrine clays and silts: outwash
deposits: minor sand and gravel deposits

GREAT UNCONFORMITY	
P R E C A M B R I A N	<p>POST-SICKLE INTRUSIONS</p> <p>Diabase</p> <p>Pegmatite and aplite</p> <p>Pink "quartz-eye" granite, quartz monzonite</p> <p>Quartz monzonite</p> <p>Pink granite and quartz monzonite, minor alaskite</p> <p>Biotite-hornblende granodiorite with dioritic to quartz dioritic contact phases; minor quartz monzonite</p> <p>Quartz monzonite, granite</p> <p>Granodiorite</p> <hr/> <p>Opachuanau Gneisses</p> <p>Biotite-hornblende intermediate gneiss</p> <p>Quartz diorite, leuco-quartz diorite</p> <hr/> <p>INTRUSIVE CONTACT</p>
	<p>SICKLE GROUP</p> <p>Biotite-muscovite-quartz schist</p> <p>Arkosic conglomerate, minor arkose</p> <p>UNCONFORMITY</p>
	<p>PRE-SICKLE INTRUSIONS</p> <p>Diorite, quartz diorite</p> <p>Hornblende gabbro, hornblendite, minor diorite and quartz diorite</p> <hr/> <p>INTRUSIVE CONTACT</p>
	<p>WASEKWAN GROUP</p> <p>Sulphide zone</p> <p>Porphyritic meta-basalt and meta-andesite</p> <p>Meta-basalt, meta-andesite</p> <p>Meta-arkose, feldspathic quartzite, minor arkosic conglomerate</p> <p>Greywacke conglomerate</p> <p>Acid and intermediate pyroclastic rocks, metamorphosed volcanoclastic rocks, meta-argillite, amphibolite</p> <p>Dacite, minor rhyolite and rhyodacite, acid tuff, agglomerate, volcanic breccia</p> <p>Porphyritic meta-basalt, meta-andesite, meta-picrite</p> <p>Meta-basalt, meta-andesite, meta-picrite; includes minor amounts of dacite, minor rhyolite and rhyodacite, acid tuff, agglomerate, volcanic breccia, acid and intermediate pyroclastic rocks, metamorphosed volcanoclastic rocks, meta-argillite, amphibolite</p> <p>Pelitic biotite gneiss</p>

quartz-biotite schists were probably derived from more argillaceous sedimentary rocks.

The Wasekwan rocks occupy almost 50% of the Ruttan Lake area with the metavolcanic rocks being much better exposed than the metasedimentary rocks. Regionally the Wasekwan series has an irregular form and consists of branching limbs and disconnected patches with a general trend of east to northeasterly.

Basic to intermediate extrusive rocks, occasionally with porphyritic varieties, constitute the major part of the lower Wasekwan volcanic sequence. Due to their similar colors and textures it is difficult to distinguish them in the field. Metabasalt is the most common rock type in the sequence and local occurrences of ellipsoidal and amygdaloidal lavas can be found. Metaandesites are almost impossible to distinguish from the basalts by field techniques.

Lenticular, easterly-trending bodies of metamorphosed rhyolite and dacite outcrop east of Ruttan Lake. These rocks are readily distinguishable from more basic varieties by their light pinkish grey color and conchoidal fracture. Many of the fine-grained acid volcanic rocks display thin flow layering consisting of quartz-felspathic and darker mafic layers. Tuffaceous beds often occur near these rhyolites and dacites.

Steeves and Lamb (1972) report two occurrences of possible ignimbrites in the map area. Varying sizes of rhyolitic clasts occur in a dacitic groundmass. Agglomerate and volcanic breccias are also found interbedded in the basic volcanic sequence. The agglomerates are usually associated with acid flows and tuffs and contain well-rounded rhyolitic clasts in a fine-grained mafic groundmass. The angular fragments of the breccia are usually basaltic in a less basic groundmass.

The Upper Wasekwan Group consists of a sequence of metasediments with isolated intercalated basic and intermediate volcanic flows. Acid and intermediate pyroclastic rocks constitute the larger portion of these rocks. The pyroclastic rocks are generally non-fragmental but occurrences of lapilli tuffs have been reported by Steeves and Lamb (1972). Volcaniclastic rocks, consisting of volcanic graywackes and siltstones, are often difficult to distinguish from flow rocks. In outcrop they are generally more rounded and weakly jointed as compared to flow outcrops which are blocky and well jointed. Meta-graywackes resemble the volcaniclastic rocks, only are lighter in color and contain visible quartz. Greywacke conglomerate with acid volcanic clasts, epidotized clasts of Wasekwan volcaniclastic metasediments and granitic clasts have also been mapped by Steeves and Lamb (1972) but are not found in

abundance.

Meta-argillite occurs as thin seams in the metavolcanic and metasedimentary rocks of the Wasekwan group. These are the only rocks in the Rusty Lake greenstone that commonly contain garnet.

The Wasekwan series has been intruded by small irregular plugs, dykes and sills composed of hornblende diorite and quartz diorite. These Pre-Sickle intrusives outcrop on the eastern side of Ruttan Lake and constitute the earliest intrusives in the area. They are younger than the Wasekwan rocks by distinct intrusive relationships. Porphyritic banded textures, various grain sizes and changes in mineralogy can be observed in these intrusive rocks.

The dominant mafic mineral present in these dark grey rocks is hornblende, which appears to have been altered at least in part to actinolite. Some of the hornblende has been altered to chlorite. The metamorphic grade is that of the upper amphibolite facies although the presence of chlorite and biotite may be due to retrograde metamorphism.

The Sickle group comprises arkosic conglomerate and sedimentary rocks which have been metamorphosed to quartz-mica schist and biotite-muscovite-quartz schist. These schists were probably derived from shale, arkose and siltstone. The relatively simple structure and low grade of metamorphism infer the Sickle rocks to be considerably

younger than the Wasekwan group and the Pre-Sickle intrusives. Milligan (1960) made the following observations for evidence of an unconformity at the base of the Sickle Group: (i) the Wasekwan and Post-Sickle rocks are more intensely folded, (ii) a slight angular unconformity was observed locally, and (iii) abundant pebbles of Wasekwan metavolcanics and metasediments and pre-Sickle intrusive rocks occur in the Sickle arkosic conglomerate. These pebbles must have been the result of erosion following deposition and intrusion of the Wasekwan rocks. Based on the mineralogy and texture, Burwash (1962) suggested that the Sickle sediments were well-sorted shallow marine shelf deposits.

Steeves and Lamb (1972) introduce the term Opachuanau gneisses as their field observations indicate that some of the gneisses are derived from Sickle rocks. In the Ruttan Lake area the most predominant gneissic rock is a biotite-hornblende intermediate gneiss but no field relations were observed which would suggest that it was derived from Sickle rocks. These gneisses are well foliated and are fine- to medium-grained. The foliation is defined by a preferred orientation of biotite and hornblende.

Response to differential glaciation, the post-Sickle intrusives show the greatest topographic relief. They constitute the youngest rocks in the Ruttan Lake area and

include hornblende-biotite granodiorite and pink gneissic granite with pegmatite and diabase dykes.

The hornblende-biotite granodiorite and quartz monzonite granite are massive, medium- to coarse-grained and usually well jointed. The granodiorite is pale pink to light grey, medium- to coarse-grained and generally massive while the quartz-rich granite is coarse-grained and appears pale pink to buff color and contains more potassium feldspar. The granite often has a gneissic texture. Pearce (1964) and Steeves and Lamb (1972) consider the quartz monzonite granite to probably be a leucocratic differentiate of the granodiorite. Granitic intrusives in the Wasekwan series have produced contact areas with variations in mineralogical composition due to assimilation. The granodiorite becomes dioritic to quartz dioritic in composition.

The pegmatite occurs mostly as sharp-edged dykes in the area and crosscuts the Sickle rocks or their metamorphosed equivalents. Two fairly large dykes of diabase composition are present just east of Ruttan Lake. These are the youngest rocks in the map area and show relatively little alteration of the constituent minerals.

Structural Geology

Pearce (1964) and Steeves and Lamb (1972) suggest two periods of folding in the Ruttan Lake area -- east-west regional foliation developed a series of isoclinal folds on all rocks older than the post-Sickle intrusions and represents the first identifiable period of deformation in the area. The diorite intrusions probably occurred prior to this folding as these intrusive masses have undergone considerable deformation. The intrusion of the granodiorite and granite caused only gentle folding but this intrusive event was followed by northeast and northwest trending faults. East of Ruttan Lake an anticline-syncline pair of folds plunges to the east and has northeasterly trending axial planes. The granitic rocks in the hinge zone of the anticline appear to postdate the folding as they are generally massive (Steeves and Lamb, 1972). Faults and shear zones in the Ruttan area occur in northeast, northwest, and easterly directions.

Poor outcrop, lack of good marker horizons and discontinuity of rock units make interpretation of the structure of the Rusty Lake greenstone belt difficult. Regionally the belt consists of steeply dipping intercalated metavolcanic and metasedimentary rocks. Regional foliation due to tectonic stresses, intrusion of the granodiorite

batholith and the effects of greenschist to amphibolite facies metamorphism have destroyed most primary structures and textures in the rocks of the Ruttan Lake area.

In most cases primary sedimentary structures are too poorly developed or preserved to conclusively determine tops of beds although relict bedding is preserved in some metasedimentary rocks of both the Wasekwan and Sickle groups. Steeves and Lamb (1972) report a few occurrences of ellipsoidal lavas in the Wasekwan Group and the occasional presence of spherical pillows. Jones (1969) regards the presence of these pillow structures to indicate subaerial extrusion flowing into shallow water rather than submarine extrusion. The occurrence of ignimbrites would be indicative of subaerial volcanic activity. The unsorted state of the coarser pyroclastic rocks and the presence of cross-bedding in some of the acid tuffs would also suggest a subaerial to shallow water environment. The presence of coarse pyroclastics such as lapilli tuffs, tuff-breccias, and agglomerates would infer proximity to the domical volcanic centre.

Metamorphism

The volcanic rocks of the Wasekwan Group and Pre-Sickle Intrusives have been considerably altered during regional

metamorphism. The metamorphic grade of most of the meta-volcanic rocks is variable and difficult to define due to the lack of indicator minerals. In the Ruttan Lake area the greenstone belt is comprised of rocks of lower amphibolite facies to epidote-amphibolite lithologies and rocks of the greenschist facies.

The rocks of the amphibolite facies are mainly fine-grained meta-basalts and meta-andesites. The major constituent minerals are hornblende and plagioclase with minor epidote. The rocks of the epidote-amphibolite facies are relatively massive and contain light green fibrous amphibole, plagioclase and epidote with small amounts of quartz. The constituents of the greenschist lithologies are green chlorite, epidote, plagioclase and quartz.

The gneisses and some of the metasedimentary rocks appear to have been metamorphosed to the lower amphibolite facies. Staurolite and appreciable amounts of garnet are found in the metasedimentary rocks and meta-argillites.

Chemistry of the Volcanic Igneous Rocks

Introduction

Considerable chemical data has been published on the volcanic rocks in the Canadian Shield. Many authors point out their chemical similarity to the volcanic rocks of

present-day island arcs and continental margins (Wilson et al., 1965; Folinsbee et al., 1968).

The Manitoba Department of Mines, Resources and Environmental Management did chemical analysis on several samples from the Rusty Lake greenstone belt which includes the Ruttan Lake ore deposit. Using the silica percentage (Goodwin, 1968) to classify the various types of extrusive and intrusive rocks, chemical variation diagrams have been constructed which distinguish three categories of basalt: olivine-alkali basalt, tholeiite and high-alumina basalt (Kuno, 1968). Due to recrystallization of the volcanic rocks in the Rusty Lake greenstone belt, the distinction between the three categories of basaltic rocks is based almost exclusively on the variation diagrams and the chemical analysis. By incorporating this data into the thesis it is hoped to draw some conclusions as to the origin of the volcanics and the geologic environment at the time of their deposition.

Results

Figure 3 shows locations of the chemically analyzed samples and Table 2 gives the chemical analysis and C.I.P.W. norms for analyzed samples in the vicinity of Ruttan Lake. The chemical analysis indicate distinctive chemical characteristics for the metavolcanics: (i) high Al_2O_3 content,

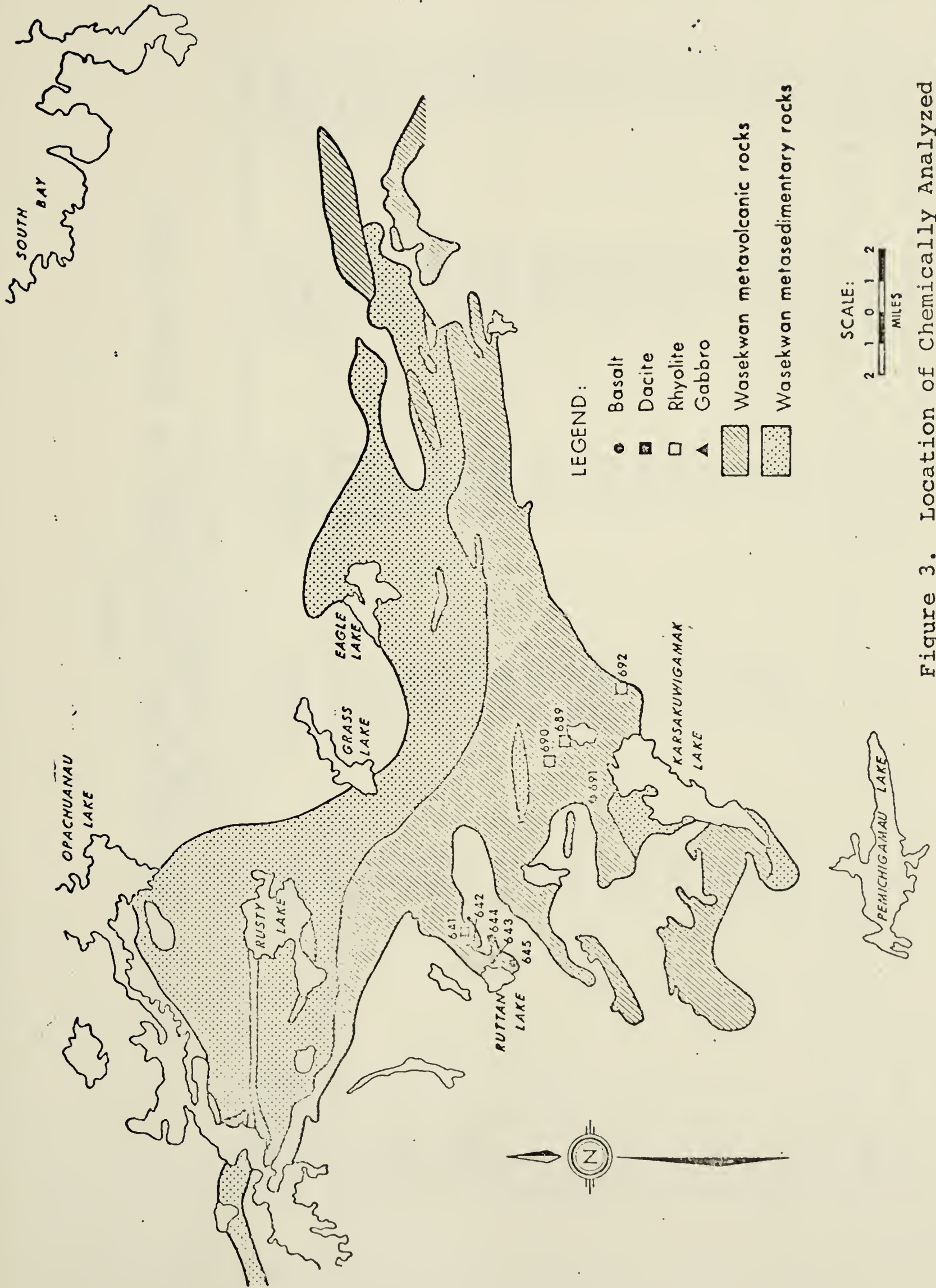


Figure 3. Location of Chemically Analyzed Samples (Steeves and Lamb, 1972)

TABLE 2

CHEMICAL COMPOSITION AND C.I.P.W. NORMS FOR VOLCANIC ROCKS
FROM THE RUTAN LAKE AREA
(FROM STEEVES AND LAMB, 1972)

Sample No. Rock Type	R-641 Dacite	R-642 Gabbro	R-643 Basalt	R-644 Basalt	R-645 Basalt
SiO ₂	58.65	44.90	51.00	46.60	51.35
Al ₂ O ₃	16.70	13.90	19.10	15.55	14.70
TiO ₂	0.75	0.73	0.66	1.45	1.81
Fe ₂ O ₃	1.70	3.43	3.26	3.27	3.65
FeO	7.21	7.49	7.14	9.49	8.26
MnO	0.15	0.21	0.21	0.26	0.27
MgO	2.82	11.30	3.12	7.15	4.80
CaO	6.27	11.70	9.35	11.95	8.50
Na ₂ O	2.40	1.90	3.42	1.98	2.87
K ₂ O	1.80	0.83	1.07	0.25	1.51
P ₂ O ₅	0.11	0.10	0.25	0.37	0.63
H ₂ O	1.26	2.60	1.33	1.81	1.84
CO ₂	0.21	0.76	0.18	0.25	0.26
Total	100.05	99.85	100.10	100.40	100.45

TABLE 2 (cont'd)

	C.I.P.W. NORMS				
Quartz	15.94	-	1.03	-	4.25
Orthoclase	10.80	5.09	6.42	1.50	9.08
Albite	20.60	13.14	29.35	17.04	24.69
Anorthite	29.91	27.93	34.09	33.37	23.15
Nepheline	-	1.91	-	-	-
Diopside	.33	19.29	4.51	12.31	7.49
Ferrosilite	10.80	-	7.24	6.19	7.02
Enstatite	6.97	-	5.79	8.60	8.68
Hedenbergite	.45	6.40	4.92	7.72	5.28
Forsterite	-	14.17	-	2.67	-
Fayalite	-	5.61	-	2.12	-
Magnetite	2.50	5.15	4.80	4.82	5.38
Ilmenite	1.45	1.44	1.27	2.80	3.50
Corundum	-	-	-	-	-
Apatite	.26	.24	.59	.87	1.49
Total	100.01	100.37	100.01	100.01	100.01

TABLE 2 (cont'd)

Sample No. Rock Type	R-689 Rhyodacite	R-690 Rhyodacite	R-691 Basalt	R-692 Rhyolite
SiO ₂	70.10	64.75	48.75	72.20
Al ₂ O ₃	14.20	17.40	16.95	13.90
TiO ₂	0.36	0.65	0.54	0.19
Fe ₂ O ₃	2.06	3.62	1.27	1.66
FeO	3.26	2.56	7.97	2.66
MnO	0.07	0.11	0.21	0.12
MgO	0.80	0.90	4.90	0.75
CaO	1.10	1.75	14.80	1.60
Na ₂ O	3.65	4.75	1.85	3.45
K ₂ O	2.70	1.45	0.45	1.95
P ₂ O ₅	0.02	0.27	0.18	0.01
H ₂ O	0.96	0.70	0.86	0.99
CO ₂	0.55	0.95	0.76	0.41
Total	99.85	99.85	99.50	99.90

TABLE 2 (cont'd)

	C.I.P.W. NORMS			
Quartz	33.86	27.35	-	39.18
Orthoclase	16.24	8.73	2.72	11.71
Albite	31.41	40.92	15.99	29.64
Anorthite	5.42	7.04	37.41	7.99
Nepheline	-	-	-	-
Diopside	-	-	15.60	-
Ferrosilite	3.89	.86	4.59	3.48
Enstatite	2.03	2.28	4.28	1.90
Hedenbergite	-	-	14.59	-
Forsterite	-	-	.67	-
Fayalite	-	-	.79	-
Magnetite	3.04	5.34	1.88	2.44
Ilmenite	.70	1.26	1.05	.37
Corundum	3.38	5.58	-	3.28
Apatite	.05	.64	.43	.02
Total	100.02	100.00	100.00	100.00

(ii) low TiO_2 content, (iii) high $\text{FeO}:\text{Fe}_2\text{O}_3$ ratios, (iv) a high CaO and correspondingly low MgO content, (v) low alkali content (especially K_2O) and (vi) high volatile content ($\text{CO}_2 + \text{H}_2\text{O}$) (Steeves and Lamb, 1972). From the C.I.P.W. norms, the basic extrusive rocks of the Rusty Lake greenstone belt display normative mineralogical characteristics of both tholeiitic and alkali-olivine basalts and thus correspond closely to Kuno's (1960) high alumina basalts. The acid and intermediate rocks all contain quartz and orthopyroxene but no olivine or nepheline, only small amounts of clinopyroxene with respect to orthopyroxene and hence tend to be more tholeiitic than the basic rocks (Steeves and Lamb, 1972).

Figure 4 shows the trend in compositional change between the calc-alkaline and tholeiitic series in an $\text{MgO} - \text{FeO} - \text{Na}_2\text{O} + \text{K}_2\text{O}$ diagram. Typical tholeiitic series show trends approximately parallel to the $\text{MgO} - \text{FeO}$ side in their early and middle stages of fractional crystallization, whereas typical calc-alkaline series show trends approximately normal to the $\text{MgO} - \text{FeO}$ side (Miyashiro, 1974). Samples of basalt and gabbro from the Rusty Lake greenstone belt show a parallel trend to the $\text{FeO} - \text{MgO}$ side while samples of rhyolite and rhyodacite are more normal to it. In general, the extrusive rocks show the high-iron type of fractionation characteristic of tholeiites.

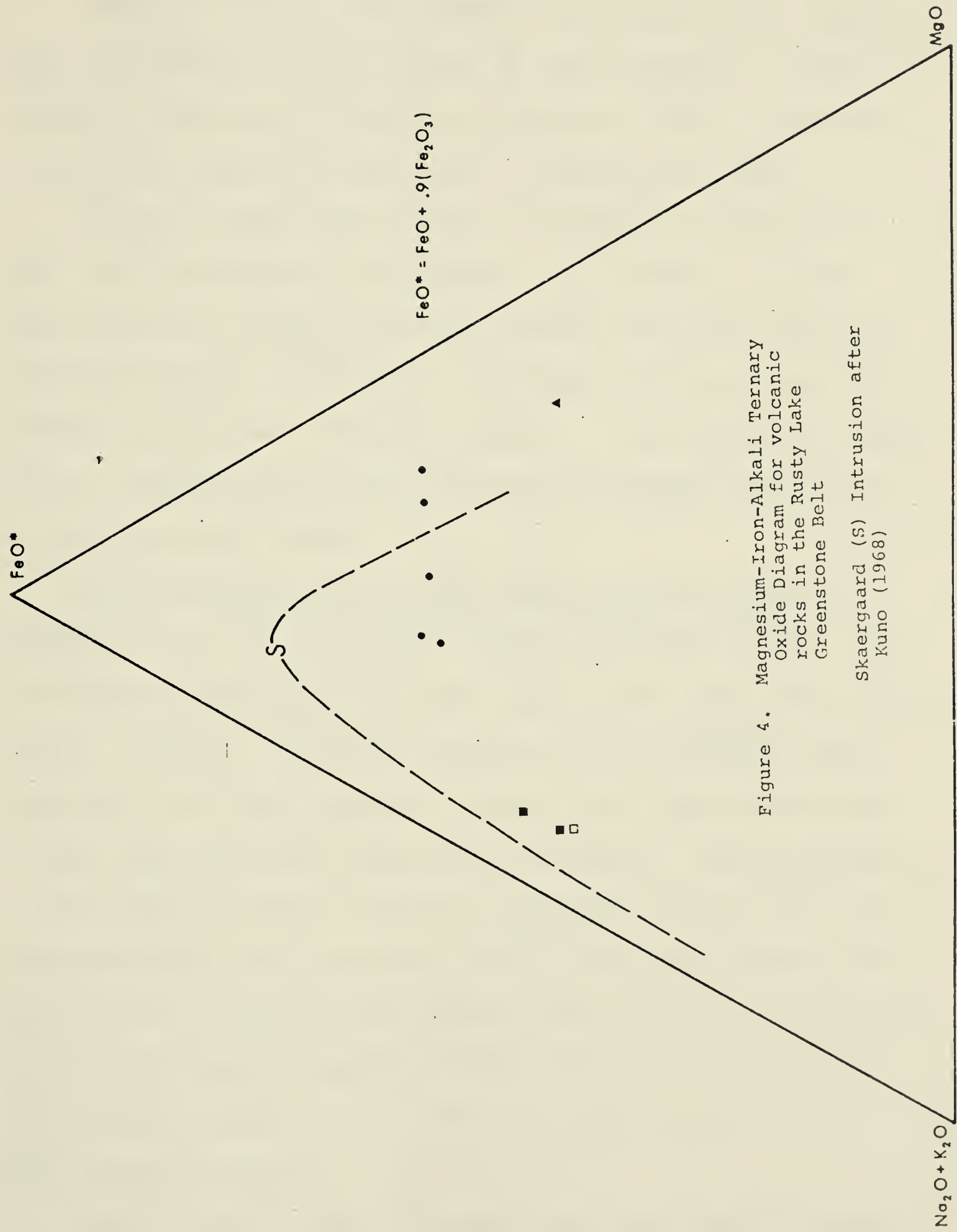


Figure 4. Magnesium-Iron-Alkali Ternary
Oxide Diagram for volcanic
rocks in the Rusty Lake
Greenstone Belt
Skaergaard (S) Intrusion after
Kuno (1968)

Figure 5 illustrates changes in SiO_2 and FeO content with increasing FeO/MgO ratios of the volcanics. Using boundary curves as defined by Miyashiro (1974), there is a gradation from calc-alkaline to tholeiitic trend.

Figure 6 shows the trends of variation of TiO_2 content with FeO/MgO in the volcanic rock series. In the calc-alkaline series, the TiO_2 content decreases with increasing FeO/MgO, whereas it increases first and then decreases in typical tholeiitic series. The resulting trend shows a depleting TiO_2 and increasing FeO/MgO from basic to acid volcanic rocks.

Calc-alkaline series rocks usually have higher K_2O contents than the associated tholeiitic series rocks with the same FeO/MgO ratios as well as with the same SiO_2 contents. Figure 7 shows K_2O content of the volcanic rocks compared with SiO_2 content. Most of the samples plotted in the tholeiitic and high-alumina fields. Those samples in the alkali-olivine field are basaltic, while those in the tholeiitic field include some of the more acidic volcanic rocks. Many of the samples plot close to the tholeiite/alkali-olivine boundary, which further indicates the transitional nature of the volcanic rocks in the Rusty Lake greenstone belt.

White et al. (1971) suggested that the Archean greenstone belts of Precambrian shields may represent oceanic

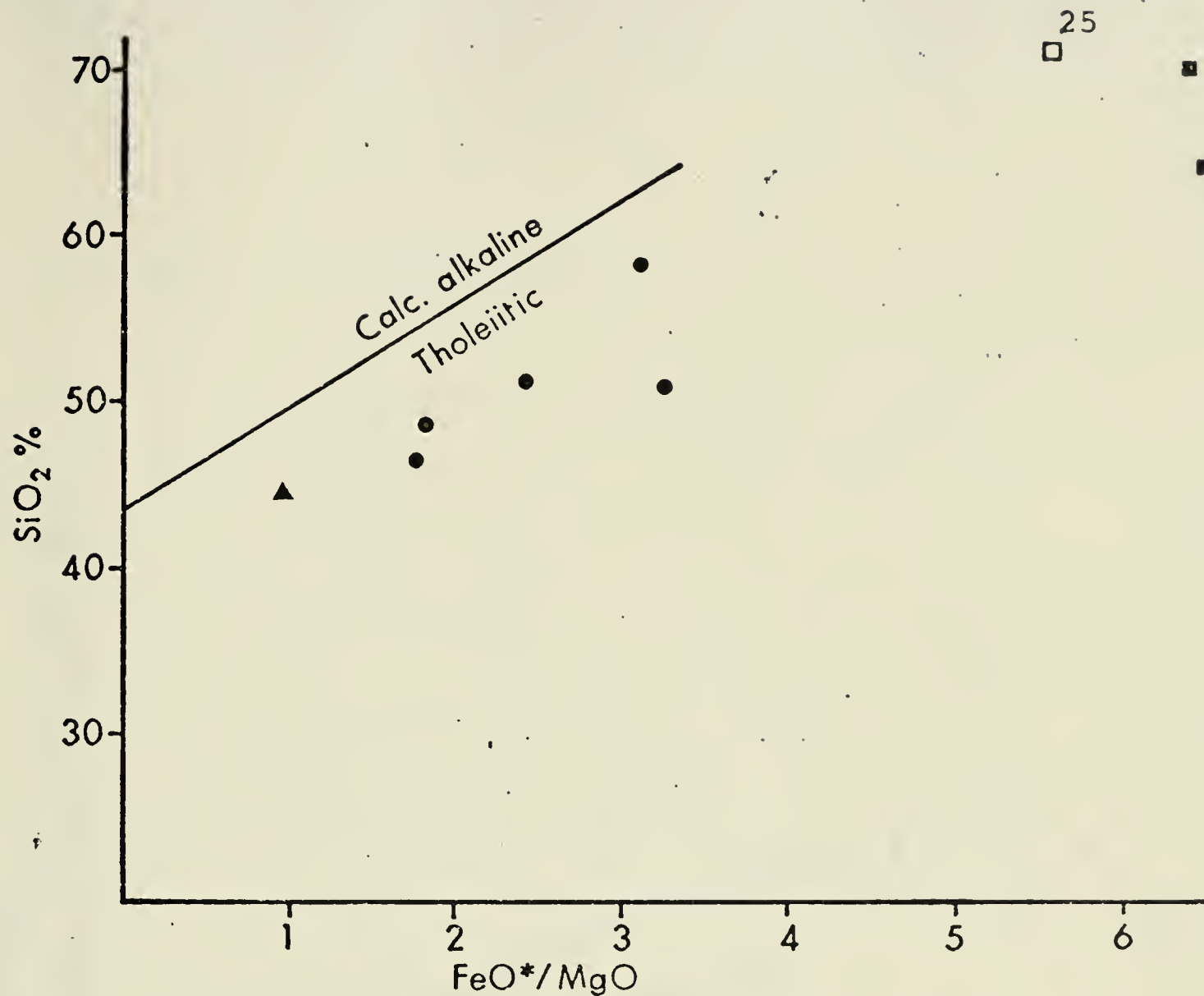


Figure 5. Changes in SiO_2 Content with increasing FeO/MgO Ratios

$$\text{FeO}^* = \text{FeO} + .9(\text{Fe}_2\text{O}_3)$$

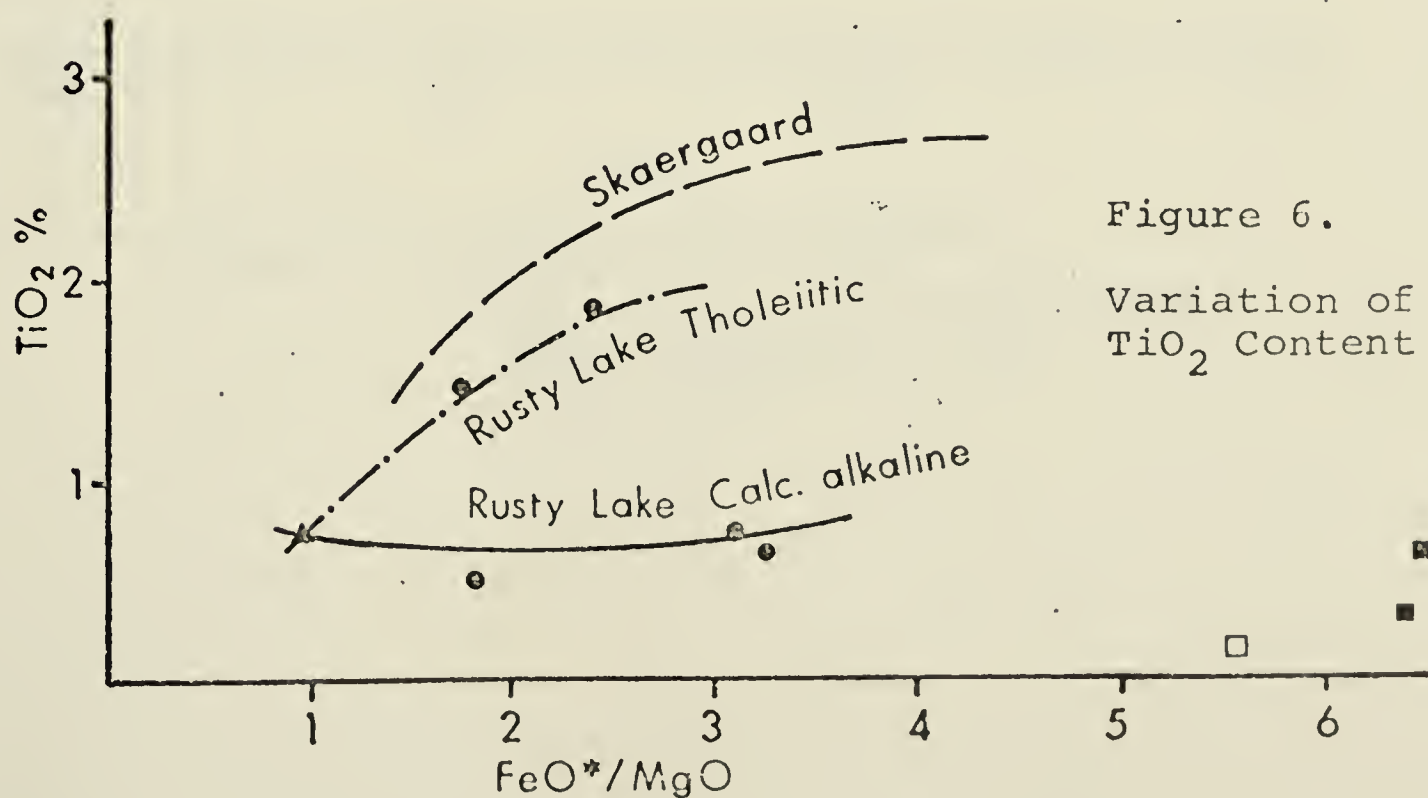


Figure 6.
Variation of TiO_2 Content

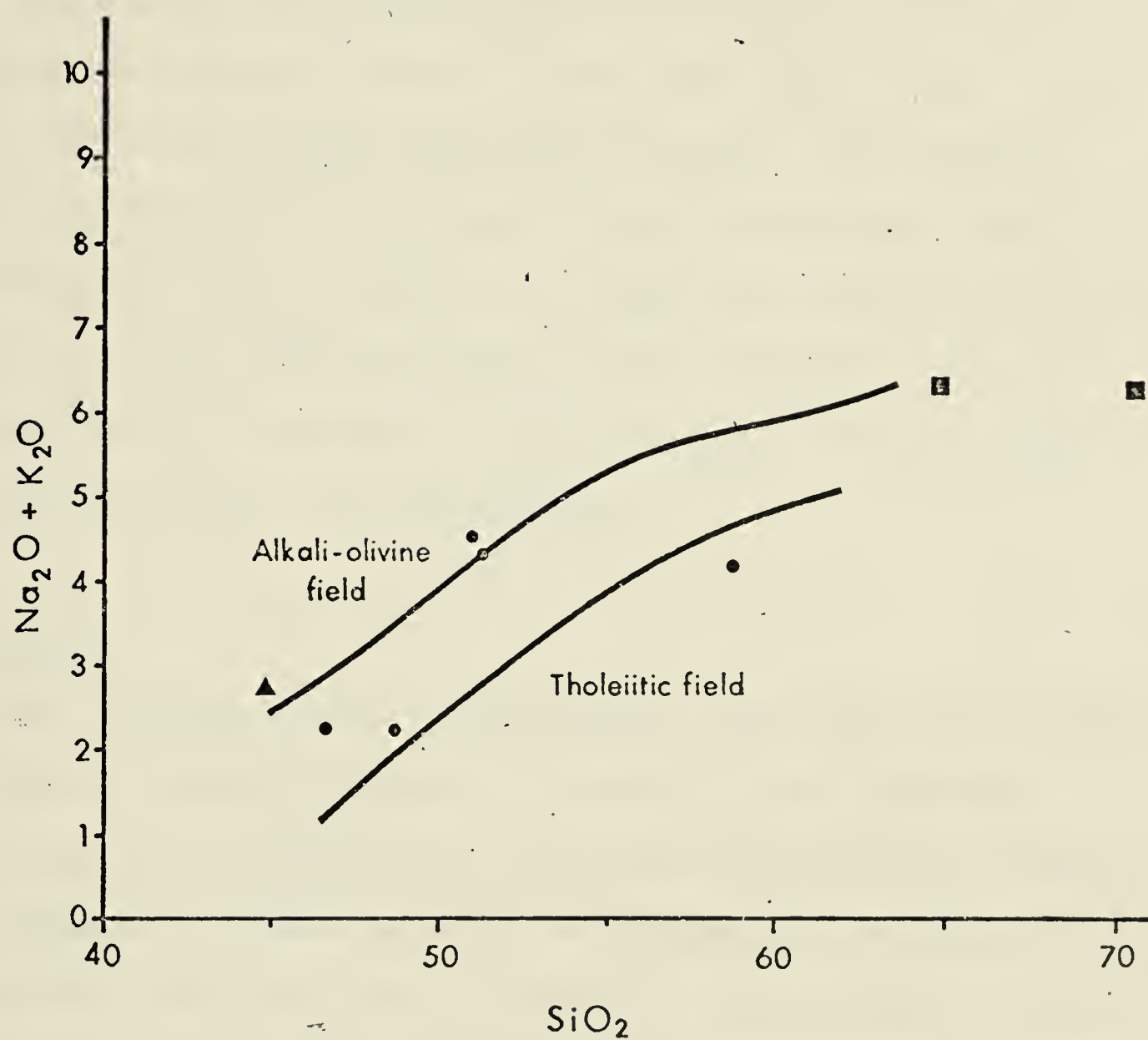


Figure 7. Alkali-Silica Diagram
Alkali-olivine and Tholeiitic
field boundaries after
Kuno (1968)

crust. Pearce et al. (1974) proposed the use of TiO_2 - K_2O - P_2O_5 ternary diagrams as a method of discriminating between oceanic and non-oceanic (continental) basalts. They concluded that Archean basalts suggest preponderant oceanic affinities. Figure 8 shows the TiO_2 - K_2O - P_2O_5 plots for a few of the Rusty Lake basalts. The results show an affinity to the oceanic field indicating the possibility that these basalts were generated under conditions similar to that of present-day oceanic basalts. The enrichment of K_2O relative to TiO_2 and P_2O_5 is most likely due to alteration and metamorphism.

Discussion

The volcanic rocks in the Ruttan Lake area are primarily basalt, andesite, dacite, rhyodacite and rhyolite. They occur as an intimately interlayered sequence of basalt and andesite followed by acid volcanic rocks ranging in composition from rhyolite to dacite. The presence of pillow structures (although usually poorly preserved) suggest that they were extruded in a subaerial to shallow marine environment. The chemistry of the acid volcanics suggests that they tend to be more tholeiitic whereas the basic rocks display characteristics of both tholeiitic and alkali-olivine basalts.

Kuno (1960) concluded that rocks with high Al content

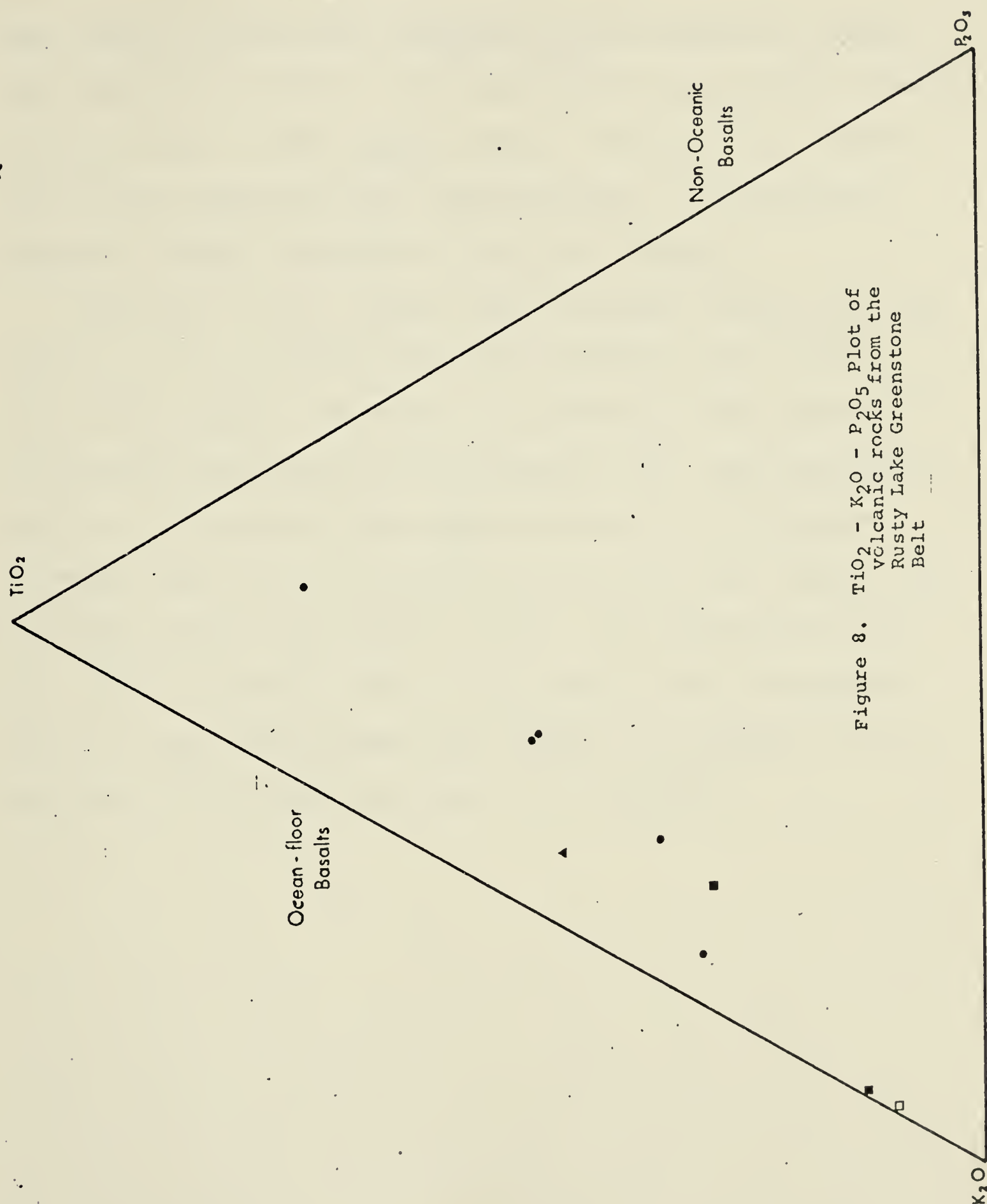


Figure 8. TiO_2 - K_2O - P_2O_5 Plot of volcanic rocks from the Rusty Lake Greenstone Belt

and found in island arc systems, are intermediate between the tholeiitic rocks of the continental side and the alkali-olivine rocks on the oceanic side. Wilson et al. (1965) state that tholeiites are characteristic of continental orogenic regions including island arc systems.

Miyashiro (1974) showed that immature island arcs are usually made up predominantly of basaltic rocks of the tholeiitic series, and that with advancing development of continental-type crust and presumably with progressive depletion of the underlying upper mantle, the predominant volcanic rocks tend to become andesite and even dacite and rhyolite of the calc-alkali series. The transitional nature of the volcanic rocks in the Rusty Lake greenstone belt, in which the Ruttan Lake deposit is located, is indicative of an island arc type of environment.

CHAPTER II GEOLOGY OF THE RUTTAN LAKE ORE DEPOSIT

A. The Host Rocks

The Ruttan Lake deposit is located in the Rusty Lake greenstone belt consisting of Archean volcanic and sedimentary rocks, a geological setting typical of many Canadian massive sulphide deposits of the same age. The deposit is controversial in origin as are many of the economic sulphides deposits in the Canadian Shield. The two main opposing theories of ore genesis are that the economic sulphide deposits originated from hydrothermal replacement of pre-existing Wasekwan rocks or that the initial derivation of ore metals was from submarine volcanic exhalation, precipitation of the metals and their incorporation in sea-floor acid volcanic flows and minor sedimentary rocks, followed by metamorphism.

Hutchinson (1973) suggests that massive pyritic base-metal sulphide deposits in volcanic rocks are of volcanogenic origin and were formed in recurrent episodes of sea-floor fumarolic activity during prolonged periods of subaqueous volcanism. The Ruttan Lake deposit is typical of massive volcanogenic stratiform Archean-type deposits. Copper-zinc mineralization occurs between basaltic-andesite flows and coarse-grained pyroclastics and felsic flows. Intercalated tuffaceous beds, and sedimentary layers of

metaargillites and cherts occur in the main volcanic sequences. These 'host' rocks for the ore have been metamorphosed to quartz-biotite-hornblende schists, quartz-biotite gneiss, quartzite, sericite and chlorite schists and are intersected with dykes of granite, gabbro, diabase and andesite.

An alteration halo of quartz sericite and chlorite-pyrite-quartz-sericite appears to envelope the ore body. Due to the greenschist facies of metamorphism these alteration zones adjacent to massive sulphide deposits are difficult to distinguish from the regionally metamorphosed country rock. Chlorite and sericite are concentrated in the footwall of the ore body. Silicification appears to decrease towards the footwall.

There are basically three parallel ore zones which strike N 70°E, dip 67° SE and plunge 45° east. Stratigraphically the sulphide bodies occur within metamorphosed dacites, rhyodacites, rhyolite, basalt and andesite which are intercalated with breccias, tuffs and cherts. Table 3 shows possible metamorphic equivalents of primary rock types commonly associated with Precambrian massive sulphide deposits (Hutchinson, 1970; Sangster, 1972). The ore bodies appear to be concordant with the enclosing steeply-dipping volcanic and metasedimentary rocks (see Figure 9).

The andesites are composed of hornblende, plagioclase,

TABLE 3

POSSIBLE METAMORPHIC EQUIVALENTS OF PRIMARY ROCK TYPES
COMMONLY ASSOCIATED WITH PRECAMBRIAN MASSIVE SULPHIDE
DEPOSITS (FROM HUTCHINSON, 1970; SANGSTER, 1972)

Primary or Low-Grade Metamorphic Rock	Medium-Grade Metamorphism	High-Grade Metamorphism
Chert	Siliceous schist	Quartzite
Pyritic, cherty iron- formation	Pyrite-pyrrhotite- magnetite mica schist	Pyrrhotite-magnetite mica quartzite
Rhyolite		
Rhyolite tuff	Quartz-feldspar- sericite gneiss	Quartz-feldspar gneiss
Rhyolite breccia		
Rhyolite agglomerate		
Andesitic tuff (chlorite-schist)	Biotite-chlorite-quartz schist	Biotite-quartz gneiss
Andesite (chlorite- schist)	Epidote-plagioclase- amphibolite	Hornblende-plagioclase- amphibolite gneiss
Basalt (chlorite-schist)	Epidote amphibolite	Amphibolite (gneiss)

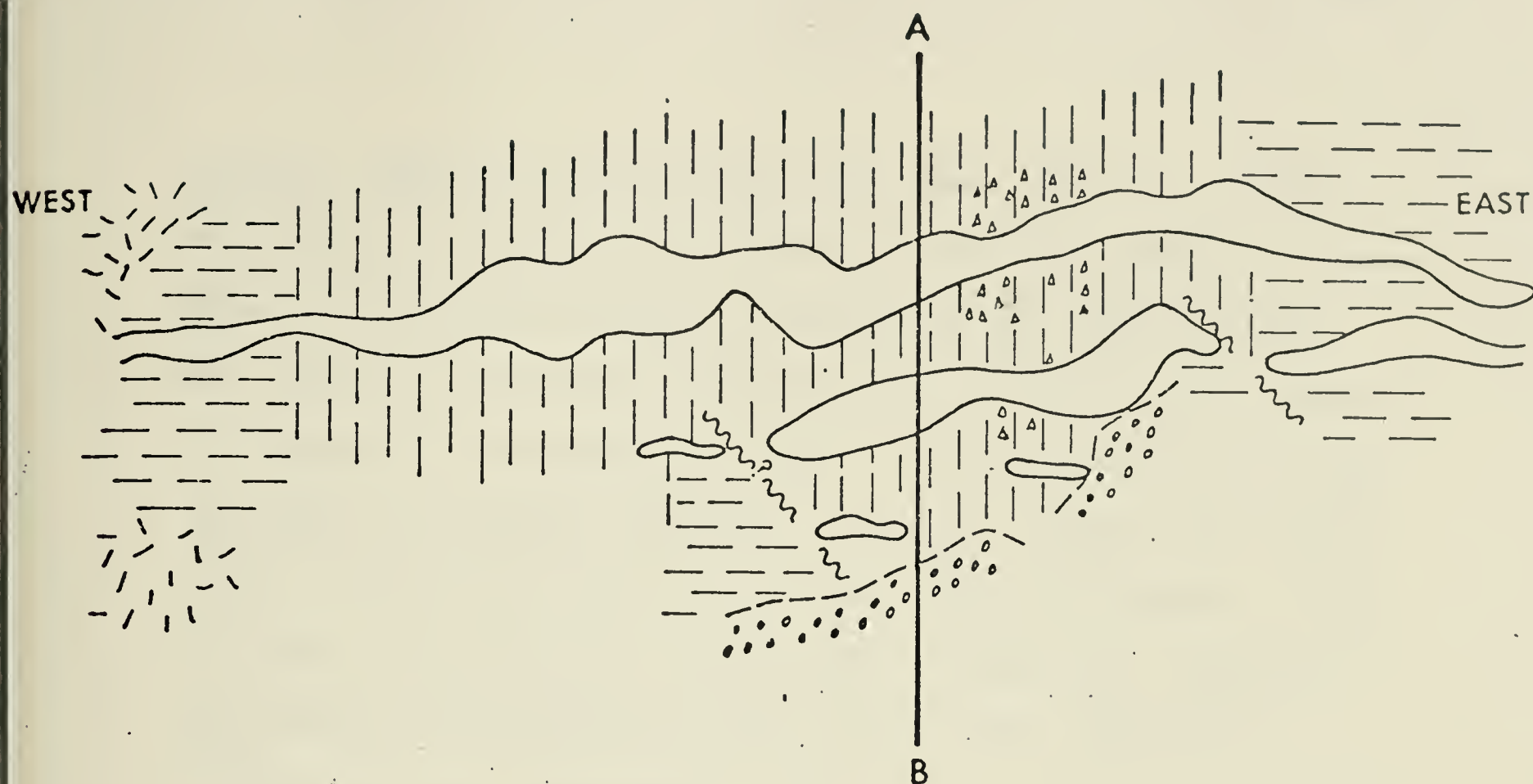
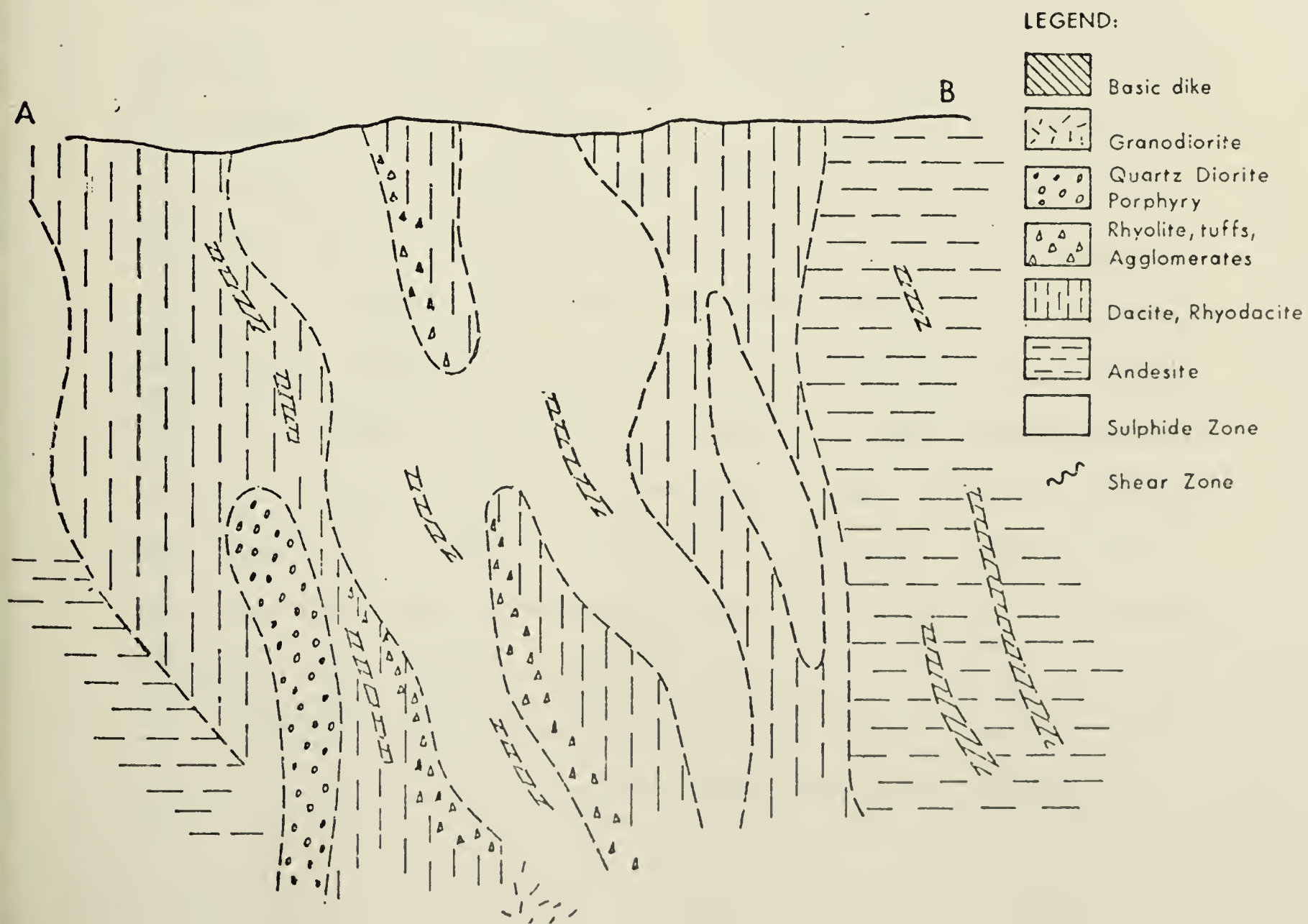


Figure 9. Plan View and Cross Section
of the Ruttan Lake Mine

SCALE:
200'



quartz, chlorite and sericite with some epidote. Quartz and calcite veinlets of secondary origin are common. These andesites are often highly chloritized and sericitized. The basalt is composed primarily of hornblende which occurs as subhedral, prismatic crystals. The plagioclase is also subhedral and poorly twinned. Biotite, epidote and actinolite are more abundant in the more altered samples. Phenocrysts of hornblende, plagioclase, magnetite, ilmenite and biotite occasionally occur in the more porphyritic metabasalts and andesites.

Dacites comprise the larger portion of the acid volcanics and are fine-grained, medium to light grey in color and are commonly porphyritic. The phenocrysts may be plagioclase, biotite, hornblende, potassium feldspar or quartz. The rhyodacite and rhyolite are greyish white to pink and have a more perfect conchoidal fracture than the dacites. They are usually fine-grained to aphanitic but may be porphyritic. Occasionally ropy textures could be recognized and optical examinations showed the groundmass to be fine-grained feldspar and quartz. Texturally and mineralogically they are similar to the dacites but are richer in quartz and potassium feldspar. Most of the dacites, rhyodacites and rhyolites show strong silicification and chloritization. Rhyolite tuffs occur as both agglomerates and breccias but it is difficult to distinguish between them. Quartz, sericite, chlorite and plagioclase constitute the groundmass

and they usually contain aggregates of chert. They are very similar in composition to the rhyolite and rhyodacite but are noticeably coarser and fragmental. Massive sulphide fragments of pyrite or chalcopyrite commonly occur in these tuffs. The agglomerate tuffs are white to greyish white and contain well-rounded rhyolitic clasts in a fine-grained more mafic groundmass. The tuff breccias are usually interbedded with basic volcanic rocks with the clasts varying in size, shape and composition. The rhyolite and dacite flows and tuffs are intercalated with argillaceous material. All the volcanic rocks show strong silicification and chloritization in the vicinity of the ore body.

Small outcrops of rhyolite tuffs near the deposit and the volcanic rocks overlying the deposit contain disseminated pyrite, but pyrrhotite, chalcopyrite and sphalerite, all of which are typical of the ore body, are absent. The larger sulphide fragments are angular or sub-rounded indicating a pyroclastic origin but with the very fine-grained fragments it is difficult to distinguish them from sulphide grains which may or may not be of pyroclastic origin.

Sinclair (1971) suggests that the presence of sulphide fragments in the volcanic rocks overlying the ore body could be due to volcanic explosion. The gneisses and intrusive rocks also show some mineralization but this usually

takes the form of disseminated pyrite and pyrrhotite. Mineralization also occurs in thin tuffaceous beds of intercalated sedimentary horizons in the volcanic sequence and in certain horizons in the sedimentary part of the sequence.

From the chemical composition of the Rusty Lake greenstone (Chapter I), the volcanic host rocks appear to have been derived by differentiation of a tholeiitic-type parent magma and chemically resemble standard tholeiitic and calc-alkalic rocks of the basalt, andesite-rhyolite association (Goodwin, 1968; Irvine and Baragar, 1971). These rocks are typically identified with the island arc or eugeosynclinal environment. Extrusion of calc-alkaline volcanics is frequently followed by orogenesis, hence accounting for the metamorphosed nature of most volcanogenic massive sulphide ores (Sangster, 1972).

B. The Sulphide Deposit

The structure of the Ruttan Lake deposit is complex with much evidence of folding, shearing and faulting. The deposit appears to be in part structurally controlled, along a northeasterly trending shear zone. The ore body is folded along with the enclosing volcanic and metasedimentary rocks. There is strong evidence that this deposit is up-turned. Although it is very difficult to determine the volcanic and intercalated sedimentary stratigraphy since there appears

to be more than one extrusion of basic lavas, zonation and distribution of the sulphide minerals suggest that the deposit has been up-turned.

The ore body is situated near the southern boundary of the greenstone belt and appears to be a structure in which mineralization occurs over a length of about 2800 feet and a width of 450 feet in the centre section but narrowing towards each end. Within this broad structure there are basically three parallel ore zones (see Figure 10).

Elsewhere, narrower ore lenses occur as separate parallel bodies, with the largest one to the west of the main ore body. This lense could possibly have been displaced from the main ore body by a northeast trending fault.

The deposit appears to be in part structurally controlled by a northeasterly trending shear zone although the precise time relationship between ore emplacement and the shearing is not known. The Ruttan ore body has undergone metamorphic effects related to regional metamorphism, dynamic metamorphism and post-Sickle intrusions, hence indicating that the ores are pre-metamorphic in age. Structures within the ores appear to be similar with those in the enclosing rocks, resulting in the possible deformation of the ore body due to slip folding and transposition. The similarity of mesoscopic structures in the ores and host rocks supports this theory.

There are two distinct types of ore - namely massive

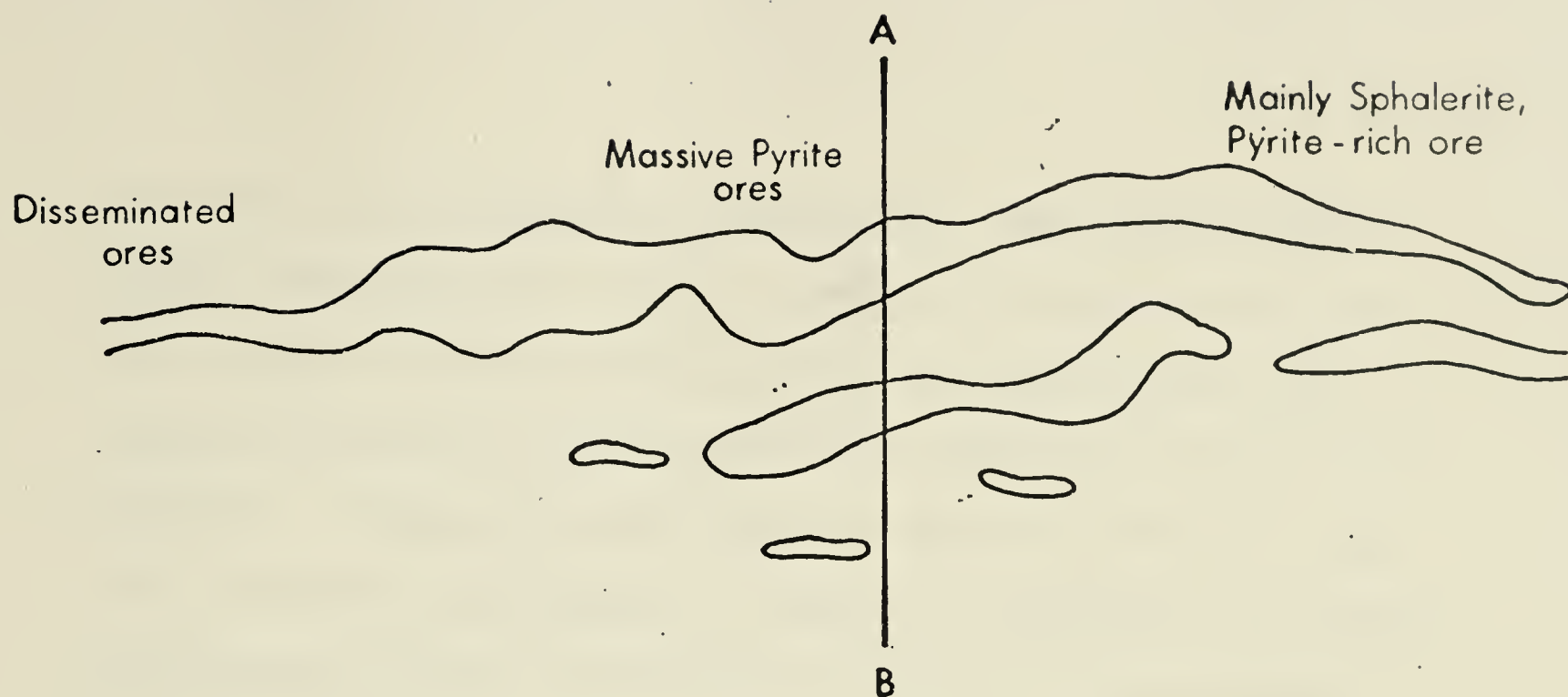
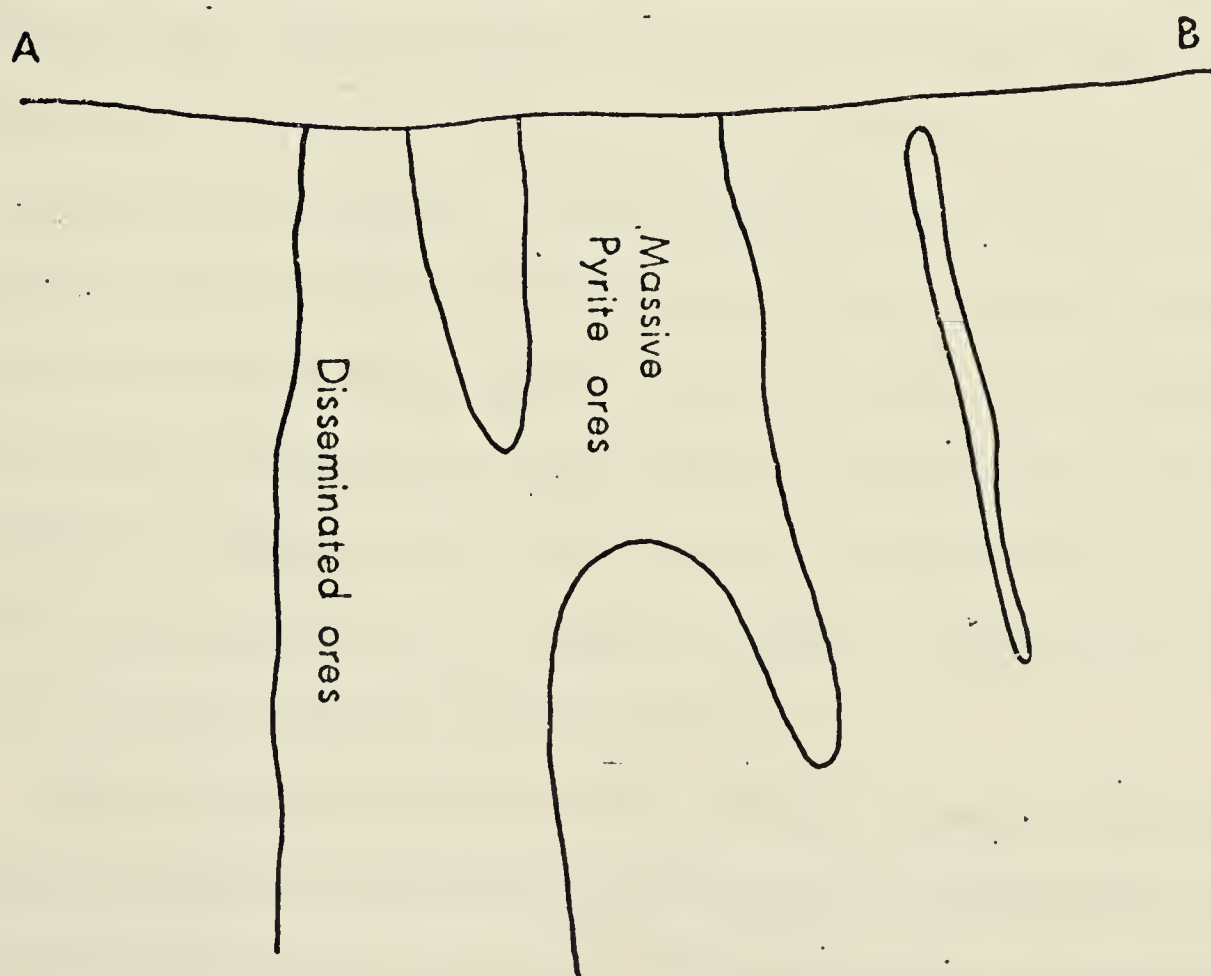


Figure 10. Plan View and Cross Section of Ruttan Lake Sulphide Zones

SCALE:
200'



sulphides and disseminated sulphides. The massive sulphides constitute the larger portion of the ore and consist mainly of fine-grained pyrite and pyrrhotite with varying amounts of chalcopyrite and sphalerite (see Photograph 1). Gangue minerals include quartz, sericite, calcite, chlorite and epidote. Within the massive ore bodies, chalcopyrite occurs irregularly throughout the sulphide but is concentrated toward the footwall and sphalerite toward the hanging wall.

The solid sulphides can be banded or massive. The sulphide bands are usually parallel to contacts of the massive ore with the wall rock except where they are strongly deformed by drag folds. Brecciation is common in pyrite-rich bands. On the hanging wall the sphalerite occurs interlayered with the pyrite giving the sulphide a distinct banded appearance. The massive chalcopyrite ores are always accompanied with pyrite, pyrrhotite and variable amounts of sphalerite. The massive sphalerite ores contain pyrite and pyrrhotite. Small amounts of gold and silver occur in the solid sulphide ores.

The sheared massive ores display weakly deformed colloform textures (Photograph 2), pyrite porphyroblasts, exsolution of chalcopyrite and pyrrhotite in sphalerite (see Photograph 3) and widespread granulation of pyrite.

The disseminated ore resembles massive ore in that it

contains the same opaque minerals and the same gangue minerals as the enclosing rocks. Pyrite, chalcopyrite, occasionally pyrrhotite, only minor amounts of sphalerite are found in the disseminated ores (see Photographs 4 and 5) and no gold or silver. Much of the disseminated ore is strongly sheared due to its location in the lower part of the ore body. The disseminated ores mostly occur in chlorite, sericite and talc schists. The talc schists decrease with depth. Chalcopyrite is found as irregular sulphide veinlets throughout the schists while the pyrite tends to parallel the foliation of the rock. In strongly sheared disseminated ores there is widespread porphyroblastic development.

Zoning is a characteristic feature of volcanogenic massive sulphide deposits. Mineralogical zoning is evident in the Ruttan deposit with chalcopyrite concentrated towards the footwall and sphalerite concentrated towards the hanging wall. Compositional zoning parallels the distribution of the two major ore sulphides with Cu/Zn ratios increasing with depth. Table 4 and Figure 11 show the results of a study of metal ratios in the ores. The eastern end or hanging wall of the ore body is zinc-rich with copper-zinc proportional to about the 800' level and then mainly copper below this.

Mineralogy of the sulphides of Ruttan Lake is relatively simple. The ore minerals identified in order of abundance

TABLE 4
Cu/Zn RATIOS

Sample #	Grid Reference	Average Cu/Zn Ratio	Remarks
1.	479 + 50	1.06	Footwall side-disseminated ores
2.	488 + 50	5.86	Massive pyrite ores
3.	495 + 30	7.60	" "
4.	500 + 50	2.25	" "
5.	501 + 50	2.82	" "
6.	502 + 50	2.12	" "
7.	503 + 60	7.43	" "
8.	505 + 00	7.60	" "
9.	506 + 00	8.60	" "
10.	508 + 00	6.69	" "
11.	510 + 00	2.31	" "
12.	512 + 00	.88	Massive pyrite-sphalerite ores
13.	514 + 00	.16	" "
14.	516 + 00	.25	" "
15.	518 + 00	.23	" "
16.	520 + 00	.76	" "
17.	522 + 00	.06	Hanging Wall Side

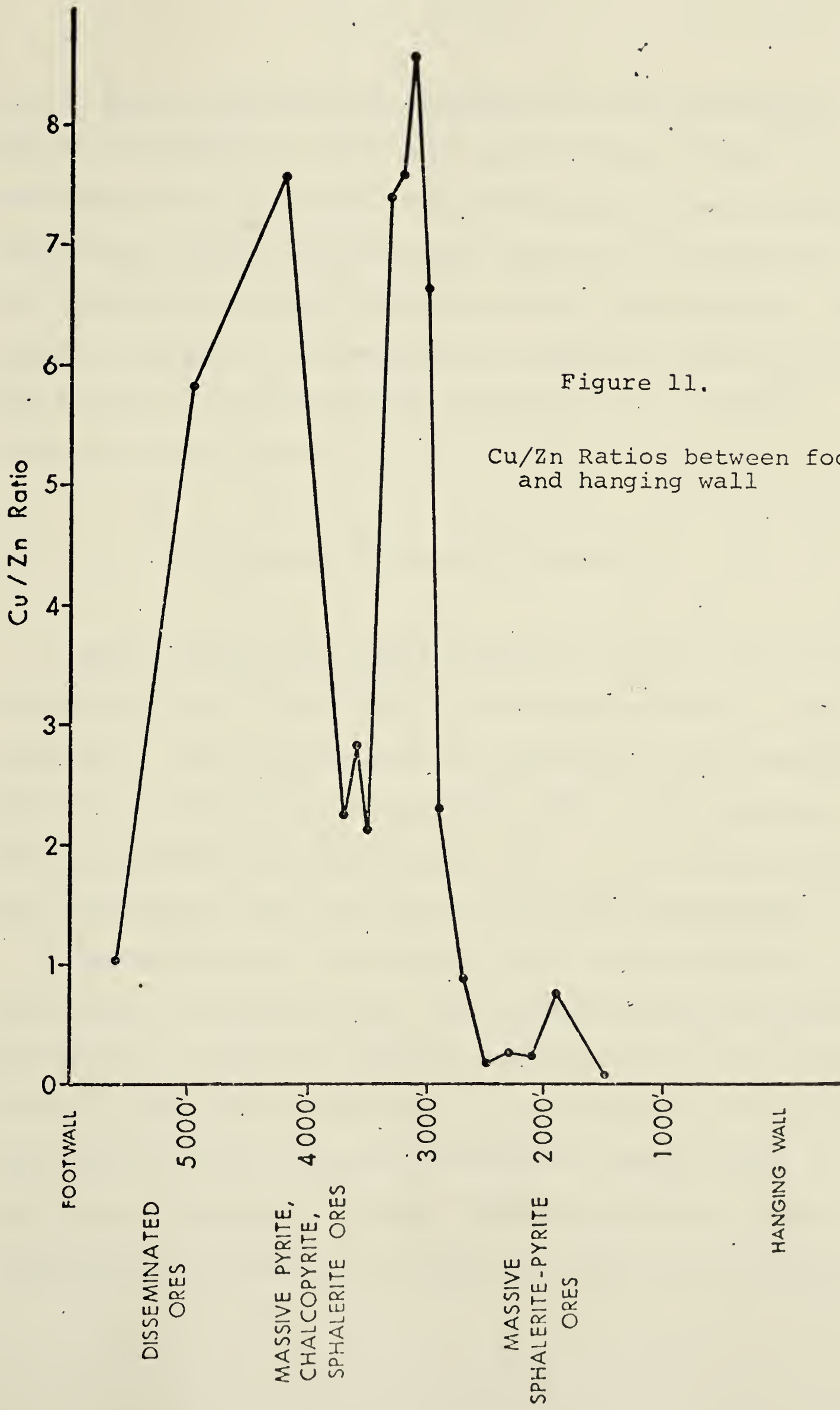


Figure 11.

Cu/Zn Ratios between footwall and hanging wall

were: pyrite, pyrrhotite, chalcopyrite and sphalerite. Galena is present in very small quantities, always as veinlets or vug fillings. The major gangue minerals identified were quartz, chlorite and sericite with secondary calcite occurring along fractures and as vug fillings. The quartz is medium- to fine-grained, massive, white in color and occurs as polycrystalline aggregates or as narrow veinlets or stringers.

Description of the ore minerals

Pyrite varies from large euhedral crystals (up to 3 cm) to subhedral grains and very fine-grained pyrite (<.1 mm in diameter). Recrystallization of chalcopyrite and sphalerite can be observed in the pyrite. The pyrite commonly occurs as massive porphyroblasts set in a matrix of gangue and chalcopyrite and can also be intensely granulated.

Pyrrhotite occurs as massive blebs and is usually associated with the pyrite. Both hexagonal and monoclinic pyrrhotite are present although the monoclinic type appears to be in the greater abundance. The method of distinguishing monoclinic from hexagonal pyrrhotite was to apply a thin film of magnetic colloid. This colloid is a dilute suspension of magnetic iron oxide in water and is prefer-

entially attracted to the ferromagnetic monoclinic pyrrhotite, imparting a dark brown coloration (see Photograph 6) (Ref. Scott, 1974). A recipe for magnetic colloid can be found in Appendix A.

Chalcopyrite is almost always associated with pyrite and appears to be replacing it. The grains are subhedral and range from 0.2 to 1 mm in diameter. In the disseminated ores the chalcopyrite occurs as veinlets and stringers. In the massive ore the chalcopyrite occurs as blebs and as fillings in small vein-like fractures. It also occurs as a coating around larger pyrite crystals in massive pyrrhotite and as unmixing intergrowths in sphalerite.

Sphalerite is the "blackjack" variety and is always associated with the pyrite and occasionally with the chalcopyrite. Exsolution of chalcopyrite and pyrrhotite along the crystal lattices can be observed. The sphalerite generally displays a dark reddish color, indicating a fairly high Fe-content.

Galena appears as veinlets and vug fillings in any observed occurrences. Cubic crystals vary from 0.5 mm to 2 mm in diameter.

Textures

The sulphide textures, structures and apparent mineral assemblages are the result of metamorphism related to the orogenic disturbance. Regional metamorphism may have caused remobilization of existing sulphide bodies and their migration to more favorable structural settings. In the Ruttan Lake ores, porphyroblastic pyrite and sphalerite, colloform or fromboidal textures in sheared massive ore, exsolution textures, widespread granulation, aggregation of individual crystals and banding can be observed. All of these textural features appear to be due to the effects of metamorphism.

Banding was observed in the sphalerite-pyrite ores. This banding is dragged out and folded due to the results of metamorphism. There is evidence that pressures were high enough to produce the flow of pyrite. This would be necessary to produce bands of pyrite from former pyrite included in the sphalerite (see Chapter IV, Fe-content in sphalerite). The pyrite grains do not exhibit cataclastic deformation and hence the banding of the ore could very well be original though modified by later tectonic events. If in fact the banding is original then it would suggest depositional of sedimentary or volcanic rocks involving substitution for certain chemical constituents following

accumulation. However, no replacement of gangue minerals by sulphides was observed in the microscopic investigation although these textures have probably been obliterated by metamorphism.

The presence of subhedral and anhedral pyrite and pyrrhotite grains embedded in sphalerite indicates syngenetic coprecipitation between pyrite, pyrrhotite and sphalerite.

Recrystallization and grain growth producing large porphyroblasts of pyrite and sphalerite surrounded by crystalline matrix of pyrrhotite and chalcopyrite suggests that the sulphides underwent fairly high grade metamorphism (Sangster, 1972).

A much more detailed textural study would have to be done on these ores to draw any definite conclusions as to their origin. Some of the textures are probably due to the diagenesis of the deposit and not necessarily due to metamorphism; but the microscopic examination offered no conclusive evidence.

Genesis

The volcanic exhalative theory and the hydrothermal replacement theory are similar in that in both cases ore deposition came from hydrothermal solutions originating

within the crust of the earth and rising along fractures or other zones of weakness. The main difference in the two theories is in the timing of the ore deposition relative to the host rocks. In the exhalative theory the massive sulphide ore formation is an integral part and coeval with the volcanic complex in which the deposits occur. That is the ore deposition takes place at or near the volcanic rock - seawater interface between successive volcanic episodes. The hydrothermal theory regards ore deposition as a secondary feature imposed on the host rocks a considerable time after their formation and lithification (Sangster, 1972).

Matsukuma and Horikoshi (1970, p. 153) have summarized the Kuroko deposits as being "stratabound, polymetallic mineral deposits genetically related to submarine acid volcanic activity of Neogene Tertiary in Japan". The many studies done on the Kuroko deposits and their unmetamorphosed nature has led to the acceptance of these as "type deposits" for volcanogenic sulphide ores and hence it is useful to compare them with Precambrian deposits of similar type (Sangster, 1972).

Studying the geochemistry of the Ruttan Lake ores should reveal some of the physicochemical conditions at the time of ore formation, determine the relationship between the ores and the Wasekwan volcanics and give evidence to substantiate a volcanogenic origin.

CHAPTER III TECHNIQUES OF GEOCHEMISTRY STUDY

A. Sulphur Isotopes

Introduction

Since sulphur constitutes a major proportion of the Ruttan Lake ore minerals, a study of the stable sulphur isotope variations was conducted to aid in interpreting mineral genesis. Sakai (1968) suggests the use of sulphur isotopes to determine certain physical and chemical factors which influenced ore deposition and hence provide clues as to the genetic relationship of the ores. Thirty-four pyrite, seventeen pyrrhotite, twelve sphalerite and twelve chalcopyrite mineral separates were analyzed for their S^{34}/S^{32} ratios.

Kulp et al. (1956), Vinogradov et al. (1956), Jensen (1959), Tupper (1960) and Stanton (1960) were among the first workers to apply sulphur isotope ratios to problems of ore genesis. Their most important conclusion is that sulphur isotope ratios vary depending on source of mineralizing solutions and may be a valuable aid in interpreting the origin of an ore deposit.

Since 1968 several detailed studies on metamorphosed stratiform deposits have been done and Rye and Ohmoto (1974) concluded:

- (i) Large-scale, premetamorphic $\delta^{34}\text{S}$ variations are generally preserved while the average $\delta^{34}\text{S}$ for sulphides in major units such as formations remain unchanged.
- (ii) Small-scale sulphur isotope changes are in many cases superimposed upon the original sulphur isotope distribution during metamorphism. These are (a) redistribution of sulphur isotopes among co-existing minerals that define the temperature of metamorphism and (b) local $\delta^{34}\text{S}$ variations which reflect the structural or chemical metamorphic history.

Rye and Rye (1974) studied the metamorphosed Homestake mine in South Dakota and showed that Fe/Mg ratios decrease in the ore zones and concluded that during metamorphism pyrite was broken down into pyrrhotite plus sulphur and that the excess sulphur was taken into solutions by the metamorphic fluids which then migrated into the dilatant zones where sulphur reacted with the wall rocks to produce iron-rich sulphides.

When detailed sulphur isotope data are combined with other geochemical data on metamorphosed deposits it should be possible to determine the chemical environments of metamorphism.

The sulphur isotope study was concerned with the two more abundant species of sulphur - S^{32} and S^{34} . Sulphide sulphur was collected as SO_2 and analyzed on the mass spectrometer as mass 66 and mass 64. Mass 66 is $S^{34}O^{16}O^{16}$ and mass 64 is $S^{32}O^{16}O^{16}$.

Sample Selection and Preparation

The samples collected for sulphur isotope analysis were obtained from the Ruttan Lake open pit and diamond drill core and represent both a vertical and horizontal distribution. Pyrite, chalcopyrite, sphalerite and pyrrhotite were analyzed from both massive and disseminated ores.

Co-existing sulphide minerals were separated by using a Franz magnetic separator, methylene tetrabromide and methylene iodide heavy liquid separation and finally by handpicking. A binocular microscope was used to check the purity and the X-ray powder diffraction method was used on some samples which were thought to be of relatively poor separation. Before burning the separated sulphides were crushed in an agate mortar.

Preparation of SO₂ for Mass Spectrometer Analysis

The sulphide sulphur was converted into SO₂ by burning the samples in a quartz-pyrex combustion line. The essential parts are a quartz combustion chamber and a vacuum line for the purification and collection of the sulphur dioxide. Using Cu₂O as an oxygen donor, the samples were oxidized at approximately 1075°C directly to SO₂. 100-200 mg of intimately mixed oxide and sulphide were packed between quartz wool plugs in an open-ended quartz tube. The sample is put into the furnace, the line is evacuated, and the combustion chamber heated to the desired temperature. Upon heating the sample the evolved H₂O fraction was removed by using a freezing trap of carbon tetrachloride, chloroform and dry ice. The CO₂ and O₂ fractions were removed by using a second freezing trap of N-pentane (ethanol) and liquid nitrogen which traps the SO₂ and allows the CO₂ and O₂ to be pumped off. After the CO₂ is removed, the SO₂ is transferred to a graduated column and the yield is recorded. Table 5 gives the SO₂ yield in % of the samples analyzed. The SO₂ is then transferred into a standard breakseal and collected.

Isotope Analysis

The sulphur isotope analyses were performed on a 12", 90° magnetic-analyzer gas source mass spectrometer by

TABLE 5

SO₂ YIELDS FOR SULPHUR ISOTOPE ANALYSIS

Sample Number	Mineral	Sample Weight mg	Actual Yield	Theoretical Yield	T°C	% Yield
R-19-1	Pyrite	15.45	231	257.6	25.8	88.0
R-20-1	"	15.75	262	262.6	26.3	97.7
R-20-2	"	15.70	250	261.8	26.5	93.4
R-22-5	"	15.56	242	259.4	26.8	91.2
R-22-6	"	16.90	267	281.8	27.5	92.4
R-21-1	"	15.62	242	260.4	26.8	90.8
R-21-2	"	14.64	227	244.05	27.0	90.8
R-15-1	"	14.60	213	243.44	26.3	85.7
R-15-2	"	15.66	233	261.11	26.3	87.4
R-121-1	"	15.25	241	254.28	25.5	93.0
R-121-2	"	14.46	230	241.11	26.0	93.5
R-24-1	"	14.44	205	240.77	25.4	83.6
R-75-1	"	15.20	206	253.4	25.2	79.9
R-75-2	"	15.91	243	265.28	26.0	89.8
R-115-1	"	14.66	220	244.4	25.9	88.2

TABLE 5 (cont'd)

Sample Number	Mineral	Sample Weight mg	Actual Yield	Theoretical Yield	T°C	% Yield
R-116-1	Pyrite	14.52	212	242.1	26.3	85.7
R-116-2	"	14.69	220	244.9	26.0	88.0
R-118-1	"	14.41	212	240.27	26.2	86.4
R-118-2	"	14.23	220	237.27	25.4	91.0
R-120-1	"	14.06	214	234.44	25.7	89.5
R-120-2	"	14.18	210	236.44	25.5	87.2
R-114-1	"	14.55	217	242.61	25.5	87.8
R-119-1	"	14.52	220	242.11	25.8	89.1
R-119-2	"	14.49	215	241.61	26.7	87.0
R-19-1	Chalcopyrite	22.2	233.5	242.04	27.4	94.1
R-19-2	"	23.13	239	252.07	27.0	92.6
R-75-1	"	22.18	240	241.72	27.6	97.0
R-75-2	"	22.67	240	247.06	27.1	94.8
R-22-5	"	21.42	220	233.44	27.6	97.5
R-22-6	"	21.30	217	232.13	27.7	91.1

TABLE 5 (cont'd)

Sample Number	Mineral	Sample Weight mg	Actual Yield	Theoretical Yield	T°C	% Yield
R-21-1	Chalcopyrite	13.55	146	147.67	26.1	96.8
R-21-2	"	22.18	231	241.72	27.5	93.2
R-116-1	"	22.68	241	247.16	26.3	95.5
R-116-2	"	21.92	229	238.88	26.3	93.8
R-114-1	"	21.68	234	236.27	26.8	96.8
R-114-2	"	21.24	235	231.47	27.1	99.1
R-116-1	Pyrrhotite	22.36	200	254.35	25.9	77.1
R-116-2	"	22.13	214	251.73	26.5	83.2
R-22-1	"	22.65	255	257.6	26.5	96.8
R-22-2	"	22.20	230	252.5	26.5	89.1
R-119-1	"	22.10	212	251.4	26.1	82.6
R-119-2	"	22.90	244	260.49	21.9	93.1
R-120-1	"	22.29	220	253.5	29.0	84.2
R-120-2	"	22.59	233	256.9	29.5	87.8
R-114-1	"	22.87	247	260.15	20.7	94.7
R-114-2	"	22.47	251	255.6	20.9	97.9
R-75-1	"	21.73	245	247.18	20.5	98.9

TABLE 5 (cont'd)

Sample Number	Mineral	Sample Weight mg	Actual Yield	Theoretical Yield	T°C	% Yield
R-15-1	Pyrrhotite	20.05	215	228.07	21.75	93.7
R-121-1	"	21.72	242	247.06	22.3	97.2
R-21-1	"	21.11	237	240.1	22.2	97.9
R-20-1	"	21.77	246	247.6	21.5	98.8
R-118-1	"	21.27	230	241.9	19.4	94.5
R-119-1	Sphalerite	24.33	232	254.49	25.9	89.4
R-119-2	"	24.09	248	251.98	26.6	96.3
R-20-1	"	23.81	250	249.05	27.5	97.8
R-20-2	"	23.72	245	248.11	27.2	97.6
R-121-1	"	23.67	237.5	247.59	27.3	93.6
R-121-2	"	22.46	228	234.93	26.3	95.0
R-15-1	"	23.33	237.5	244.03	27.0	95.1
R-15-2	"	23.19	234	242.57	26.0	94.5
R-120-1	"	23.36	239	244.3	26.5	95.7
R-120-2	"	23.73	243	248.2	27.0	95.6
R-118-1	"	23.46	253	245.4	27.0	100.7
R-118-2	"	23.97	254	247.6	27.0	100.2

alternately introducing a standard sample and simultaneously collecting mass 64 and mass 66. The laboratory standard or line standard was calibrated against various SO_2 artificial standards with well-known δS^{34} values (i.e. Cañon Diablo troilite sulphur has a ratio of $\text{S}^{32}/\text{S}^{34} = 22.21$ per mil or $\delta \text{S}^{34} = 0$ per mil). Samples enriched in S^{34} are isotopically heavy relative to the standard and have positive per mil values; negative per mil values indicate depletion of S^{34} relative to the standard.

The calibration was conducted in 1974 and Table 6 lists standards of known isotopic composition which were analyzed to determine a correction formula for the obtained results (by S. Burnie, Say-Lee Kuo, R. Haverslew).

The correction formula used is:

$$\delta \text{S}_{\text{C.D.T.-x}}^{34} (\text{‰}) = \delta \text{S}_{\text{L.S.-x}}^{34} (\text{‰}) \times 1.158 + 4.5$$

where $\delta \text{S}_{\text{C.D.T.-x}}^{34}$ = δS^{34} of unknown against δS^{34} of Cañon Diablo Troilite
 $\delta \text{S}_{\text{L.S.-x}}^{34}$ = δS^{34} of unknown against δS^{34} of Line Standard.

Results

The results of the isotopic analyses are represented using the following expression:

TABLE 6

CALIBRATION OF SO₂ LINE STANDARD (1974)

Standards	$\delta^{34}\text{S}$ Line Standard	$\delta^{34}\text{S}$ Cañon Diablo Troilite
NBS #120 (Native Sulphur)	- 2.63	+ 1.45
NBS #200 (Galena, Ivigtut)	- 3.3	+ 0.68
Peace River Troilite	- 3.2	+ 0.79
PbS Line Standard	- 8.83	- 5.73
BaSO ₄ ("merck")	- 1.46	+ 2.8
Pine Creek NW (Sour Gas)	+ 16.4	+ 23.49
McMaster "Ag ₂ S"	- 8.5	- 5.34

* Calibrated by S. Burnie, S.L. Kuo and R. Haverslew, 1974

$$\delta S^{34} \text{ ‰} = \frac{(S^{34}/S^{32})_{\text{sample}} - (S^{34}/S^{32})_{\text{standard}}}{(S^{34}/S^{32})_{\text{standard}}} \times 1000$$

In Table 7 the description and location of samples analyzed are listed, the analytical results from the study are listed in Table 8 and $\Delta \delta S^{34}$ in co-existing sulphides are listed in Table 9. Figures 12 and 13 are cross sections illustrating sample locations and the variance in sulphur isotope ratios with respect to horizontal and vertical dispersion in the ore body. Frequency distribution of the δS^{34} values obtained in the study are illustrated using a histogram in Figure 14.

B. Fe-Content in Sphalerite

Introduction

Since sphalerite is one of the most important ore minerals of the Ruttan Lake deposit and because it is one of the more refractory sulphides and can display a wide range of Fe content as a function of conditions of formation, it may be used to decipher environments of sulphide deposition and deformation. Kullerud (1953), Barton and Toulmin (1966), Clark (1966), Boorman (1967), Scott and Barnes (1971), Boorman et al. (1971) and Scott (1974) have concluded that the iron content of sphalerite co-existing with pyrite and pyrrhotite is very sensitive to variations

TABLE 7

DESCRIPTION AND LOCATION OF SAMPLES USED FOR SULPHUR ISOTOPE ANALYSIS

Sample Number	Description	Grid Location and Depth
R-15-1	Massive sphalerite with pyrite, pyrrhotite	502 + 00 E 300 ft.
R-15-2	Massive sphalerite with pyrite, pyrrhotite	502 + 00 E 500 ft.
R-19-1	Massive chalcopyrite, pyrite, pyrrhotite and sphalerite	498 + 00 E 900 ft.
R-20-1	Massive pyrite, sphalerite and pyrrhotite	498 + 00 E 200 ft.
R-20-2	Massive pyrite, sphalerite and pyrrhotite	498 + 00 E 500 ft.
R-21-1	Massive pyrite with chalcopyrite, pyrrhotite	498 + 00 E 700 ft.
R-21-2	Massive pyrite with chalcopyrite, pyrrhotite	498 + 00 E 800 ft.
R-22-5	Massive pyrite, chalcopyrite and pyrrhotite	498 + 00 E 550 ft.

TABLE 7 (cont'd)

Sample Number	Description	Grid Location and Depth
R-22-6	Massive pyrite, chalcopyrite and pyrrhotite	499 + 00 E 400 ft.
R-24-1	Disseminated pyrite in chlorite-biotite schist	514 + 00 E 1000 ft.
R-75-1	Massive pyrite, chalcopyrite and pyrrhotite	509 + 00 E 200 ft.
R-75-2	Massive pyrite, chalcopyrite and pyrrhotite	509 + 00 E 400 ft.
R-114-1	Massive pyrite, pyrrhotite and chalcopyrite	510 + 00 E 100 ft.
R-115-1	Massive pyrite, pyrrhotite and chalcopyrite (minor)	490 + 00 E 200 ft.
R-116-1	Massive pyrite, pyrrhotite and chalcopyrite	511 + 00 E 100 ft.
R-116-2	Massive pyrite, pyrrhotite and chalcopyrite	511 + 00 E 200 ft.
R-118-1	Massive sphalerite and pyrite with minor pyrrhotite	504 + 00 E 100 ft.
R-118-2	Massive sphalerite, pyrite and pyrrhotite	504 + 00 E 200 ft.

TABLE 7 (cont'd)

Sample Number	Description	Grid Location and Depth
R-119-1	Massive sphalerite, pyrite	506 + 00 E 200 ft.
R-119-2	Massive sphalerite, pyrite and pyrrhotite	506 + 00 E 400 ft.
R-120-1	Massive sphalerite, pyrite, pyrrhotite	512 + 00 E 200 ft.
R-120-2	Massive sphalerite, pyrite, pyrrhotite	512 + 00 E 500 ft.
R-121-1	Massive sphalerite, pyrite, and pyrrhotite	516 + 00 E 150 ft.
R-121-2	Massive sphalerite, pyrite, and pyrrhotite	516 + 00 E 400 ft.

TABLE 8

RESULTS OF SULPHUR ISOTOPE ANALYSIS

Sample Number	Isotopic Composition in $\delta^{34}\text{S}$ (per mil)			
	Pyrite	Pyrrhotite	Chalcopyrite	Sphalerite
R-15-1	1.68	1.15		1.06
R-15-2	1.62	0.57		1.49
R-19-1			0.76	
R-20-1	2.11	0.64		1.15
R-20-2	1.78	0.78		1.22
R-21-1	1.44	0.76	1.32	
R-21-2			1.62	
R-22-5	- .24	0.35	0.15	
R-22-6	.98	0.35	- .10	
R-24-1	1.04			
R-75-1	1.57	0.97	0.56	
R-75-2	0.99	0.70	0.70	
R-114-1	0.57	0.34	0.65	
R-115-1	0.84			
R-116-1	0.55	0.24	1.08	
R-116-2	0.37	0.24	0.79	
R-118-1	1.58	2.18		1.50
R-118-2	1.61	2.51		1.07

TABLE 8 (cont'd)

Sample Number	Isotopic Composition in $\delta^{34}\text{S}$ (per mil)			
	Pyrite	Pyrrhotite	Chalcopyrite	Sphalerite
R-119-1	1.64	2.73		1.12
R-119-2		2.73		
R-120-1	2.11	1.64		1.41
R-120-2	1.74	1.45		1.73
R-121-1	0.74	1.32		0.79
R-121-2	0.10	1.36		0.79

TABLE 9
 $\Delta \delta^{34}\text{S}$ IN CO-EXISTING SULPHIDES
 FROM RUTTAN LAKE

Sample Number	Mineral Pair	$\Delta \delta^{34}\text{S}$
R-15-1	pyrite - sphalerite	.62
R-15-2	" "	.13
R-20-1	" "	.96
R-20-2	" "	.56
R-118-1	" "	.08
R-118-2	" "	.54
R-119-1	" "	.52
R-120-1	" "	.70
R-120-2	" "	.01
R-121-1	" "	.05
R-121-2	" "	.69
R-21-1	pyrite - chalcopyrite	.12
R-22-5	" "	.39
R-22-6	" "	1.08
R-75-1	" "	1.01
R-75-2	" "	.29
R-114-1	" "	.08
R-116-1	" "	.53
R-116-2	" "	.42
R-15-1	pyrite - pyrrhotite	.53
R-15-2	" "	1.05
R-20-1	" "	1.47
R-20-2	" "	1.00
R-118-1	" "	.60
R-118-2	" "	.90
R-119-1	" "	1.09
R-120-1	" "	.47
R-120-2	" "	.29

TABLE 9 (cont'd)

Sample Number	Mineral Pair	$\Delta \delta^{34}\text{S}$
R-121-1	pyrite - pyrrhotite	.58
R-121-2	" "	1.26
R-21-1	" "	.68
R-22-5	" "	.59
R-22-6	" "	.63
R-75-1	" "	.60
R-75-2	" "	.29
R-114-1	" "	.23
R-116-1	" "	.31
R-116-2	" "	.13

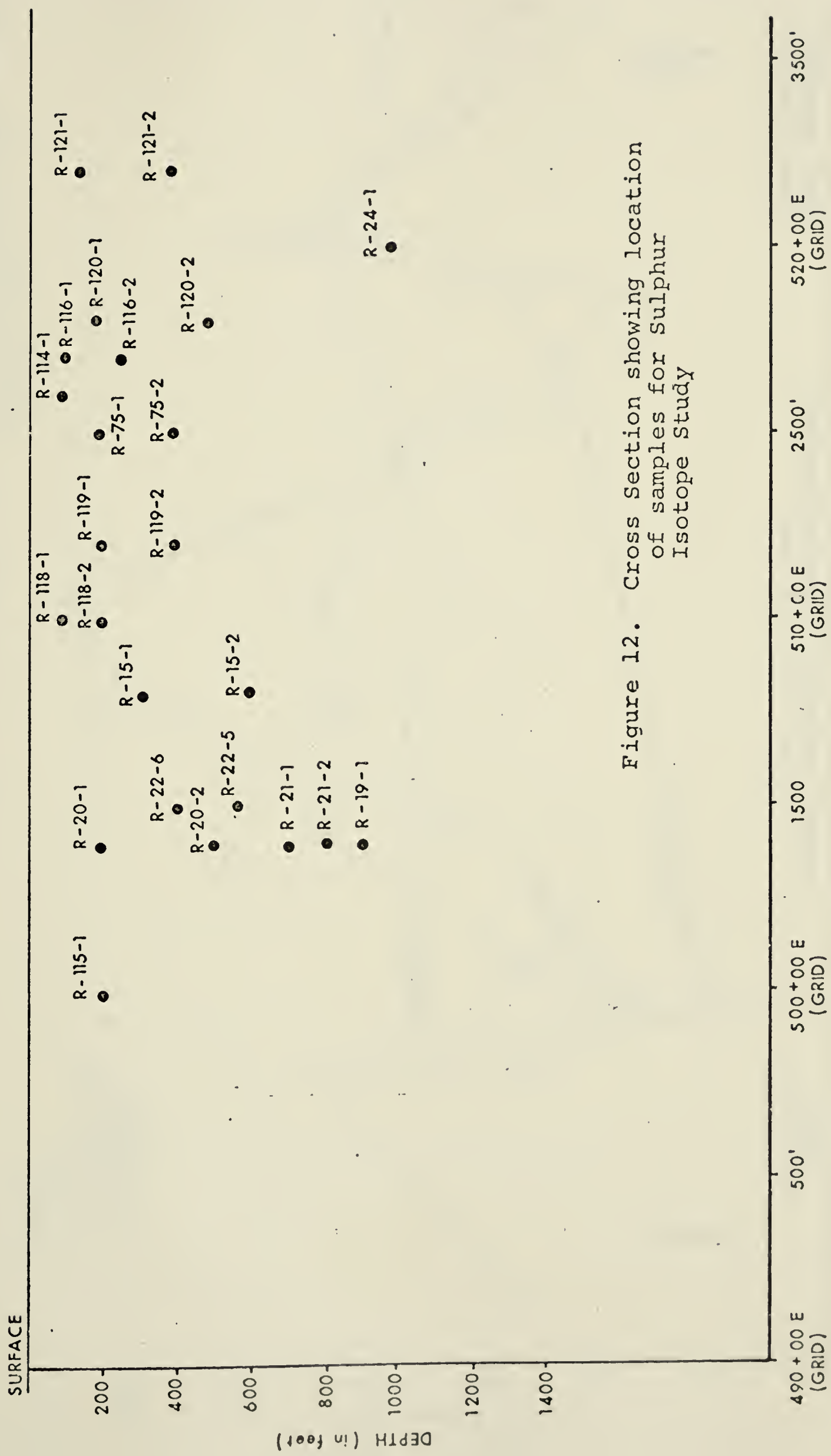
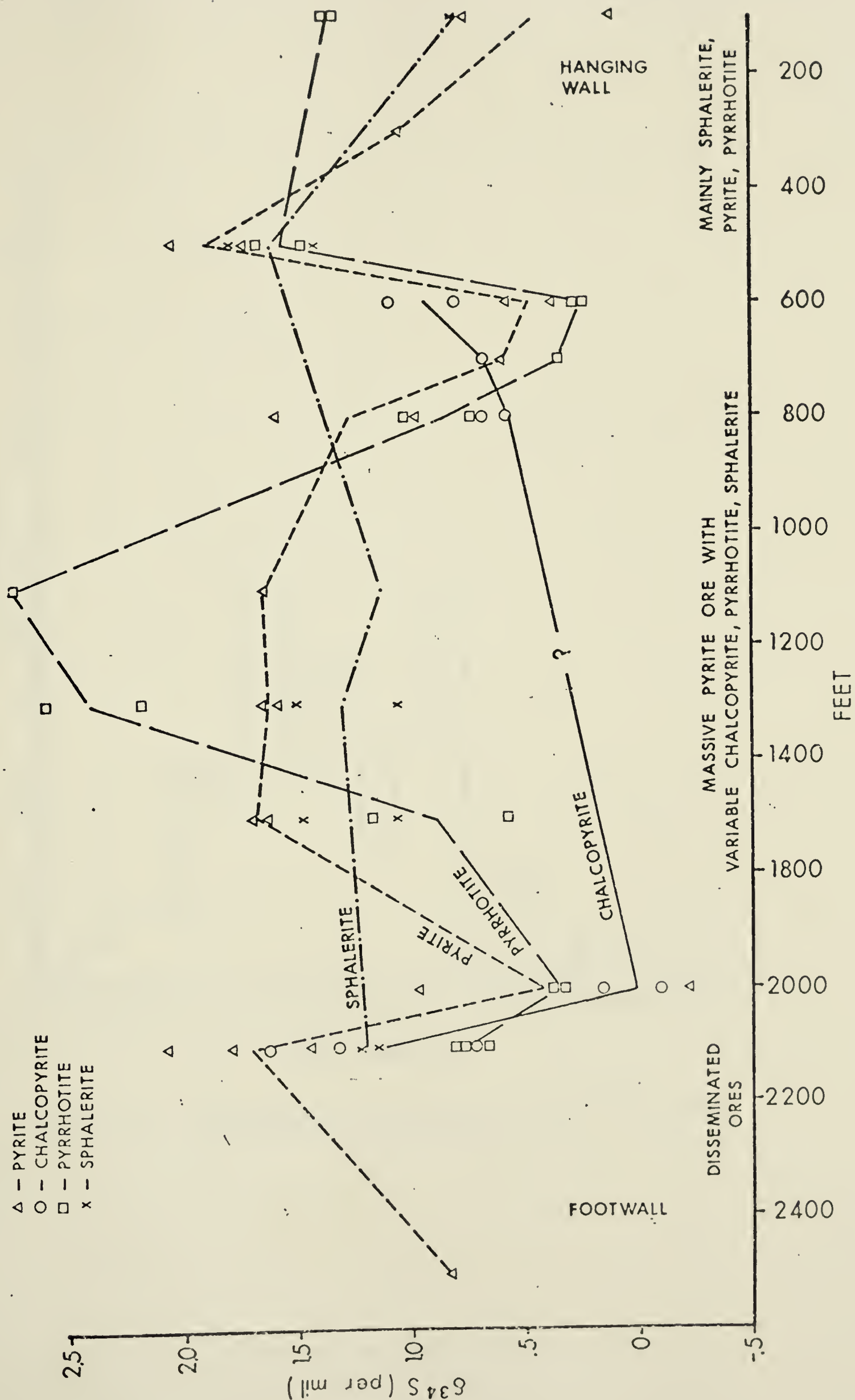


Figure 12. Cross Section showing location of samples for Sulphur Isotope Study

Figure 13. Distribution of Isotope Results between Footwall and Hanging Wall

Symbols:

- △ - PYRITE
- - CHALCOPYRITE
- - PYRRHOTITE
- x - SPHALERITE



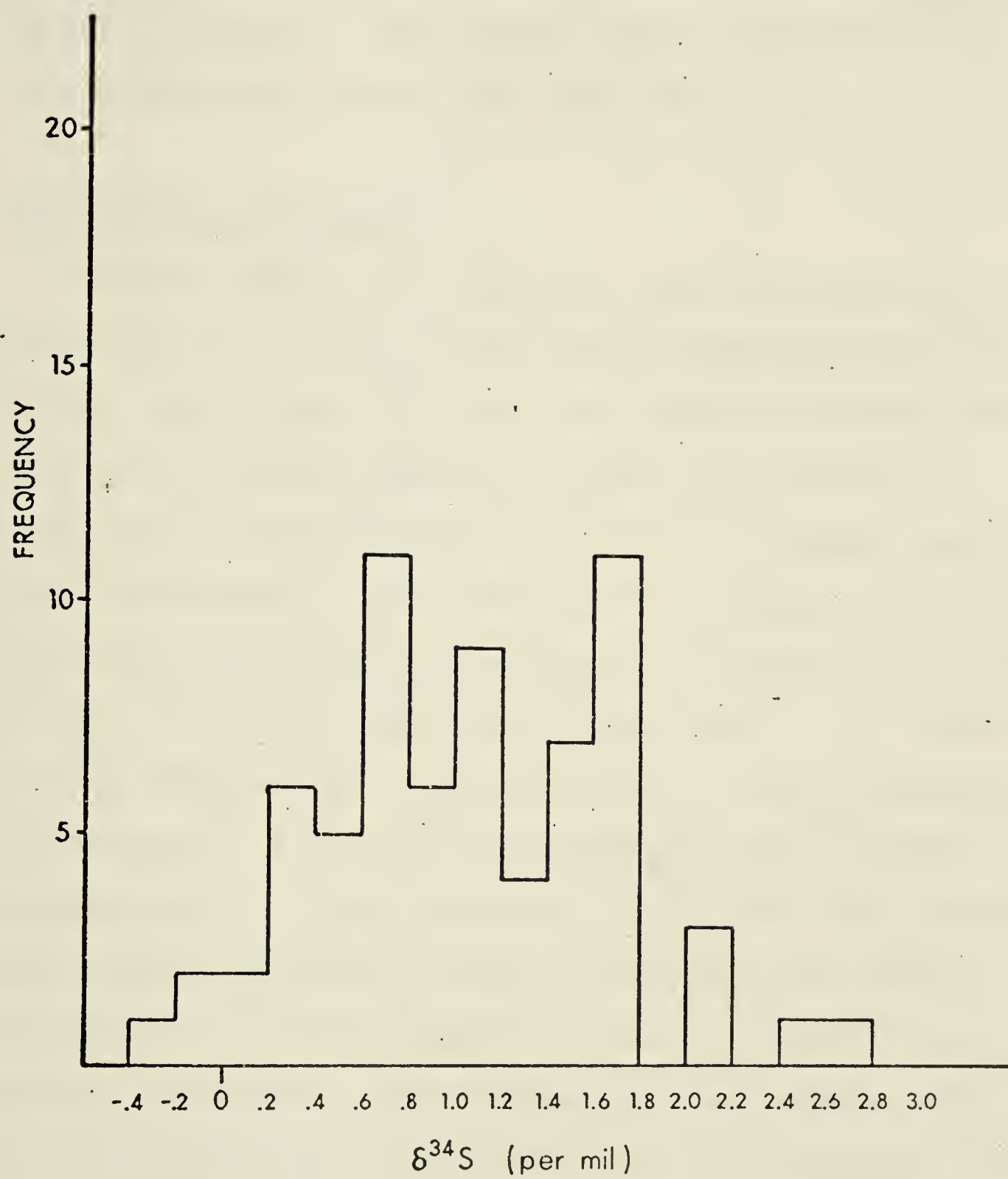


Figure 14. Frequency Distribution of $\delta^{34}\text{S}$ Values

in pressure and temperature of ore formation and the fugacity of sulphur. The method used in determining the iron content was on an A.R.L. EMX microprobe.

Experimental Procedure

Twenty samples were selected which represent both a horizontal and vertical distribution throughout the ore deposit (see Figure 15). All the samples analyzed contained co-existing sphalerite, pyrite and pyrrhotite. Specimens of the sulphides were mounted in epoxy, polished and carbon-coated. Both wavelength and energy dispersive techniques were used on the microprobe and the discrepancy between the two was found to be negligible. A 15 kV operating voltage and a focussed beam were used throughout the analysis. A list of the standards used and their compositions are found in Table 10. Fe and S were determined against standard 1 and Zn was determined against standard 3. Cd was determined against standard 2 and Mn against standard 4. Full corrections for atomic number (Z), absorption (A) and characteristic fluorescence effects (F) were made using computer programs EMPADOR VII (by Rucklidge and Gasparri, 1969) and EDATA (by D.G.W. Smith, personal communication).

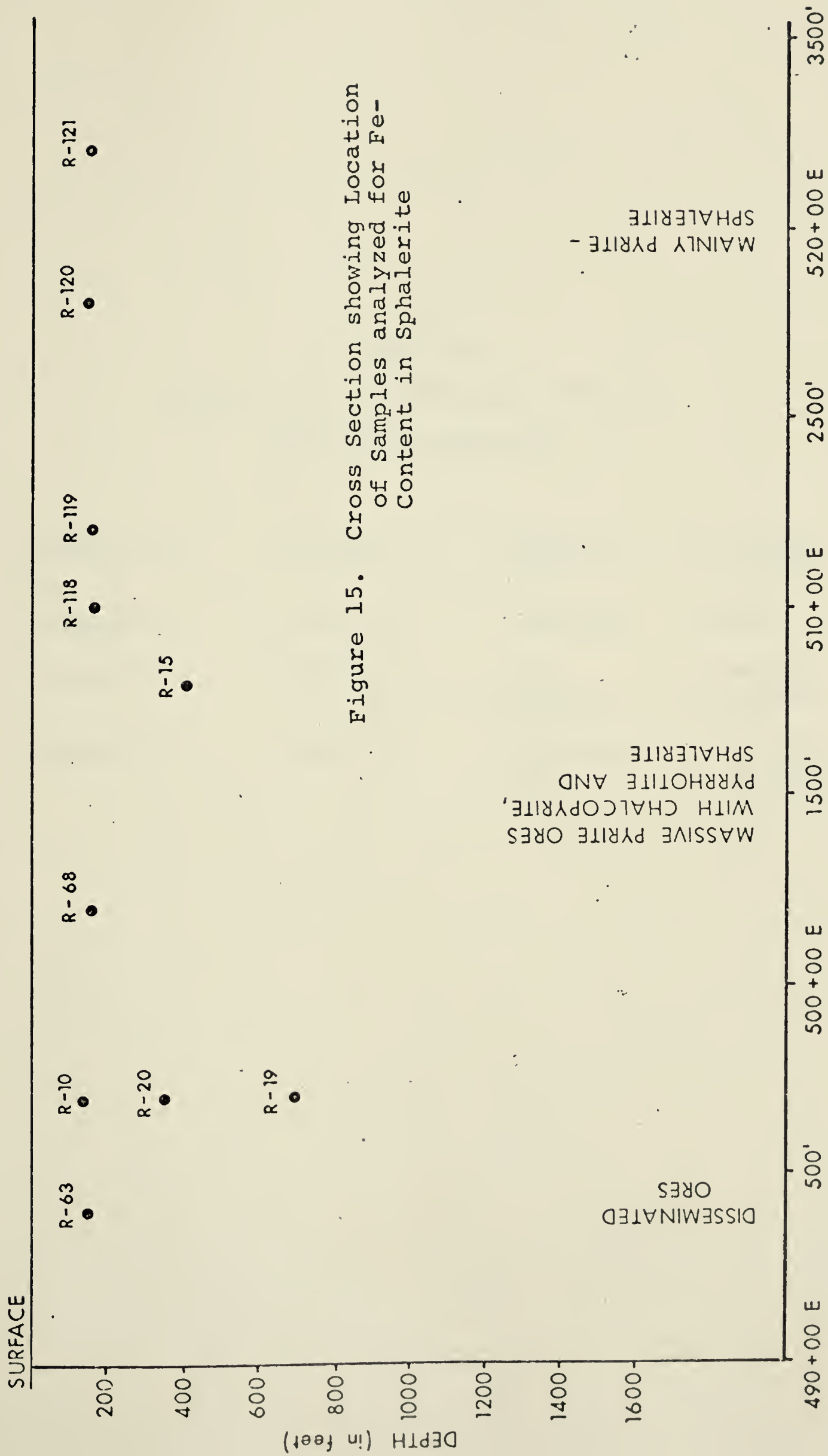


Figure 15. Cross Section showing Location of Samples analyzed for Fe-Content in Sphalerite

TABLE 10
COMPOSITION OF STANDARDS USED IN
MICROPROBE ANALYSIS

Standard 1	EPS/22-1	Sulphur	-	38.25%
		Fe	-	61.75%
Standard 2	EPS/7-8	Cadmium	-	100%
Standard 3	EPS/22-6	Zinc	-	66.8%
		Sulphur	-	32.60%
Standard 4	EPS/7-10	Manganese	-	99.879%
		Fe	-	0.109%
		Al	-	0.012%

Results

The initial results for individual grains (after ZAF corrections), together with the calculated metal:non-metal ratios appear in Table 11. Mole percent of FeS was calculated from the observed weight percent of Fe of each grain analyzed. Both analyzed and calibrated values are shown in Table 12. Figure 16 shows a statistical distribution plotted as a histogram of FeS mole percent. The compositional spread for Fe content in sphalerites co-existing with pyrite and pyrrhotite vary from 7.13 to 12.64 mole percent FeS with a mean mole percent of 10.69.

C. Pb Isotopes

Introduction

Ore leads were used for model lead dating to determine the age and genesis of Ruttan Lake mineralization. Model lead interpretations are based on the ratios of the lead isotopes Pb^{204} , Pb^{206} , Pb^{207} and Pb^{208} in common lead. Radioactive decay of ^{238}U and ^{235}U to the radiogenic isotopes ^{206}Pb and ^{207}Pb , respectively and ^{232}Th to the radiogenic isotope ^{208}Pb produce variations in the lead isotope composition as compared to an original or "primeval" lead, which existed at the time of formation of the earth. ^{204}Pb has no long-lived radioactive parent as it is non-radiogenic and hence its absolute abundance in the earth

TABLE 11

RESULTS OF MICROPROBE STUDY SHOWING COMPOSITION OF SPHALERITE IN
WEIGHT PERCENT AND THE METAL:NON-METAL RATIO

Sample #	Element	Average Wt %	Atomic Wt %	Atomic Amount	Metal:Non-Metal Ratio (Metal:Non-Metal)
19-3-1	Fe	6.89	55.85	.12	
	Zn	59.15	65.37	.90	1.02:1.05
	S	33.96	32.06	1.05	.97
	Mn	NA			
	Cd	ND			
19-3-2	Fe	7.37	55.85	.13	
	Zn	58.35	65.37	.89	1.02:1.07
	S	34.29	32.06	1.07	.95
	Mn	NA			
	Cd	ND			
19-3-3	Fe	7.03	55.85	.13	
	Zn	59.26	65.37	.91	1.04:1.05
	S	33.71	32.06	1.05	.99
	Mn	NA			
	Cd	ND			

TABLE 11(cont'd)

Sample #	Element	Average Wt %	Atomic Wt %	Atomic Amount	Metal:Non-Metal Ratio (Metal:Non-Metal)
19-3-4	Fe	7.10	55.85	.13	
	Zn	58.44	65.37	.89	1.02:1.07
	S	34.46	32.06	1.07	.95
	Mn	NA			
	Cd	ND			
19-3-5	Fe	8.29	55.85	.15	
	Zn	58.33	65.37	.89	1.04:1.04
	S	33.38	32.06	1.04	1.0
	Mn	NA			
	Cd	ND			
19-3-6	Fe	7.81	55.85	.14	
	Zn	57.69	65.37	.88	1.02:1.08
	S	34.50	32.06	1.08	.94
	Mn	NA			
	Cd	ND			

TABLE 11 (cont'd)

Sample #	Element	Average Wt %	Atomic Wt %	Atomic Amount	Metal:Non-Metal Ratio (Metal:Non-Metal)
R-20-1	Fe	8.50	55.85	.15	
	Zn	57.48	65.37	.88	1.03:1.06
	S	34.01	32.06	1.06	.97
	Mn	NA			
	Cd	ND			
R-20-2	Fe	8.78	55.85	.16	
	Zn	57.48	65.37	.88	1.04:1.05
	S	33.75	32.06	1.05	.99
	Mn	NA			
	Cd	ND			
R-20-3	Fe	8.77	55.85	.16	
	Zn	57.21	65.37	.86	1.02:1.06
	S	34.02	32.06	1.06	.96
	Mn	NA			
	Cd	ND			

TABLE 11 (cont'd)

Sample #	Element	Average Wt %	Atomic Wt %	Atomic Amount	Metal:Non-Metal Ratio (Metal:Non-Metal)
R-20-4	Fe	8.42	55.85	.15	
	Zn	57.48	65.37	.88	1.03:1.06
	S	34.10	32.06	1.06	.97
	Mn	NA			
	Cd	ND			
R-10-72	Fe	5.75	55.85	.10	
	Zn	60.86	65.37	.93	1.03:1.02
	S	32.80	32.06	1.02	1.01
	Mn	.13	54.94	.002	
		<u>99.54</u>			
R-15-72	Fe	8.65	55.85	.15	
	Zn	57.95	65.37	.89	1.04:1.04
	S	33.25	32.06	1.04	1.0
	Mn	0.00	54.94	--	
		<u>99.85</u>			

TABLE 11 (cont'd)

Sample #	Element	Average Wt %	Atomic Wt %	Atomic Amount	Metal:Non-Metal Ratio (Metal:Non-Metal)
R-19-2	Fe	7.36	55.85	.13	
	Zn	58.47	65.37	.89	1.02:1.03
	S	33.06	32.06	1.03	.99
	Mn	.12	54.94	.002	
		<u>99.01</u>			
R-20-5	Fe	8.66	55.85	.16	
	Zn	58.38	65.37	.89	1.05:1.05
	S	33.59	32.06	1.05	1.0
	Mn	.04	54.94	.0007	
	Co	.04	58.93	.0006	
		<u>100.71</u>			
R-63-73	Fe	5.01	55.85	.09	
	Zn	62.27	65.37	.95	1.04:1.04
	S	33.33	32.06	1.04	1.0
	Mn	.03	54.94	.0005	
	Co	.04	58.93	.0006	
		<u>100.68</u>			

TABLE 11 (cont'd)

Sample #	Element	Average Wt %	Atomic Wt %	Atomic Amount	Metal:Non-Metal Ratio (Metal:Non-Metal)
R-68-73	Fe	6.37	55.85	.11	
	Zn	60.43	65.37	.92	1.03:1.03
	S	33.11	32.06	1.03	1.0
	Mn	.11	54.94	.002	
	Co	.05	58.93	.0008	
		<u>100.07</u>			
R-118-73	Fe	6.92	55.85	.12	
	Zn	59.63	65.37	.91	1.03:1.03
	S	33.15	32.06	1.03	1.0
	Mn	.20	54.94	.004	
		<u>99.90</u>			
R-119-73	Fe	7.63	55.85	.14	
	Zn	58.90	65.37	.90	1.04:1.03
	S	33.04	32.06	1.03	1.01
	Mn	.18	54.94	.003	
		<u>99.65</u>			

TABLE 11 (cont'd)

Sample #	Element	Average Wt %	Atomic Wt %	Atomic Amount	Metal:Non-Metal Ratio (Metal:Non-Metal)
R-120-73	Fe	6.19	55.85	.11	
	Zn	60.17	65.37	.92	1.03:1.03
	S	33.09	32.06	1.03	1.0
	Mn	.23	54.94	.004	
	Co	.04	58.93	.0006	
		<u>99.72</u>			
R-121-73	Fe	7.29	55.85	.13	
	Zn	58.86	65.37	.90	1.03:1.03
	S	33.00	32.06	1.03	1.0
	Mn	.17	54.94	.003	
	Co	.04	58.93	.0007	
		<u>99.36</u>			

Abbreviations: NA - not analyzed
 ND - not detected

TABLE 12

CALIBRATED FeS MOLE % FROM MICROPROBE RESULTS

Sample #	Av Wt % Fe	Av Wt % Zn	Av Wt % S	Fe S Wt %	Zn S Wt %	Fe S mole %
19-3-1	6.89	59.15	33.96	10.84	89.2	9.88
19-3-2	7.37	58.35	34.29	11.60	88.4	10.59
19-3-3	7.03	59.26	33.71	11.07	88.93	10.10
19-3-4	7.10	58.44	34.46	11.18	88.82	10.2
19-3-5	8.29	58.33	33.38	13.05	86.95	11.93
19-3-6	7.81	57.69	34.50	12.29	87.71	11.22
20-1-1	8.50	57.48	34.01	13.38	86.62	12.23
20-1-2	8.78	57.48	33.75	13.82	86.18	12.64
20-1-3	8.77	57.21	34.02	13.80	86.2	12.62
20-1-4	8.42	57.48	34.10	13.25	86.25	12.17
R-120-73	6.21	60.34	33.18	9.77	90.23	8.90
R-10-72	5.78	61.14	32.95	9.10	90.90	8.28
R-121-73	7.34	59.24	33.21	11.55	88.45	10.37
R-15-72	8.66	58.04	33.29	13.63	86.37	12.46
R-19-72	7.43	59.05	33.39	11.70	88.3	10.68
R-20-72	8.60	57.97	33.35	13.54	86.46	12.38
R-63-73	4.98	61.85	33.10	7.84	92.16	7.13
R-68-73	6.37	60.39	33.09	10.03	89.97	9.14
R-118-73	6.93	59.69	33.18	10.91	89.09	9.95
R-119-73	7.86	59.11	33.16	12.06	87.94	11.01

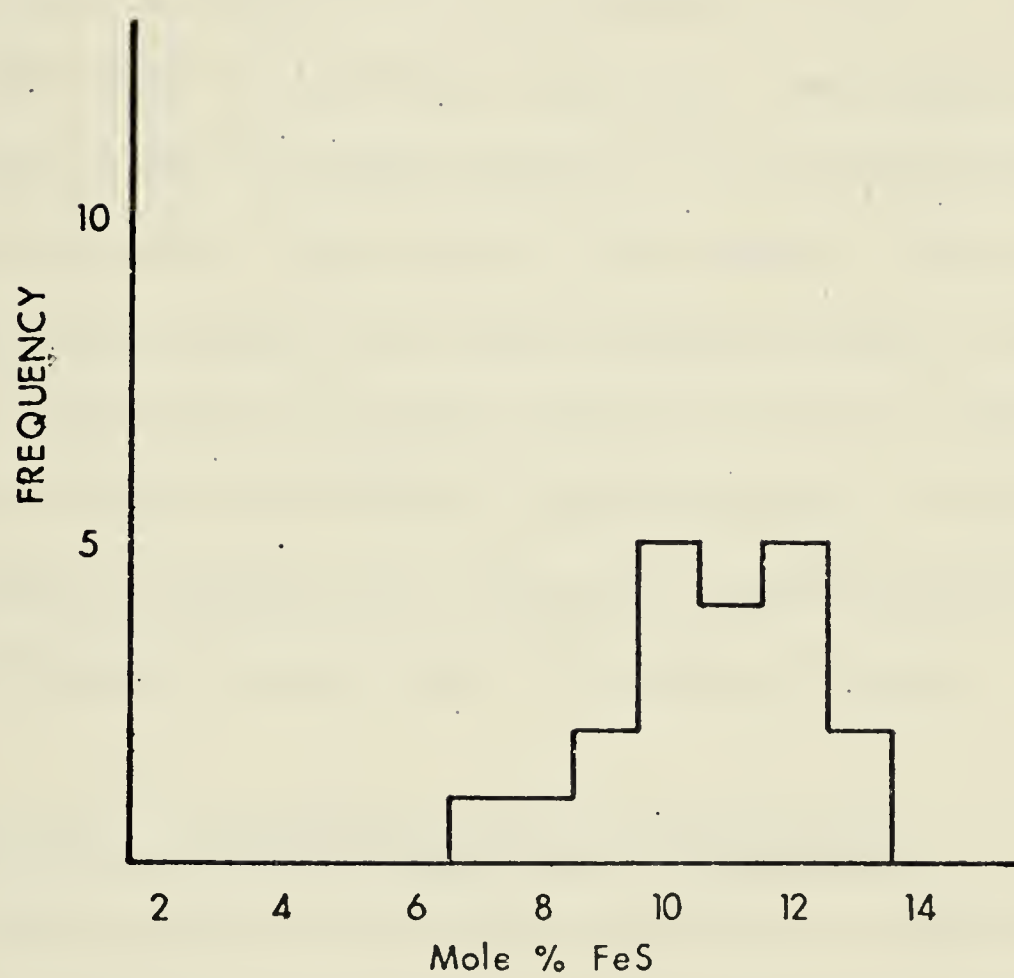


Figure 16. Frequency Distribution of FeS
Mole % from Fe-Content
in Sphalerite

has not changed since primeval times. Reasonably assuming that the earth began with some primeval lead, then the lead isotope values of this primeval lead are adopted from the least radiogenic leads found - i.e. the values in the troilite phase of meteorites (Tatsumoto, 1973). Common lead then consists of primeval lead plus radiogenic lead consisting of the isotopes generated by uranium and thorium decay since the formation of the Earth. The radiogenic atoms become mixed with the primeval atoms of the original lead. Since the isotopic ratios in common lead have not changed since the time of mineralization, then the obtained Pb ratios represent the isotopic composition of lead in the source region at the time of mineralization.

Theoretical Considerations and Ore Genesis

The genesis of most ore deposits is not easily understood, and age relationships among sulphide minerals and between them and their host rocks are often difficult problems, of economic as well as scientific interest. Ages calculated for sulphide minerals depend on the assumption of some particular model for the genesis of lead ores in general.

Lead isotope ratios have been applied to the problems of ore genesis and it is generally accepted that they have evolved through a sequence of different stages.

(i) Single-stage leads: a number of ores and igneous rocks have leads that evolved under conditions where the only changes in the value of the parent/daughter ratio are due to radioactive decay. Stanton and Russel (1959) demonstrated how single-stage model leads could be used for interpreting deposits referred to as "submarine exhalative" associated with island arcs. These produce a single-stage growth curve. The conformity with and small departures from the apparent single-stage growth curve could be explained by the perfect and imperfect degree of mixing (multiple reworking of sediments - Brown, 1965 and Armstrong, 1968) or leaching of lead from large volumes of rock of several isotopically heterogeneous source materials at differing geological periods (Doe et al., 1966). Hence 'single-stage leads' only approximate an evolution under single-stage conditions. It would be surprising if single-stage conditions could persist unaltered by geological events throughout the 4.5 b.yrs. of geological history.

(ii) Two-stage or anomalous leads: it has become apparent that since the accumulation of hundreds of lead isotope analysis, that they can yield valuable information about the particular histories of ore deposits. Early workers in the field who considered them in detail, included Eberhardt, Geiss and Houtermans (1955), Cahen et al. (1958) and Russel

and Farquhar (1957). Anomalous leads can be explained by quite simple models and sometimes yield more precise information about the genesis of a deposit. The simplest process to produce anomalous leads is a two-stage evolution in which lead evolved in an effectively closed system from lead of troilitic composition 4.57 billion years ago until some later event at time t and that caused the $^{238}\text{U}/^{204}\text{Pb}$ ratio to vary. Anomalous leads may be the result of the mixing of two ordinary leads or a mixture of ordinary lead with lead produced in one or more different U-Th-Pb environments (Russel and Farquhar, 1960). Two-stage or more complex systems can best be recognized by analyzing several samples from a deposit and graphing them on a $^{207}\text{Pb}/^{204}\text{Pb}$ versus $^{206}\text{Pb}/^{204}\text{Pb}$ plot.

(iii) Multi-stage systems: Many igneous rocks and ore deposits have undergone more than two stages of lead isotopic evolution. Although interpretation of the three-stage systems is extremely difficult, some three-stage systems result in parallel linear isochrons which can be interpreted by making small changes in the parameters of the single- and two-stage systems. Small variations in $^{238}\text{U}/^{204}\text{Pb}$ values can explain many apparent three-stage lead systems but it is often difficult to incorporate available geologic factors. Theoretical consideration of simplified multi-stage models has been made by Kanasewich (1962), Kanasewich and Slawson (1964) and Ulrych (1964) on anomalous ore leads (mainly from Ivigtut, Greenland)

and they conclude that evolution of the leads in many ores did occur under conditions involving more than two stages.

Use of these models must be based on assumptions regarding the parameters U, V and W where

$$U = {}^{238}\text{U}/{}^{204}\text{Pb}$$

$$V = {}^{235}\text{U}/{}^{204}\text{Pb}$$

$$W = {}^{232}\text{Th}/{}^{204}\text{Pb}$$

It is also necessary to have precise knowledge of the geophysical constants - initial time t_0 and a_0 , b_0 and c_0 to accurately use model lead dating. Several revisions for a_0 , b_0 , c_0 and t_0 have been made and the ones used to construct the growth curve were based on work done by Tatsumoto (1973) and Jaffey et al. (1971) and $\mu = 8.7$ by Russel et al. (1967).

Experimental Procedures

A total of eight lead isotope determinations were made from purified samples of chalcopyrite, pyrite and pyrrhotite. A detailed description of the extraction procedure of lead from sulphide minerals is found in Appendix B. The resulting Pb solution was carried through a careful dithizone extraction procedure to ensure a pure sample. The amount of Pb extracted from each sulphide sample varied from 2 μg to 50 μg ,

which was then loaded on silica gel on a Rhenium filament. All reagents used in the analytical work were purified and precautions were taken to prevent any contamination from any reagents or glassware used in the extraction procedure. All glassware used in the present work is cleaned in hot concentrated HNO_3 , rinsed in triple distilled "pure" water and then wrapped in parafilm. Only triple distilled water is used in the preparation of reagents for the extraction of Pb.

The Pb sample was loaded on a filament of pure rhenium, which had been outgassed at 3 amps for approximately 3 hours under vacuum. The outgassing removes any lead contamination on the surface of the filament. The sample is then loaded on the filament using the silica gel and phosphoric acid loading method as devised by Akishin et al. (1957) and Cameron et al. (1969) and modified by Tatsumoto (1973). For a detailed description of this loading procedure see Appendix C.

Analytical Methods and Instrumentation

The samples were run on a 12" radius, 90° sector, single filament, solid source mass spectrometer in the Department of Physics, University of Alberta. In a vacuum of 5×10^{-8} atm, the samples were ionized with a filament current of 1.65 to 2.25 amps at an operating voltage of 4.5 kV in order to obtain the best peak shape and steady emission. Pb emission started after the decay of potassium and varied at different filament currents from one run to another.

The mass spectrometer was put in the scanning mode and would graphically display the Pb peaks of 204, 206, 207 and 208. Ten to fifteen scans were made for each sample and the ratios for $^{206}\text{Pb}/^{204}\text{Pb}$, $^{207}\text{Pb}/^{204}\text{Pb}$ and $^{208}\text{Pb}/^{204}\text{Pb}$ of the ore leads were recorded on a magnetic tape. These were then processed by a computer program to calculate a set of mean ratios for each sample.

Accuracy of Results

Precautions taken to avoid contamination in the Pb preparation have been mentioned. Error due to instrumentation must also be considered. Isotopic fractionation is the most serious and seemed to vary depending upon the length of time a sample is run and the filament current used. Through experimentation it was found that the most stable emission and best peak shapes occurred when the sample was in a slightly decaying mode. The most steady emission was found using a filament current between 1.85 amps and 2.0 amps.

The Broken Hill Pb-standard was used as a test for the reliability of the mass spectrometer. The obtained results were compared with previous work (see Table 13).

Results

The results of the study of lead isotope compositions in the Ruttan Lake ores are presented as ratios of a radiogenic isotope to the non-radiogenic isotope whose abundance does not change with time - $^{206}\text{Pb}/^{204}\text{Pb}$, $^{207}\text{Pb}/^{204}\text{Pb}$ and $^{208}\text{Pb}/^{204}\text{Pb}$. Table 14 are the parameters used to obtain the best growth curve in which to plot the analytical results. The parameter constants used were $\mu = 8.70$, $a_o = 9.307$ and $b_o = 10.294$ and $\mu = 8.79$, $W = 38.33$.

Figure 17 shows the location of samples analyzed in the Pb-isotope study. The measured results of the Pb isotopic abundance and mean standard deviations for all samples analyzed are listed in Table 15.

TABLE 13

INTERLABORATORY COMPARISON OF BROKEN HILL GALENA STANDARD
USED IN Pb ISOTOPE STUDY

	$^{206}\text{Pb}/^{204}\text{Pb}$	$^{207}\text{Pb}/^{204}\text{Pb}$	$^{208}\text{Pb}/^{204}\text{Pb}$
Average of Cooper et al., (1969) and Stacey et al., (1969)	16.004	15.394	35.668
Average of Kuo and Folinsbee (1974)	15.941	15.326	35.443
Haverslew (1975)	15.9923	15.2805	35.5734

TABLE 14

PB GROWTH CURVE PARAMETERS
 (FROM DR. BAADSGAARD AND S.L. KUO, PERSONAL COMMUNICATION USING
 APL PROGRAMS DATE 76 AND DATE 86)

Million Yrs.	$a_O = 9.307$ $b_O = 10.294$ $\mu = U^{238}/Pb^{204} = 8.7$ $206_{Pb}/204_{Pb}$ $207_{Pb}/204_{Pb}$	$a_O = 9.346$ $b_O = 10.218$ $c_O = 29.476$ $\mu = 8.79$ $W = Th^{232}/Pb^{204} = 38.33$ $206_{Pb}/204_{Pb}$ $208_{Pb}/204_{Pb}$
0		18.32 38.42
500	17.55 15.82	17.62 37.56
1000	16.80 15.75	16.86 36.68
1500	15.98 15.65	16.04 35.78
2000	15.09 15.47	15.16 34.85
2500	14.13 15.18	14.20 33.90
3000	13.10 14.71	13.17 32.93
3500	11.98 13.94	12.06 31.93
4000	10.64 12.46	10.86 30.91
4500	9.46 10.59	9.56 29.82

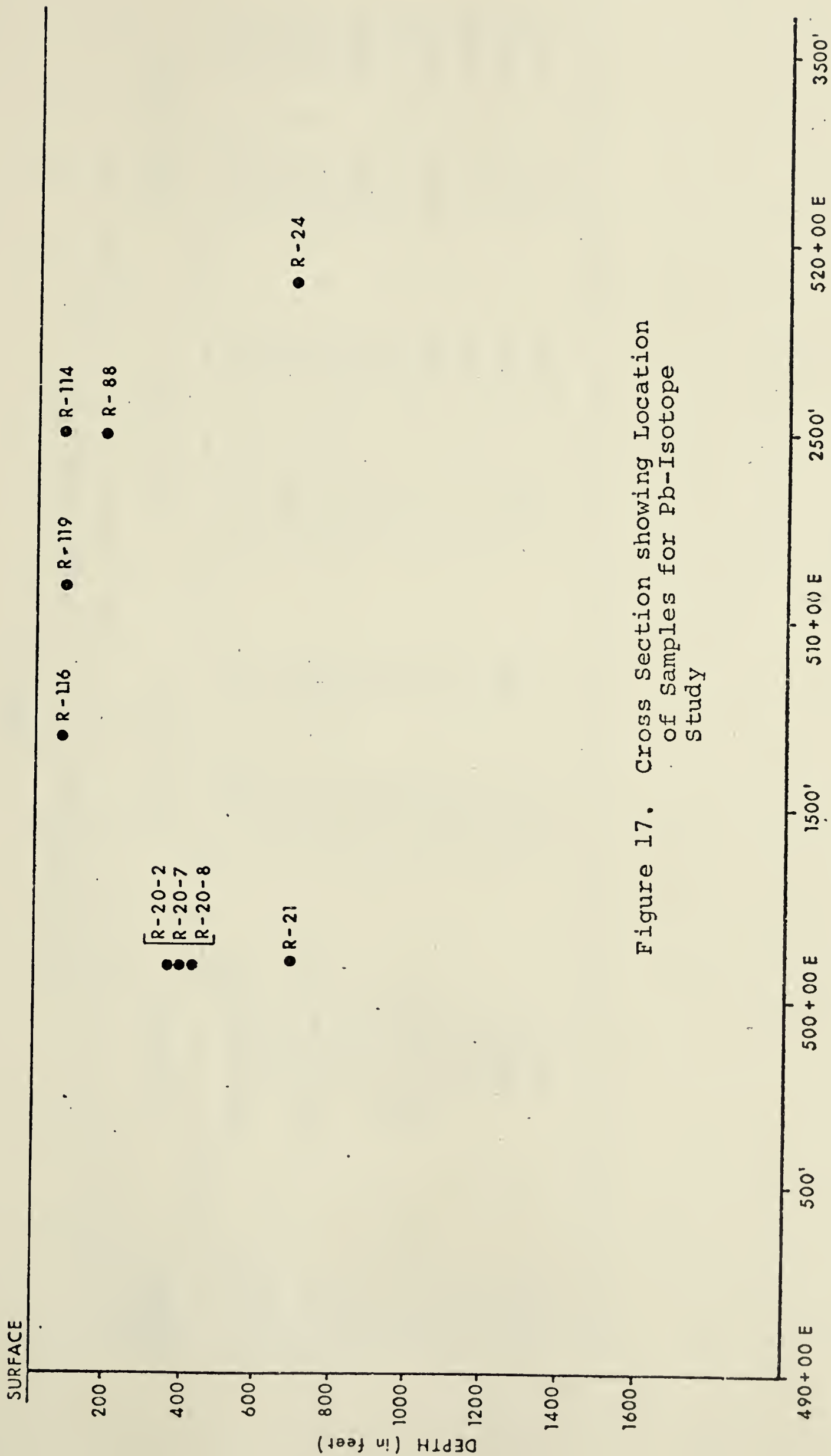


Figure 17. Cross Section showing Location of Samples for Pb-Isotope Study

TABLE 15

LEAD ISOTOPE DATA OF THE RUTTAN LAKE ORES

Sample Number	Sulphide	$^{206}\text{Pb}/^{204}\text{Pb}$	$^{207}\text{Pb}/^{204}\text{Pb}$	$^{208}\text{Pb}/^{204}\text{Pb}$
R-116-1	Chalcopyrite	17.269 \pm .0084	15.429 \pm .0075	36.820 \pm .0180
R-20-2	Pyrite	15.53 \pm .0853	15.09 \pm .0802	34.89 \pm .1842
R-21-4	Chalcopyrite	18.81 \pm .0261	15.63 \pm .0216	38.00 \pm .0527
R-88-7	Pyrite	17.66 \pm .0257	15.41 \pm .0224	36.88 \pm .0541
R-114-1	Pyrrhotite	17.27 \pm .0789	15.60 \pm .0708	37.07 \pm .1692
R-119-2	Pyrrhotite	17.29 \pm .0694	15.61 \pm .0203	36.98 \pm .0558
R-24-4	Pyrite	18.58 \pm .0736	15.39 \pm .0608	37.37 \pm .1483
R-20-7	Pyrite	15.71 \pm .0634	15.21 \pm .0616	34.99 \pm .1405
R-20-8	Pyrite	15.62 \pm .0478	15.21 \pm .0465	35.13 \pm .1087

D. Trace Elements in Ores

Introduction

A study of the distribution of trace elements Fe, Ba and Mn in the ores and country rocks was undertaken to see if they showed any particular zonation pattern. From previous studies of other massive sulphide stratiform-type deposits one could expect compositional zoning of Fe, Ba and Mn within the deposit and hence aid in interpreting the stratigraphic sequence of the complex volcanic and intercalated sedimentary rocks found in the Ruttan Lake ore body.

Experimental Procedure

The samples were analyzed by the laboratory of Resource Associates of Alaska in Fairbanks, Alaska. Each sample was treated with aqua regia and the dissolved specimen was then evaporated to dryness and taken up with 1 N HCl. Atomic absorption spectroscopy was performed on these solutions for Fe, Ba and Mn.

Results

Forty-one samples were selected from various representative parts of the deposit as well as from the hanging and footwall rocks giving both vertical and horizontal cross sections. Table 16 gives a description and location

TABLE 16

LOCATION AND DESCRIPTION OF SAMPLES ANALYZED FOR TRACE ELEMENTS

Sample Number	Grid Location and Depth	Description
R-6	498 + 00 E 150 ft.	Quartz-biotite schist with sphalerite, pyrite and pyrrhotite
R-10	498 + 00 E 75 ft.	Disseminated pyrite, chalcopyrite and sphalerite in quartz, felspar, biotite schist
R-15	502 + 00 E 400 ft.	Massive sphalerite, pyrite and pyrrhotite
R-19	498 + 00 E 1000 ft.	Massive chalcopyrite, pyrite with minor sphalerite
R-20	498 + 00 E 200 ft.	Massive pyrite, sphalerite and pyrrhotite
R-21	498 + 00 E 700 ft.	Massive pyrite
R-23	504 + 00 E 400 ft.	Disseminated pyrite, sphalerite and pyrrhotite in quartz-biotite gneiss
R-24	514 + 00 E 700 ft.	Chlorite-biotite schist with disseminated pyrrhotite, pyrite and minor chalcopyrite
R-25	510 + 00 E 1100 ft.	Chlorite-biotite schist with disseminated pyrite and pyrrhotite

TABLE 16 (cont'd)

Sample Number	Grid Location and Depth	Description
R-26	510 + 00 E 1200 ft.	Disseminated pyrrhotite, pyrite and chalcopyrite in quartz-biotite gneiss
R-27	524 + 00 E 1800 ft.	Massive pyrite, pyrrhotite with minor chalcopyrite
R-29	491 + 00 E 200 ft.	Massive pyrite, chalcopyrite and pyrrhotite
R-30	493 + 00 E 400 ft.	Massive pyrite with trace of chalcopyrite and sphalerite
R-31	501 + 00 E 100 ft.	Massive pyrite, pyrrhotite
R-32	504 + 00 E 500 ft.	Disseminated pyrite, pyrrhotite, chalcopyrite in quartz, biotite, chlorite schist
R-34	520 + 00 E 1400 ft.	Massive pyrite, pyrrhotite with minor chalcopyrite
R-35	493 + 00 E 50 ft.	Disseminated pyrite-pyrrhotite in chlorite-biotite schist
R-50	501 + 00 E 225 ft.	Pyrite-pyrrhotite and chalcopyrite in chlorite-talc schist

TABLE 16 (cont'd)

Sample Number	Grid Location and Depth	Description
R-51	501 + 00 E 240 ft.	Massive pyrite-chalcopyrite
R-52	500 + 00 E 50 ft.	Biotite, quartz, hornblende gneiss with disseminated pyrite
R-53	504 + 00 E 100 ft.	Massive pyrite, pyrrhotite and chalcopyrite
R-54	504 + 00 E 150 ft.	Chlorite-biotite-talc schist with pyrite-pyrrhotite-chalcopyrite
R-55	504 + 00 E 200 ft.	Massive pyrite, pyrrhotite and chalcopyrite
R-58	487 + 00 E 200 ft.	Footwall; granite breccia with disseminated pyrite
R-60	489 + 00 E 200 ft.	Footwall; epidortized meta-andesite with disseminated pyrite
R-62	490 + 00 E 150 ft.	Footwall; biotite-quartz-feldspar gneiss
R-65	492 + 00 E 150 ft.	Massive pyrite, chalcopyrite and pyrrhotite
R-66	494 + 00 E 150 ft.	Blebs of chalcopyrite in quartz, pyrite and pyrrhotite

TABLE 16 (cont'd)

Sample Number	Grid Location and Depth	Description
R-67	498 + 00 E 160 ft.	Chalcopyrite-pyrrhotite in chlorite-biotite schist; minor pyrite
R-68	496 + 00 E 150 ft.	Massive sphalerite, pyrite and pyrrhotite; vuggy
R-69	502 + 00 E 190 ft.	Massive pyrite, chalcopyrite
R-70	501 + 00 E 160 ft.	Massive pyrite, chalcopyrite
R-71	500 + 00 E 125 ft.	Chlorite-biotite-talc schist with disseminated pyrite, pyrrhotite, chalcopyrite
R-74	510 + 00 E 100 ft.	Biotite-quartz-sericite schist with disseminated pyrite
R-75	509 + 00 E 250 ft.	Massive pyrite with minor chalcopyrite
R-76	510 + 00 E 300 ft.	Sericite schist with disseminated pyrite
R-79	492 + 00 E 50 ft.	Biotite-chlorite-hornblende schist with minor pyrite

TABLE 16 (cont'd)

Sample Number	Grid Location and Depth	Description
R-86	506 + 00 E 150 ft.	Quartz-biotite gneiss with stringers of chalcopyrite, pyrrhotite
R-87	508 + 00 E 150 ft.	Massive pyrite and chalcopyrite with quartz; near contact with biotite-quartz; hornblende gneiss
R-88	510 + 00 E 175 ft.	Massive pyrite-chalcopyrite-pyrrhotite
R-91	536 + 00 E 500 ft.	Quartz-biotite-hornblende gneiss
R-92	522 + 00 E 500 ft.	Quartz-biotite-hornblende gneiss with disseminated pyrite
R-99	502 + 00 E 500 ft.	Quartz-biotite-hornblende gneiss
R-100	504 + 00 E 225 ft.	Chlorite-biotite schist with disseminated chalcopyrite, pyrite, pyrrhotite
R-108	520 + 00 E 500 ft.	Biotite-hornblende-quartz gneiss
R-109	536 + 00 E 500 ft.	Biotite-hornblende schist

TABLE 16 (cont'd)

Sample Number	Grid Location and Depth	Description
R-112	510 + 00 E 800 ft.	Biotite-quartz-chlorite schist with disseminated pyrite
R-113	502 + 00 E 800 ft.	Massive quartzite with disseminated pyrite
R-114	510 + 00 E 325 ft.	Massive pyrite, chalcopyrite
R-115	510 + 00 E 290 ft.	Massive pyrite, pyrrhotite and chalcopyrite
R-116	510 + 00 E 250 ft.	Massive pyrite, pyrrhotite and chalcopyrite
R-118	504 + 00 E 200 ft.	Massive sphalerite, pyrite and pyrrhotite
R-119	506 + 00 E 200 ft.	Massive sphalerite, pyrite and pyrrhotite
R-120	512 + 00 E 150 ft.	Massive sphalerite-pyrite with minor pyrrhotite
R-121	516 + 00 E 150 ft.	Massive sphalerite-pyrite with minor pyrrhotite

of the samples analyzed and Figure 18 graphically shows the sample distribution. The analytical results are listed in Table 17.

SURFACE

DEPTH (in feet)

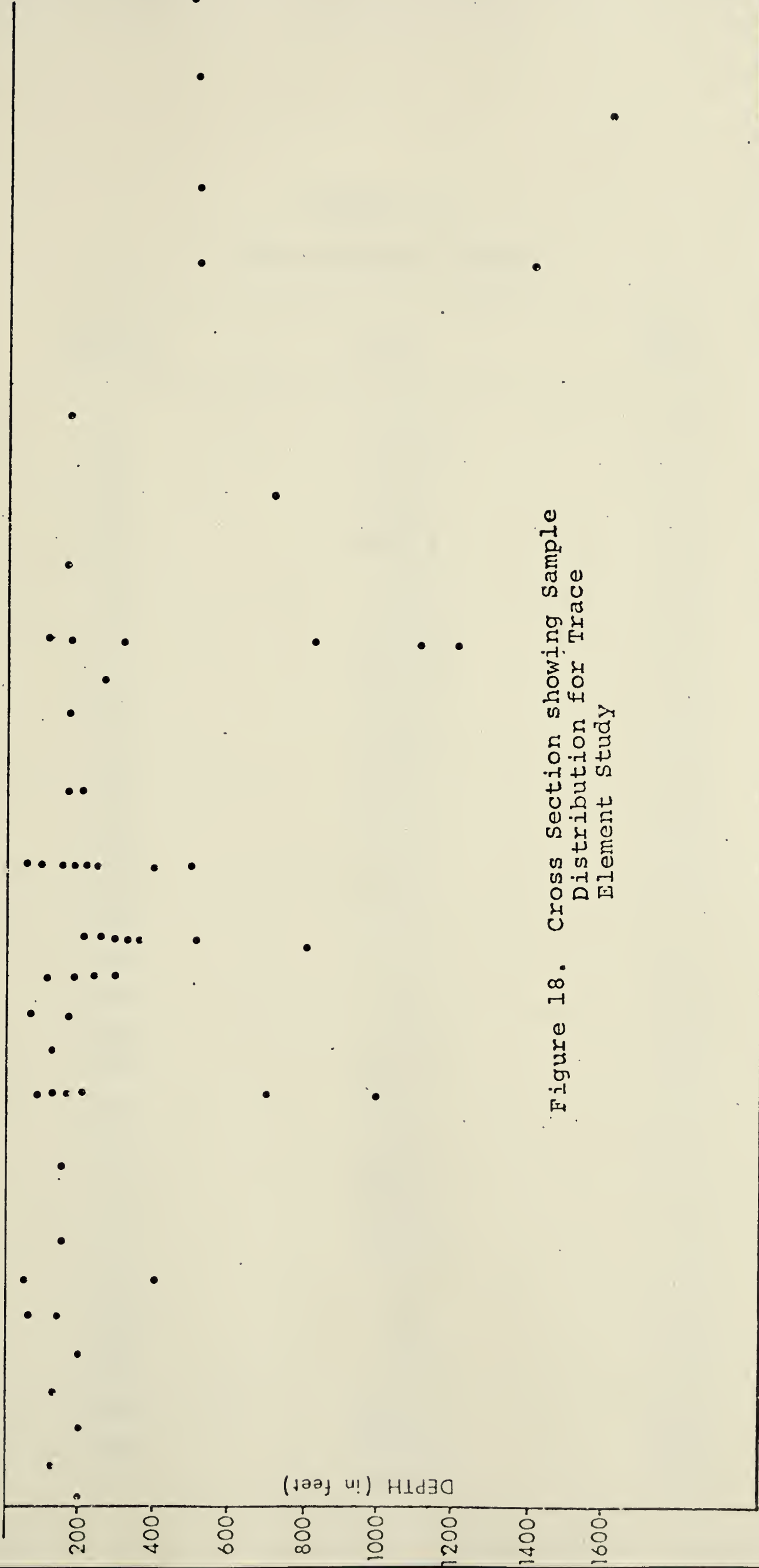


Figure 18. Cross Section showing Sample
Distribution for Trace
Element Study

490 + 00 E 500' 500 + 00 E 1500' 510 + 00 E 2500' 520 + 00 E 3500' 101

TABLE 17
TRACE ELEMENT RESULTS

Sample Number	Fe/Mn	Ba (ppm)
R-6	150.0	<10
R-10	793.3	<10
R-15	105.5	<10
R-19	6000.0	<10
R-20	19.4	<10
R-21	875.0	<10
R-23	203.8	<10
R-24	666.7	<10
R-25	400.0	<10
R-26	520.8	<10
R-27	1000.0	250
R-29	600.0	<10
R-30	1000.0	<10
R-31	875.0	<10
R-32	403.8	<10
R-34	729.2	240
R-35	500.0	<10
R-50	1400.0	<10
R-51	857.1	<10
R-52	500.0	<10
R-53	1500.0	<10
R-54	500.0	<10
R-55	625.0	10
R-58	72.7	<10
R-60	29.4	<10
R-62	50.0	80
R-63	400.0	<10
R-65	1400.0	<10
R-66	631.6	<10

TABLE 17 (cont'd)

Sample Number	Fe/Mn	Ba (ppm)
R-67	1080.0	<10
R-68	318.2	<10
R-69	545.4	<10
R-70	857.1	<10
R-71	550.0	<10
R-74	400.0	10
R-75	538.5	<10
R-76	550.0	<10
R-79	628.6	10
R-86	103.4	10
R-87	325.0	<10
R-88	117.1	<10
R-91	80.0	180
R-92	71.4	320
R-99	150.0	100
R-100	240.0	10
R-108	90.5	300
R-109	100.0	240
R-112	52.6	60
R-113	260.0	30
R-114	777.8	<10
R-115	1000.0	<10
R-116	700.0	<10
R-118	227.3	<10
R-119	227.3	<10
R-120	141.2	<10
R-121	150.0	40

CHAPTER IV INTERPRETATIONS - DISCUSSION

A. Sulphur Isotopes

The sulphur isotope data from Ruttan Lake pyrite, chalcopyrite, sphalerite and pyrrhotite show a remarkably narrow range of values. Average $\delta^{34}\text{S}$ values for pyrite was 1.21 per mil, .76 per mil for chalcopyrite , 1.18 per mil for sphalerite and 1.01 per mil for pyrrhotite. The standard deviation of the $\delta^{34}\text{S}$ values is $\pm .18$ per mil and indicates the narrow range of sulphur isotopic composition. The mean sulphur isotopic composition of the sulphides is not significantly different from that of the meteoritic sulphur and is well within the range for igneous sulphur of possible upper mantle origin (Ault and Kulp, 1959; Thode, 1963).

Early workers in the field of sulphur isotope studies interpreted isotopic values for sulphides not far from the meteoritic standard or the approximate average value of the Earth's crustal sulphur as originating from a deep-seated igneous origin. Since then Sangster (1968) and Sasaki (1970) have shown that seawater sulphates could have had an extensive role in volcanic-type stratabound ores. Ohmoto et al. (1970) and Kajiwara (1971) have interpreted isotopic data from both sulphates and sulphides in the

Kuroko ores of Japan and concluded that the source of sulphur was of seawater origin. Rye and Ohmoto (1974) have demonstrated that sulphides which precipitated from magmatic sulphur can exhibit a wide range of $\delta^{34}\text{S}$ values while sulphides precipitated from non-magmatic sulphur, such as seawater, can have a modest range of $\delta^{34}\text{S}$ values near 0 per mil.

Barnes (1967) states that if the source of sulphur is not the mantle but rather a portion of the crust that has undergone metamorphism under conditions where sulphur is mobilized, then the δS^{34} values of the hydrothermal sulphur-bearing minerals would be an average value of the sulphur assimilated in that portion of the crust. If the metamorphism results in the formation of magmas, the homogenizing effects that occur during the last stages of the magmatic process should result in the characteristic narrow spread in δS^{34} values of the sulphides derived from intrusive bodies.

Due to lack of any preserved sulphate minerals in the Ruttan ores, it was not possible to obtain the sulphur isotope composition of any sulphates. However, since the ores are definitely of premetamorphic age which may have reduced sulphate to sulphide, we cannot rule out the source of sulphur as being from seawater. A line of evidence from trace element distribution in sulphides (Ba, Fe/Mn) indicates

that increasing contamination of seawater (see section on discussion of trace element distribution) which is consistent with an increase in sulphur isotope ratios of sulphides towards the upper part of the deposit, indicating either a decrease in oxidation or an increase in pH or both.

Sulphur isotope geothermometry is based on the equilibrium sulphur isotope fractionations between co-existing sulphur-bearing compounds. Isotopic fractionation of sulphur between synthetic sulphide mineral pairs as a function of temperature and duration of reaction time has been investigated by many authors (Kajiwara and Sasaki, 1969; Kajiwara and Krouse, 1971; Rye and Czamanske, 1969). Figure 19 shows curves based on experimental and theoretical data by Kajiwara and Krouse (1971). Czamanske and Rye (1974) have discussed the differences between the curves produced by various laboratories but concluded that the relative position of the curves among the minerals will not change. Table 9 shows the isotopic composition of co-existing sulphide pairs from Ruttan Lake ores which have been used to calculate the per mil deviations between specific sulphide pairs. Using the geothermometric plots by Kajiwara and Krouse (1971) from Figure 19, one can determine an isotopic temperature for the Ruttan Lake ores. See Figures 20 and 21 for data of isotopic

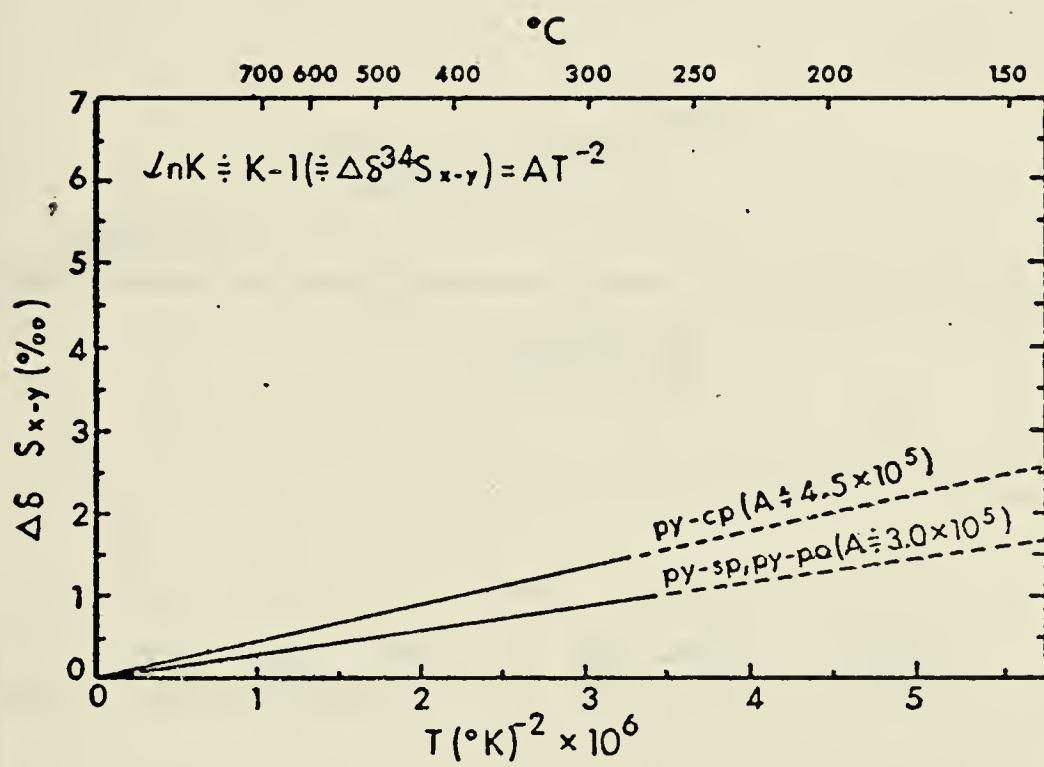
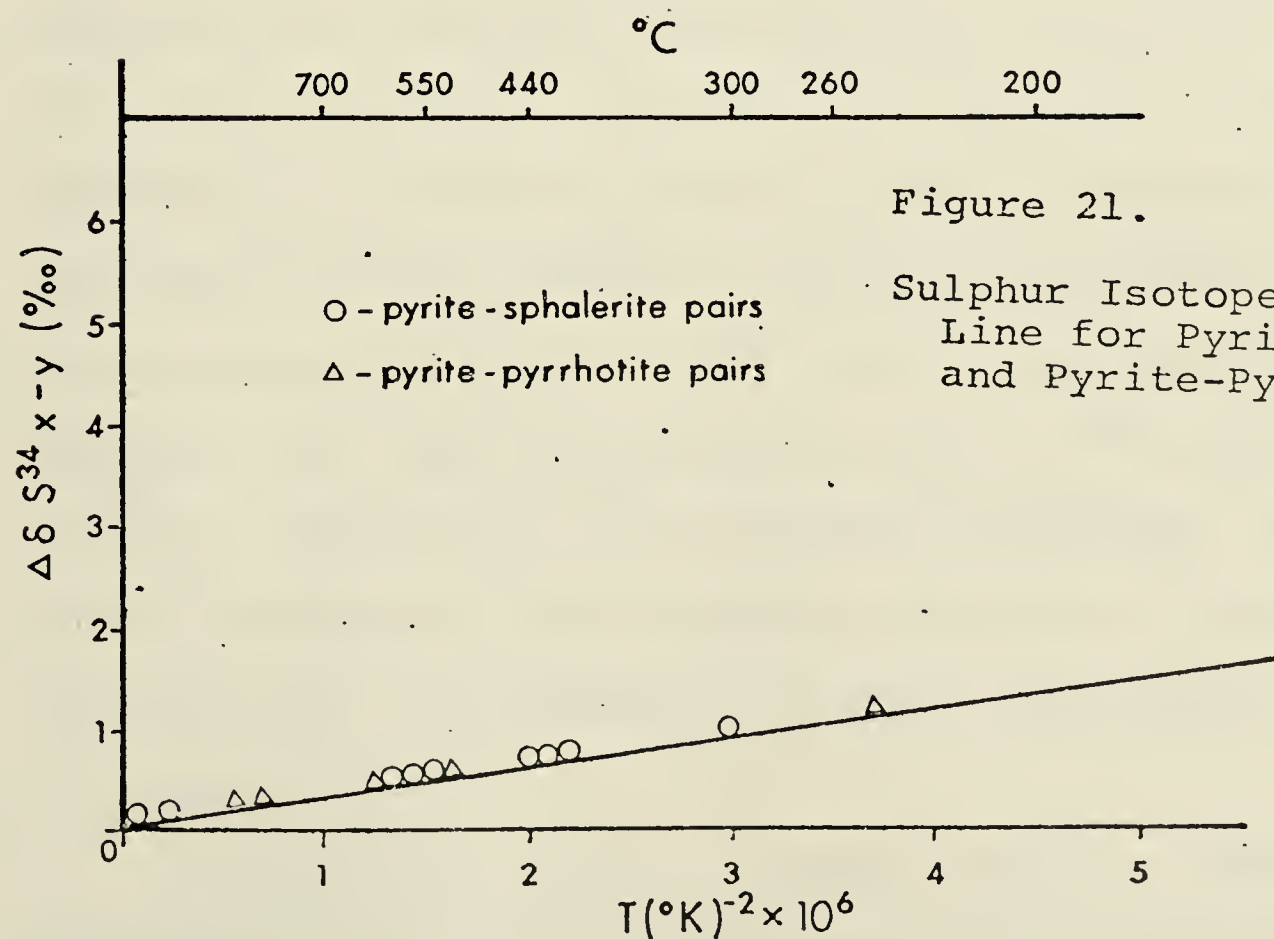
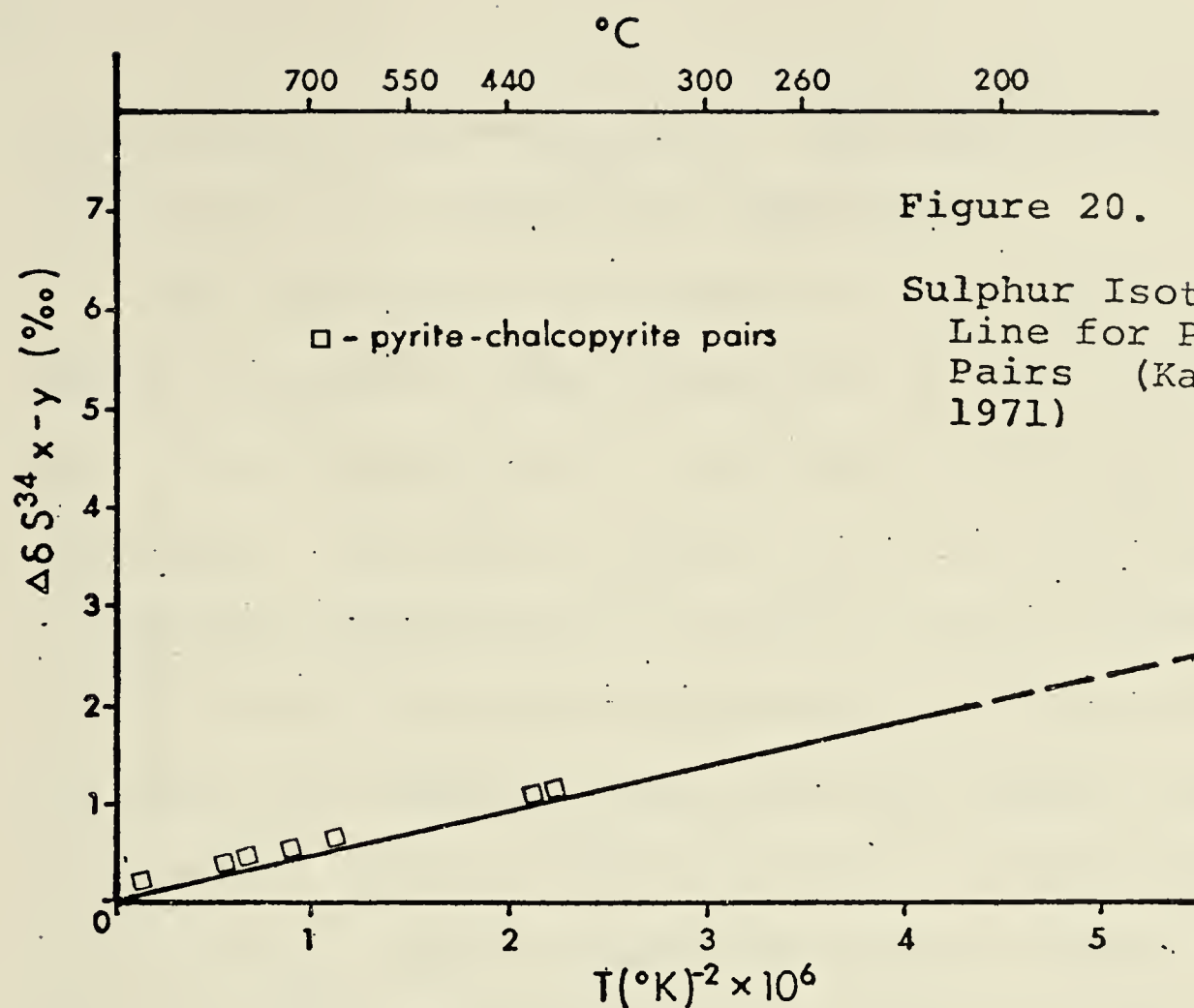


Figure 19. Geothermometric Plot by Kajiwarra and Krouse, 1971



fractionation between pyrite - chalcopyrite and pyrite - sphalerite as a function of temperature.

The application of sulphur isotope thermometer to a deposit depends on the suitability of the samples. Samples that crystallized in equilibrium with each other are necessary. The use of mineral pairs may give geologically reasonable temperatures as long as the two minerals were formed in equilibrium with solutions having uniform temperature and chemical states (Rye and Ohmoto, 1974). The theoretical trend of fractionation of sulphur isotopes in co-existing, cogenetic sulphide species (Sakai, 1968) is that the $\delta^{34}\text{S}$ enrichment would be pyrite > pyrrhotite > sphalerite > chalcopyrite > galena. Although no galena samples were analyzed, this trend can be seen in the other four sulphides from the Ruttan Lake ores and could imply equilibrium between the mineral pairs. Figures 22 and 23 are plots showing isotopic fractionation between $\delta^{34}\text{S}$ (pyrite-pyrrhotite) and $\delta^{34}\text{S}$ (pyrite-chalcopyrite) and between $\delta^{34}\text{S}$ (pyrite-pyrrhotite) and $\delta^{34}\text{S}$ (pyrite-sphalerite), respectively in co-existing sulphides. The results show no definite linear pattern and hence it cannot be certain that the sulphides did attain equilibrium or closely approached it.

Although the sulphur isotopic values of individual sulphides is variable in different parts of the deposit

Figure 22. Sulphur Isotope Fractionation
between co-existing Pyrite-
Sphalerite and Pyrite-
Pyrrhotite

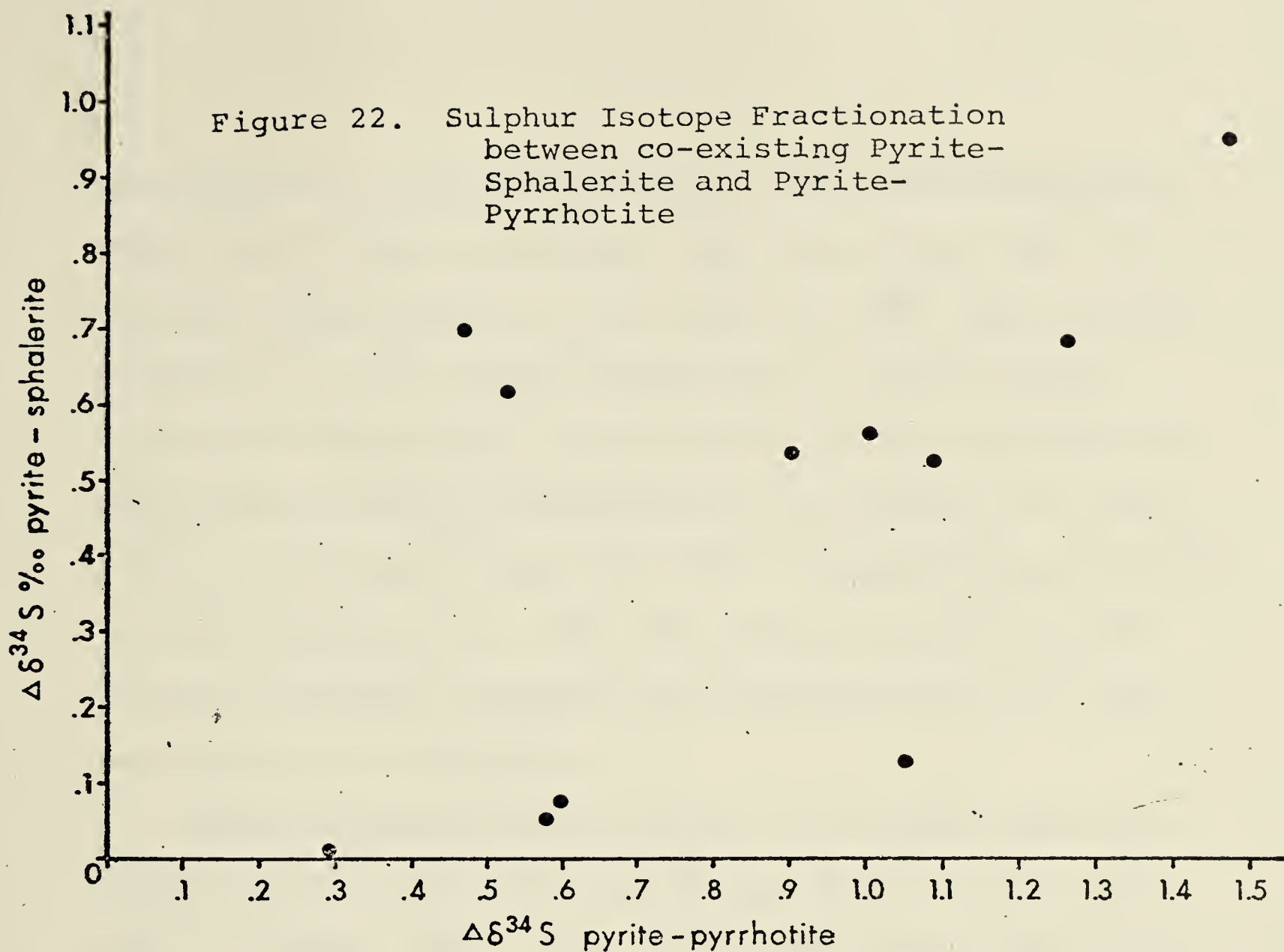
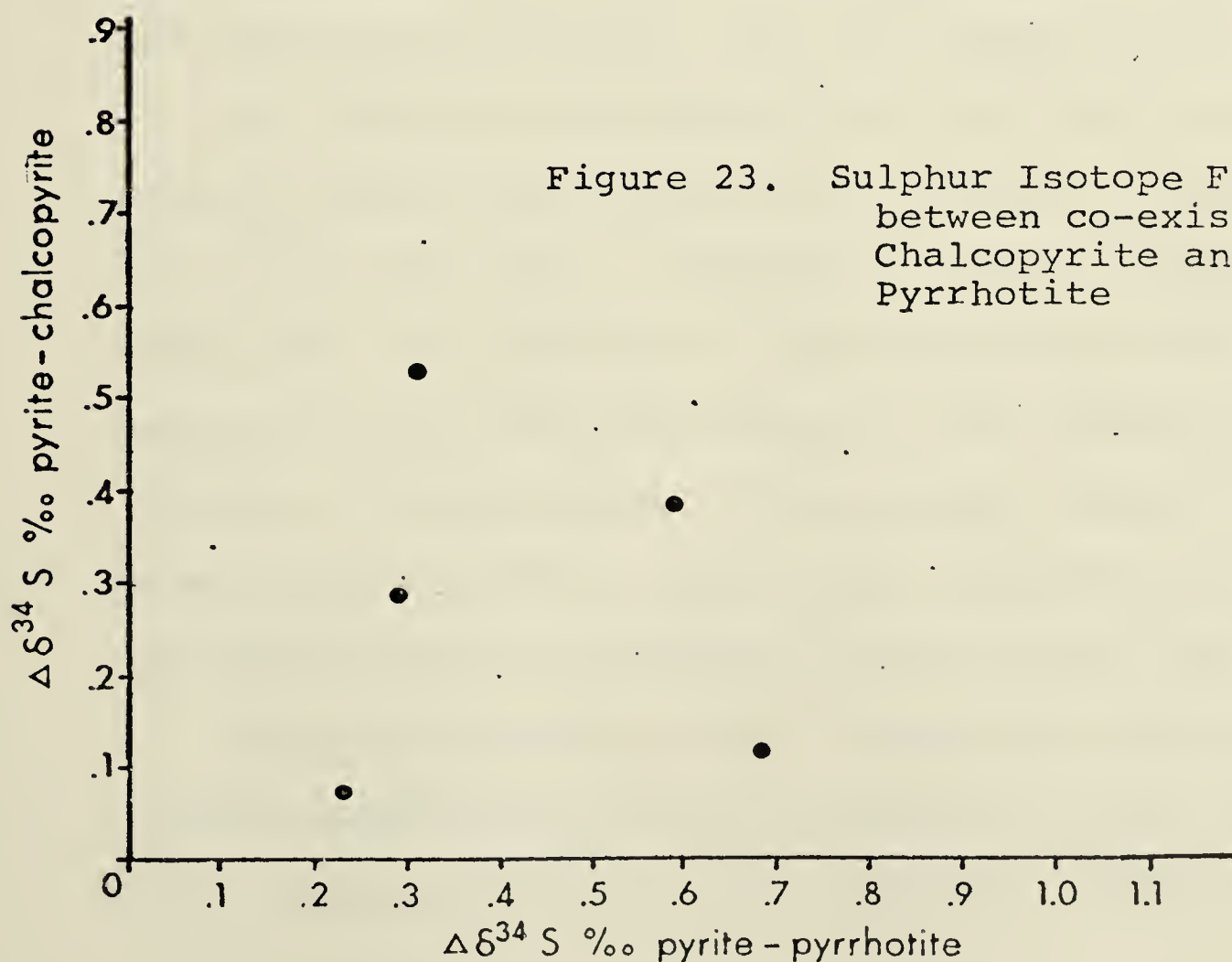


Figure 23. Sulphur Isotope Fractionation
between co-existing Pyrite-
Chalcopyrite and Pyrite-
Pyrrhotite



(see Figure 13), the fractionation among co-existing sulphide species show relatively small variations and a decreasing fractionation in the order of $\Delta\delta S^{34}$ (pyrite-chalcopyrite) $> \delta S^{34}$ (pyrite-sphalerite) $> \delta S^{34}$ (pyrite-pyrrhotite) indicating the attainment of isotopic exchange equilibrium among the sulphides during original ore deposition. If fractionation of δS^{34} of co-existing sulphides had been preserved but were not reduced by metamorphism then the cogenetic sulphide pairs should reveal the temperature of ore formation.

Using suitable sulphide pairs and careful sampling, temperatures of deposition or metamorphism can be determined to within $\pm 40^\circ\text{C}$, even considering the uncertainty in the fractionation factors (Rye and Ohmoto, 1974).

The isotopic temperatures derived from the geothermometric plots range from 250°C to greater than 700°C in the Ruttan Lake ores. Although the higher temperatures could have been attained in hydrothermal deposits, there appears to be a definite effect on the isotopic fractionation due to metamorphism. The isotopic temperatures appear more likely to reflect metamorphic temperatures attained in the greenschist to amphibolite facies of the host rocks.

In the environment of ore deposition, other aqueous sulphur species which become important are SO_4 , HSO_4^- , KSO_4^- , NaSO_4^- and HS^- but Rye and Ohmoto (1974) have shown

that the major factors which control the sulphur isotopic composition of hydrothermal minerals are:

- (i) temperature, which determines the fractionations between sulphur-bearing species;
- (ii) $\delta^{34}\text{S}_{\Sigma\text{S}}$, which is controlled by the source of sulphur; and
- (iii) pH and $f\text{O}_2$, which along with temperature, determine the proportions of oxidized and reduced sulphur species in solution.

Ohmoto (1972) suggested that changing physical-chemical conditions, particularly partial pressure of oxygen ($f\text{O}_2$) and pH can induce isotopic variation in the aqueous sulphur species despite a homogeneous source of sulphur in the ore solution and hence it would be possible to have a very wide range of isotopic composition in the sulphide minerals, particularly if the deposition occurs in an oxidizing alkaline environment.

Figure 24. (from Ohmoto, 1972) indicates that in the low $f\text{O}_2$ and low to neutral pH range the $\delta^{34}\text{S}$ of aqueous H_2S and that of the precipitating minerals is little affected by changes in $f\text{O}_2$ and pH so that the precipitating sulphide minerals from such a solution exhibit homogeneous $\delta^{34}\text{S}$ values similar to the mean sulphur isotopic composition of the ore-depositing solution.

Results from the study on Fe content in sphalerite

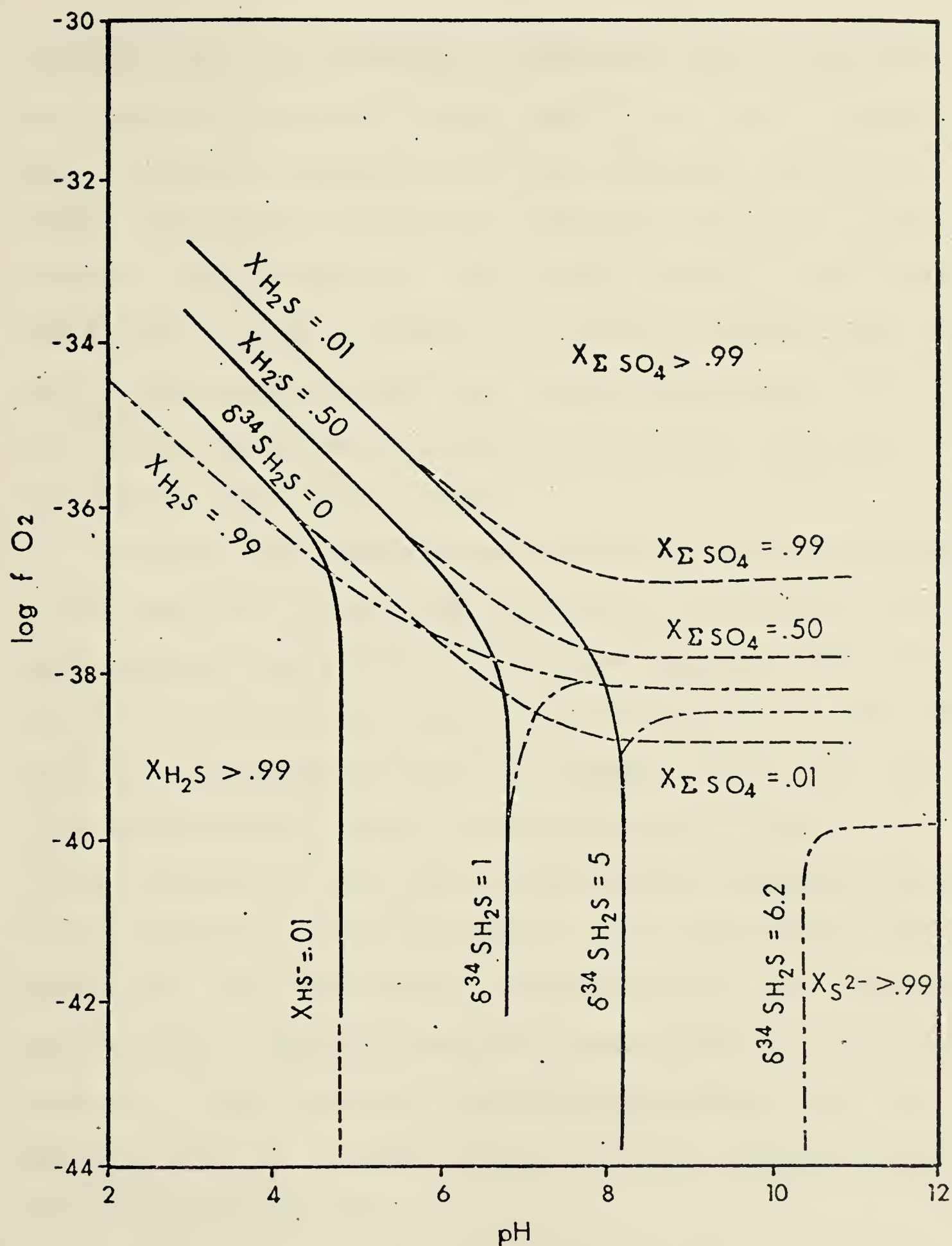


Figure 24. Influence of $f\text{O}_2$ and pH on Mole Fractions of Aqueous Sulphur Species assuming $T = 250^\circ\text{C}$, Molarity of Total Alkalies is 1.0 and $\delta^{34}\text{S}_{\Sigma\text{S}} = 0$ per mil (from Ohmoto, 1972, p. 257, 258)

indicate that the chemistry of the ore-forming solutions at Ruttan Lake were of low fO_2 and fS_2 and low or neutral pH. A probable temperature of ore formation was 200° to 250°C (from the Fe content in sphalerite results and the sulphur isotope results). The narrow range in δS^{34} values and a mean δ value of close to 0 per mil suggests that H_2S must have been the predominant sulphur species in the ore-depositing solutions which formed the Ruttan Lake ores (from Figure 24, Ohmoto, 1972).

Although one cannot classify the types of ore deposits or say very much about their genesis on the basis of sulphur isotope values alone, the narrow range in $\delta^{34}S$ values and near magmatic mean value from the Ruttan Lake ores indicates a homogeneous source of sulphur. The slight increase in sulphur isotopic composition and of barium towards the stratigraphic top of the deposit suggests possible assimilation of seawater sulphur. With the average $\delta^{34}S$ value near zero, the source of the depositing ore solution was magmatic. Homogenization or redistribution of sulphur isotopes of the sulphides by metamorphism have been superimposed upon the original sulphur isotope distribution among co-existing minerals.

B. Fe Content in Sphalerite

Sphalerites for which complete analyses were made all approach stoichiometric Zn - Fe - S. The average metal to non-metal ratio for the twenty sphalerite grains analyzed was .985. The range of FeS mole percent was 7.13 to 12.64 and averaged 10.69

Barton and Toulmin (1966), Clark (1966) and Scott and Barnes (1971) pointed out that the iron content in sphalerite co-existing with pyrite and pyrrhotite was very sensitive to variations in temperature and fugacity of sulphur. The use of the iron content in sphalerite co-existing with pyrite and pyrrhotite as a geothermometer may be applied to the Ruttan Lake deposit if it is assumed that (Scott, 1974):

- (i) the sphalerite-pyrrhotite-pyrite attained equilibrium at the temperature of ore formation,
- (ii) the relation between activity and molality of FeS in sphalerite does not change in the sphalerite-pyrite field at temperatures below 300°C and,
- (iii) the inversion of hexagonal pyrrhotite to monoclinic pyrrhotite does not affect the slope of the pyrite-pyrrhotite-sphalerite solvus.

The physical-chemical variables defining the iron content of sphalerite in the Zn - Fe - S system are temperature, fugacity of sulphur and total pressure. Application of the experimental results to sphalerite from the Ruttan Lake deposit gives a temperature of formation between 160° and 210°C (see Figure 25). For this temperature range the probable fS_2 range lies between 10^{-13} and 10^{-17} (see Figure 26). In the three phase assemblages (pyrite + pyrrhotite + sphalerite) the equilibrium fugacity of sulphur is fixed by the pyrite-pyrrhotite buffer system, therefore the iron content of sphalerite is more restricted as it is only a function of the total pressure at a given temperature (Scott, 1974). From Figure 27 we can estimate a total pressure involved during ore deposition from approximately 6 to 6.2 kilobars in the temperature range 160-210°C. Since the isobars of Scott and Barnes (1971) are extrapolated ones at pressures higher than one kilobar, these pressure values are only tentative. These changes in physicochemical conditions of the ore-forming solution could be explained by use of fO_2 - pH diagrams. From work done by Sato (1971) an estimated fugacity of oxygen for the above temperature range would vary from 10^{-40} to 10^{-50} atm and pH could vary from 3.6 to 5.0. Common occurrences of sericite and quartz mineral assemblages near the hanging wall in the Ruttan ore body suggests

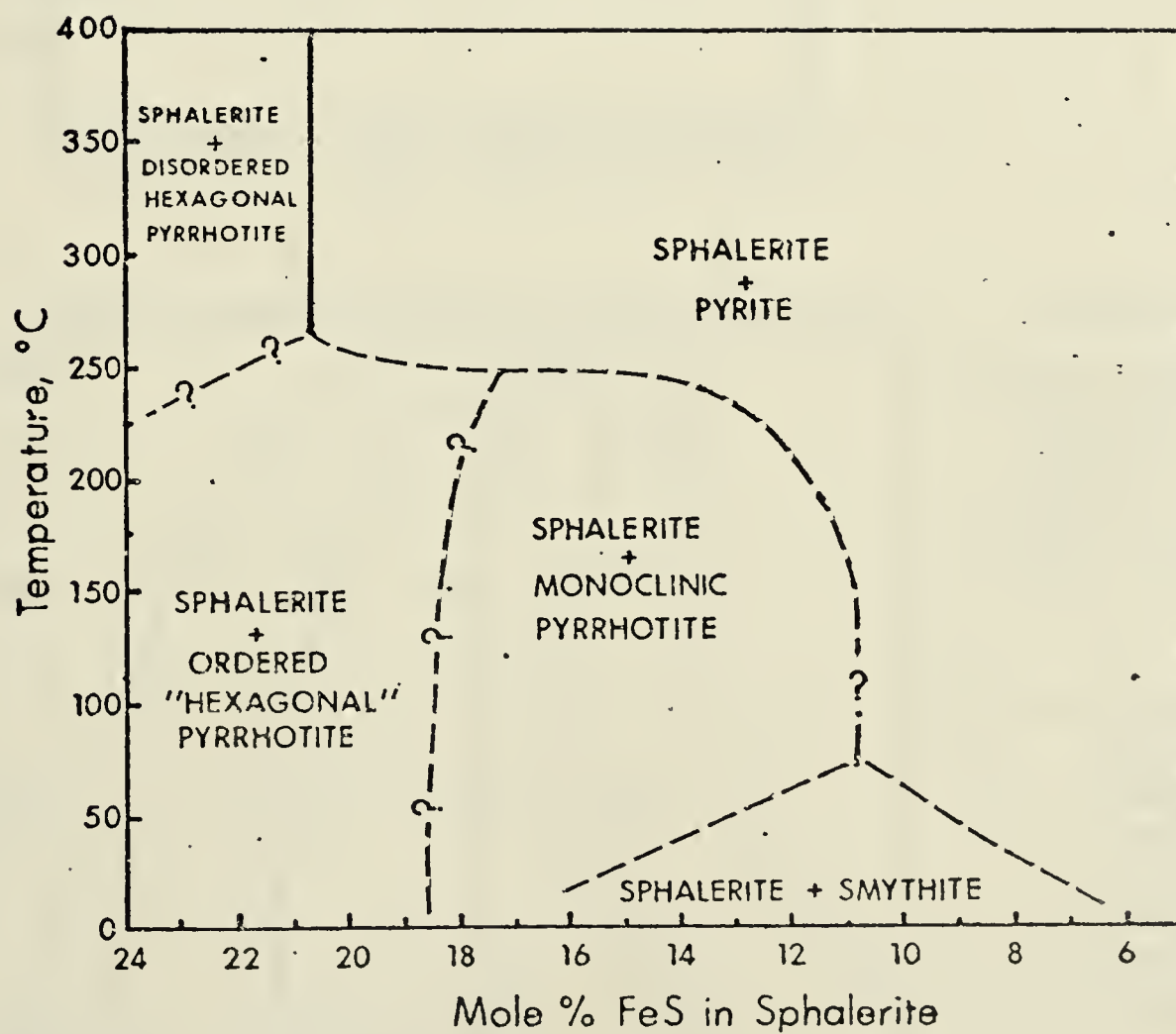


Figure 25. FeS - ZnS - S System at Low Temperatures (from Scott and Kissin, 1973, Econ. Geol. 68, p. 478)

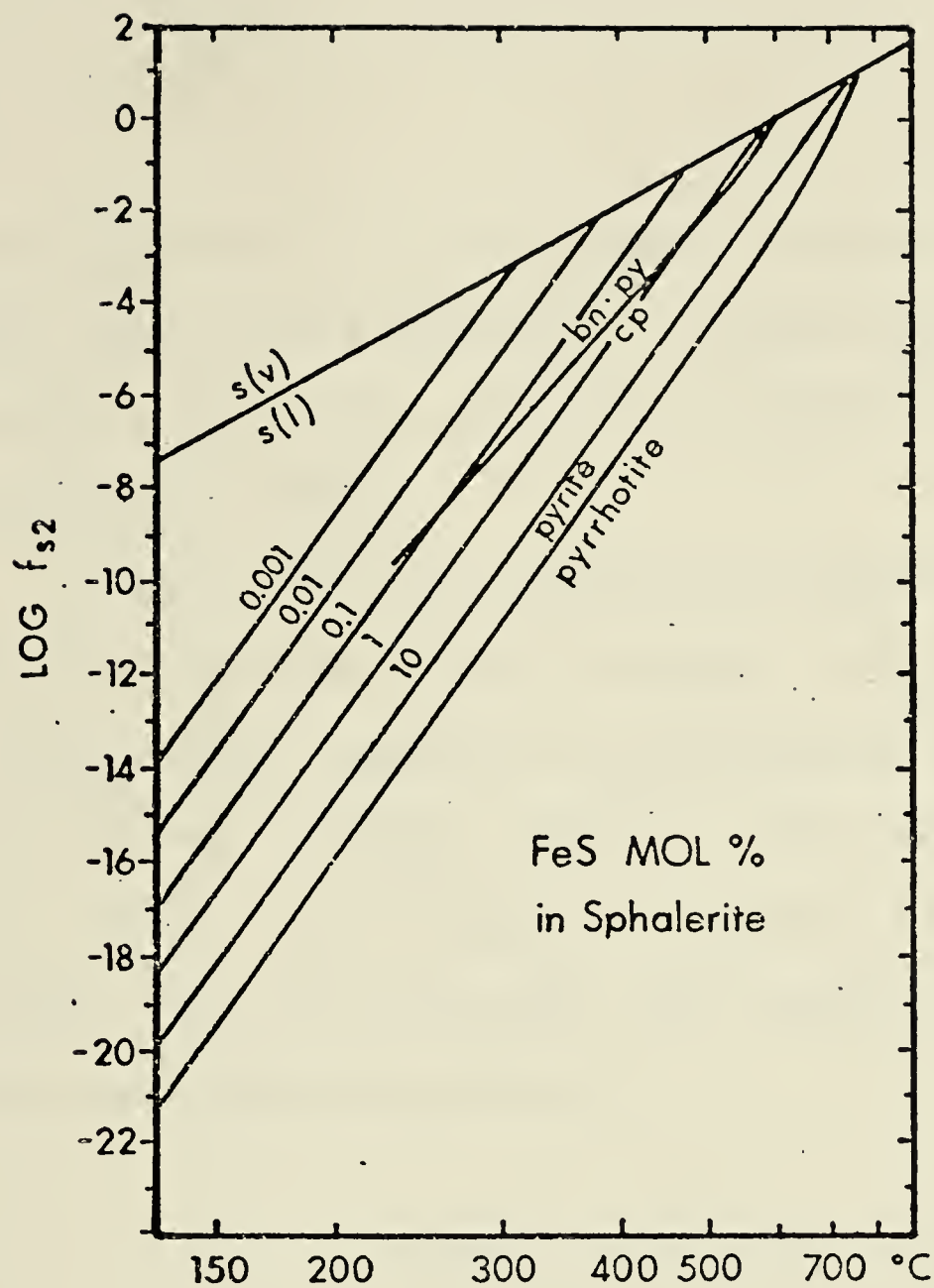


Figure 26.

Temperature - f_{S_2}
Diagram showing
Fe-content in
Sphalerite in
Equilibrium with
Pyrite (from
Scott, 1974)

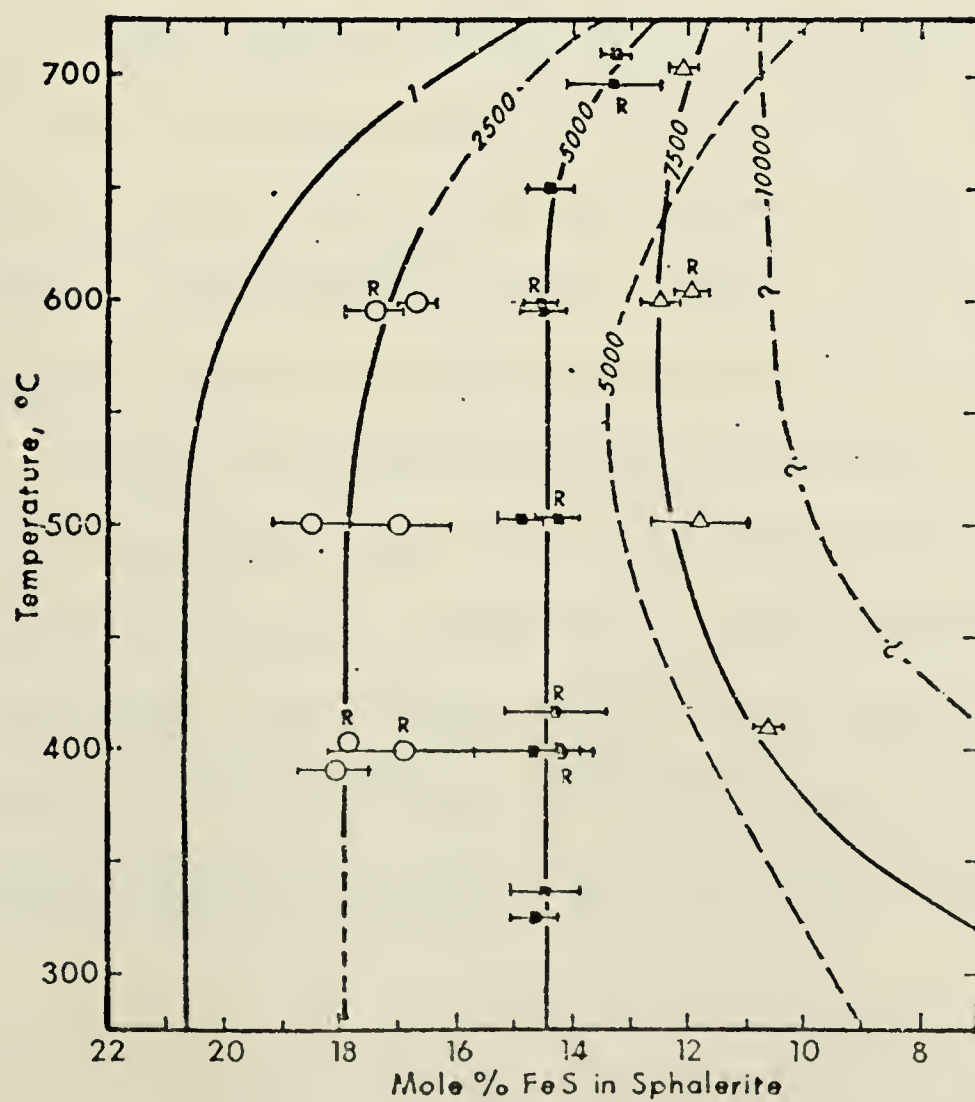


Figure 27.

Isobars for the
FeS-ZnS-S
System (from
Scott, 1973,
Econ. Geol.
68, p. 469)

- - Measured / Extrapolated Isobar
- - - - Calculated Isobar (Scott & Barnes, 1971)
- - 2.5 kb Experiments
- - 5 kb Experiments
- △ - 7.5 kb Experiments
- R - Reversol

that the pH of the ore-forming solution was near neutral at the time of ore formation or became more neutral towards the upper part of the ore body as sulphur isotopes became heavier (Helgeson, 1969).

Since "the iron content of sphalerite is unusually resistant to post mineral changes" (Barnes, 1967), its use in studying the genesis of metamorphosed massive sulphide deposits can be very useful. However, until more experimental studies on the Zn - Fe - S system in pyrite field at temperatures below 300°C is available, the results of this study cannot be considered conclusive.

C. Isotopic Data of Ore Lead

From Figures 28 and 29 it can readily be observed that the lead isotope ratios from the Ruttan Lake ore minerals display a distinctly anomalous linear relationship. Armstrong (1968), Stanton and Russel (1959), and Russel et al. (1966) suggest mixing to explain such anomalous leads.

That the anomalous lead line does not cut the growth curve suggests that more than a two-stage lead evolution occurred, hence a multi-stage model must be considered. An integrated age of the source leads can be calculated from the slope R $(^{207}\text{Pb}/^{204}\text{Pb})/(^{206}\text{Pb}/^{204}\text{Pb})$ of the best fit straight line through the data. See Appendix D for method of calcu-

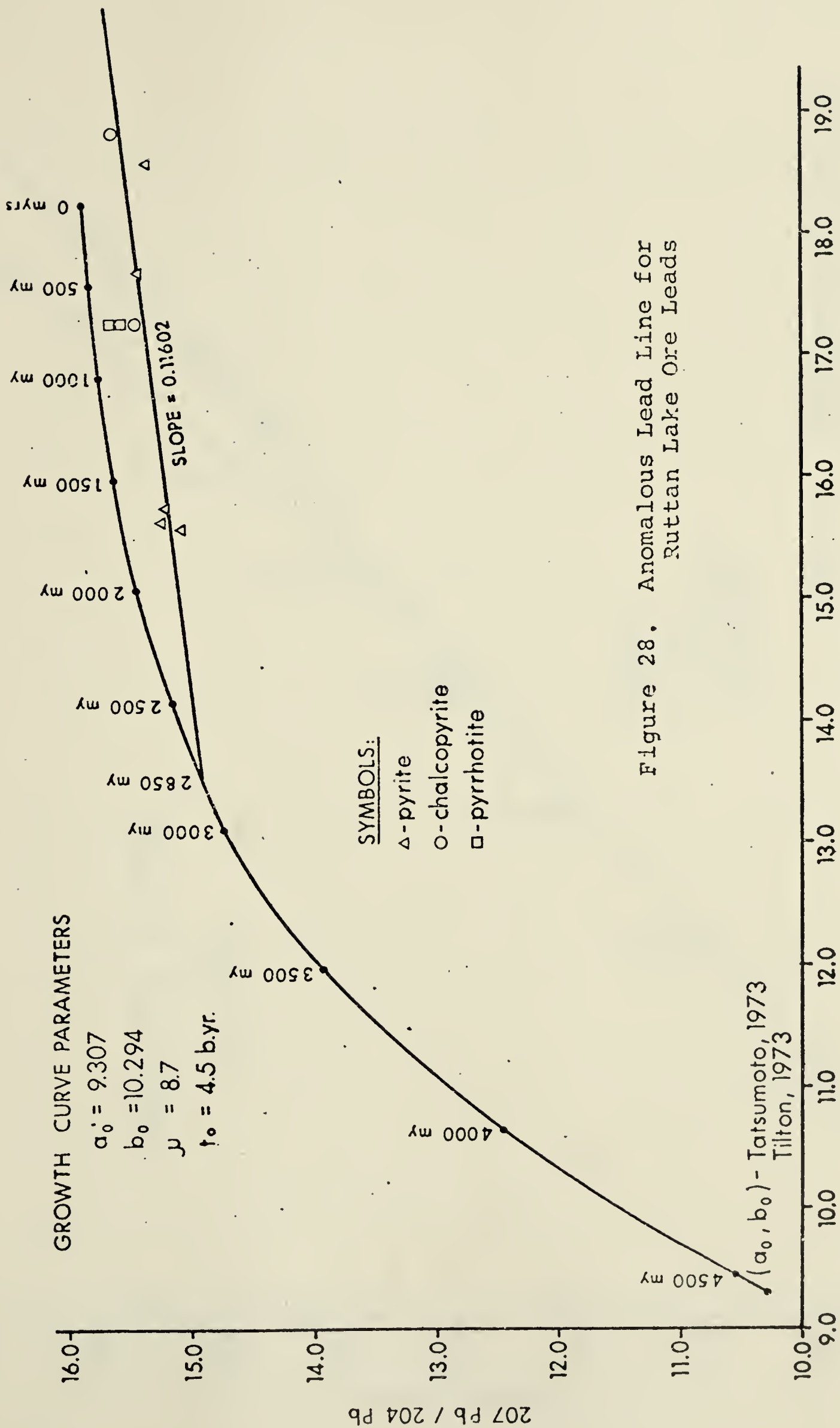
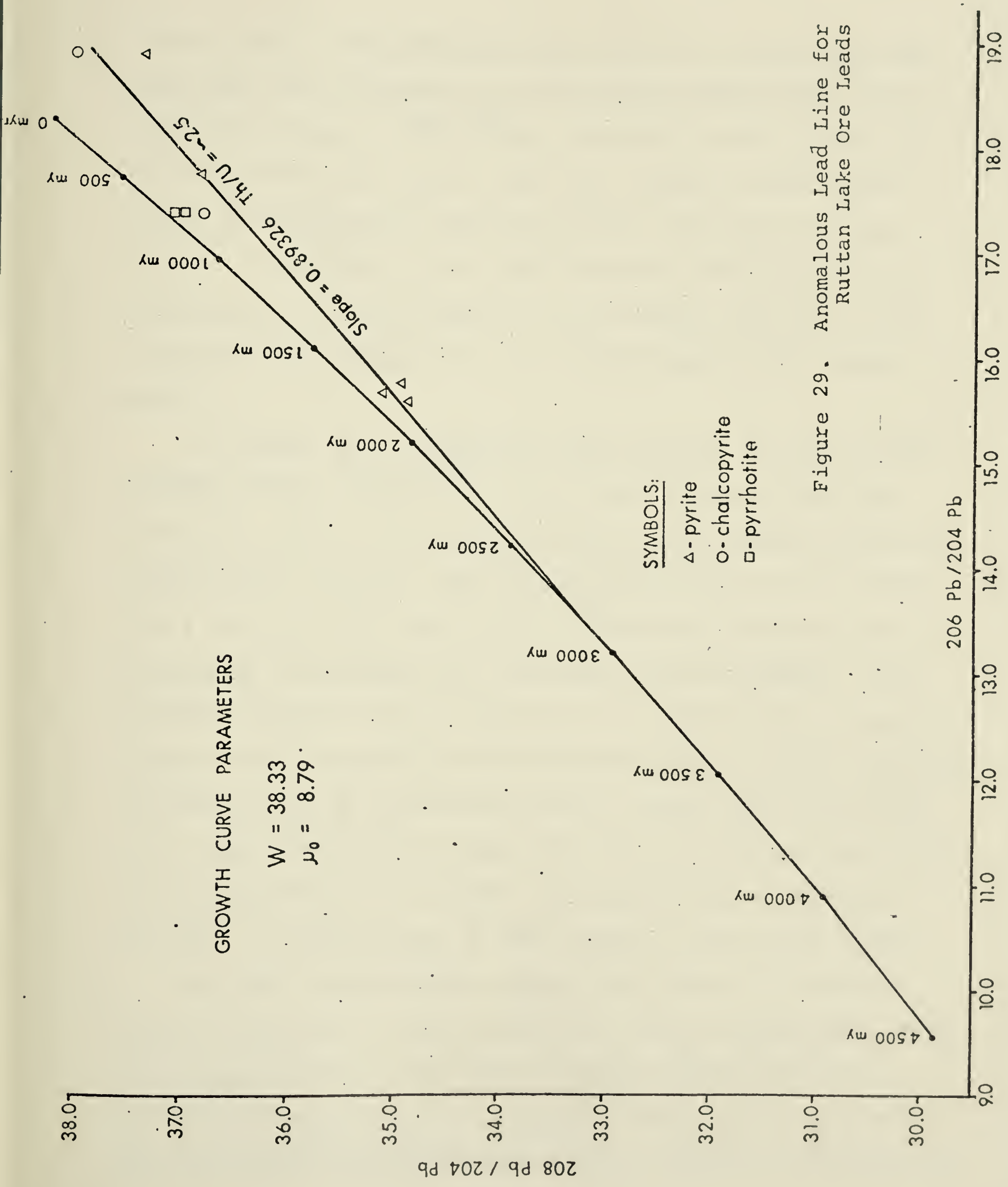


Figure 28. Anomalous Lead Line for Rutan Lake Ore Leads



lating slope. The anomalous lead line is $R = 0.116$ and this line does not intersect any single-stage growth curve with a reasonable value of $^{238}\text{U}/^{204}\text{Pb}$. Slope $R = 0.116$ results in an integrated model age of 1900 m.y., which is meaningless unless mineralization occurred recently (from APL program DATE76). Assuming $\mu = 8.7$, the anomalous uranium-lead line intersects the growth curve at approximately 2850 m.y., providing an upper limit on t , in a three-stage or four-stage model.

In Figure 29 an anomalous lead line best fit with slope $R(^{208}\text{Pb}/^{204}\text{Pb})/(^{206}\text{Pb}/^{204}\text{Pb})$ can be drawn through the data and hence confirms the anomalous lead mixing pattern involving open-system evolution. The slope is estimated to be 0.89326 and a value of Th/U ratio in the integrated source system is calculated to be about 2.45 (from APL program DATE86). That the Th/U anomalous line intersects the growth curve at approximately the same period as the uranium-lead line might indicate the source age of the Ruttan Lake ore leads to be about 2850 m.y. The lineal pattern means that the ore lead in the region was incorporated in a crustal environment with a rather restricted or narrow range of Th/U ratios in the source rocks.

Why the two pyrrhotite samples plot above the best fit line is uncertain. From the polished section microscopy, most of the pyrrhotite in the Ruttan deposit appears to be of a secondary origin, hence the radiogenic composition of lead in the pyrrhotites may differ from that of pyrite and chalcopyrite.

The more relevant age limit is where t_2 and t_3 approach each other, which is the time at which uranium isotopes were generating lead isotopes in the ratio R .

$$R = \frac{\lambda' e^{\lambda' t_R}}{137.8 \lambda e^{\lambda t_R}} \quad (\text{Russel et al., 1954})$$

This turns out to be $t_R = 1140$ m.y. which is the maximum value t_3 can have.

Validity of the lead model interpretation depends on the validity of the assumptions used in the model. The dates 1140, 1900 and 2850 m.y. are limiting values and from them one can construct various reasonable models, some of which may be more acceptable based on geologic evidence:

(i) the data supports a three or higher stage development of lead isotopes,

(ii) for a three-stage model, ages t_1 , t_2 and t_3 specify the relevant events. The source of lead must have been prior to t_1 , when ordinary lead was produced from a well-mixed sub-crustal portion of the earth and subsequently introduced into the crust. There was no radiogenic addition of lead at this time. Growth is presumed to be along a single-stage curve until time t_1 when the lead was emplaced in an environment where uranium was a minor element as compared to lead. The maximum age for t_1 is 2850 m.y. but it may be older. At t_1 remobilization and homogenization due to some major event

appears to have occurred causing variable amounts of radiogenic lead to be generated. The age t_2 , when a new source of uranium was supplied, can occur between 1900 and 1140 m.yrs. The 1900 m.y. corresponds with the Hudsonian orogeny which may have caused remobilization followed by an anomalous lead mineralization era. However, this would have to imply final mineralization, hence $t_3 = 0$. It is more likely that a massive amount of uranium was introduced just prior to 1140 m.y. and that the lead was abstracted shortly thereafter and mixed with the older lead formed during the event t_1 . Since this time the radioactive decay of U/Pb and Th/Pb have been proportional so as to form the linear relationship with radioactivity increasing as time decreases.

Armstrong and Cooper (1971) have proposed a tectonic-petrogenetic model for lead isotope evolution in volcanic island arcs involving a mixture or interaction process between mantle and crust and the pelagic sediments taken into the mantle by its convection current are probably the major source of lead for stratabound ore deposits.

Kuo and Folinsbee (1974) pointed out that in metallogenic provinces flanking ancient craton margins or island arcs, most mineral deposits are more likely to behave in a combination of "episodic-random" mixing and "continuous-random" mixing, and that anomalous ore leads are frequently encountered peripheral to regions in which conformable (or

stratabound) ore leads occur. The anomalous leads of the Ruttan Lake deposit seem to further substantiate this point.

In summary, the lead from the Ruttan Lake ores were derived from a well-mixed subcrustal portion of the earth sometime in early Archean time. At this time they were removed from the primary source into a crustal environment and underwent remobilization during the Hudsonian orogenies to display a distinctly anomalous linear relationship.

D. Trace Elements

Figure 30 shows a decrease in Fe/Mn ratios and Figure 31 shows an increase in Ba in the Ruttan Lake ores from the footwall to the hanging wall. The increase in Ba towards the upper part of the ore body would suggest an increasing contamination of seawater and hence would support a syngenetic relationship between the deposition of the volcanics and of the ore fluids or that sulphide deposition took place on the sea floor in a basin-like depression (McMillan, 1969).

The dispersion of Fe and Mn in massive sulphide deposits and their relationship to marine environments has been studied by many authors. Goodwin (1964) indicated that manganese decreases in concentration in the pyritic zone and this decrease reflects the decrease in carbonate content.

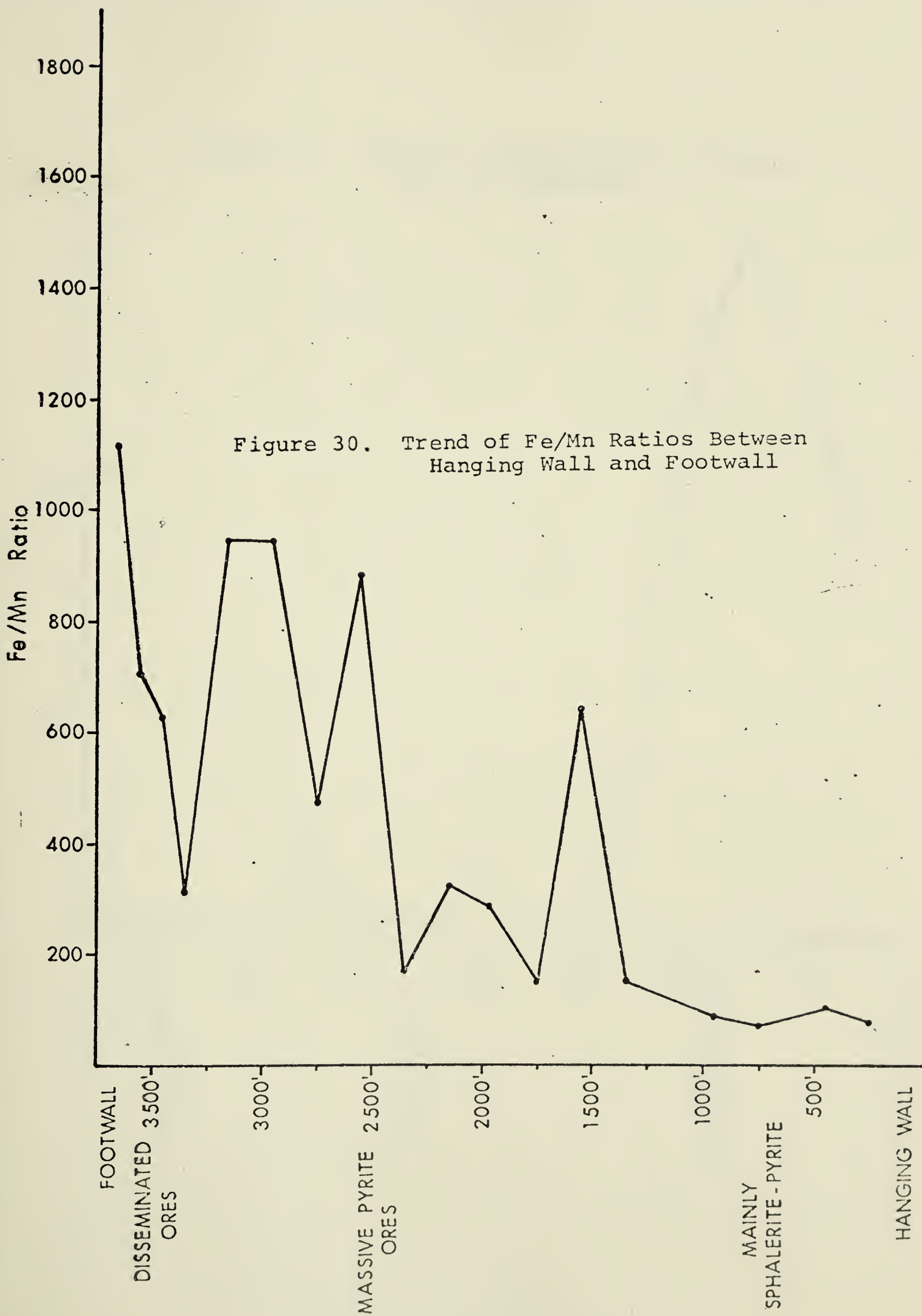
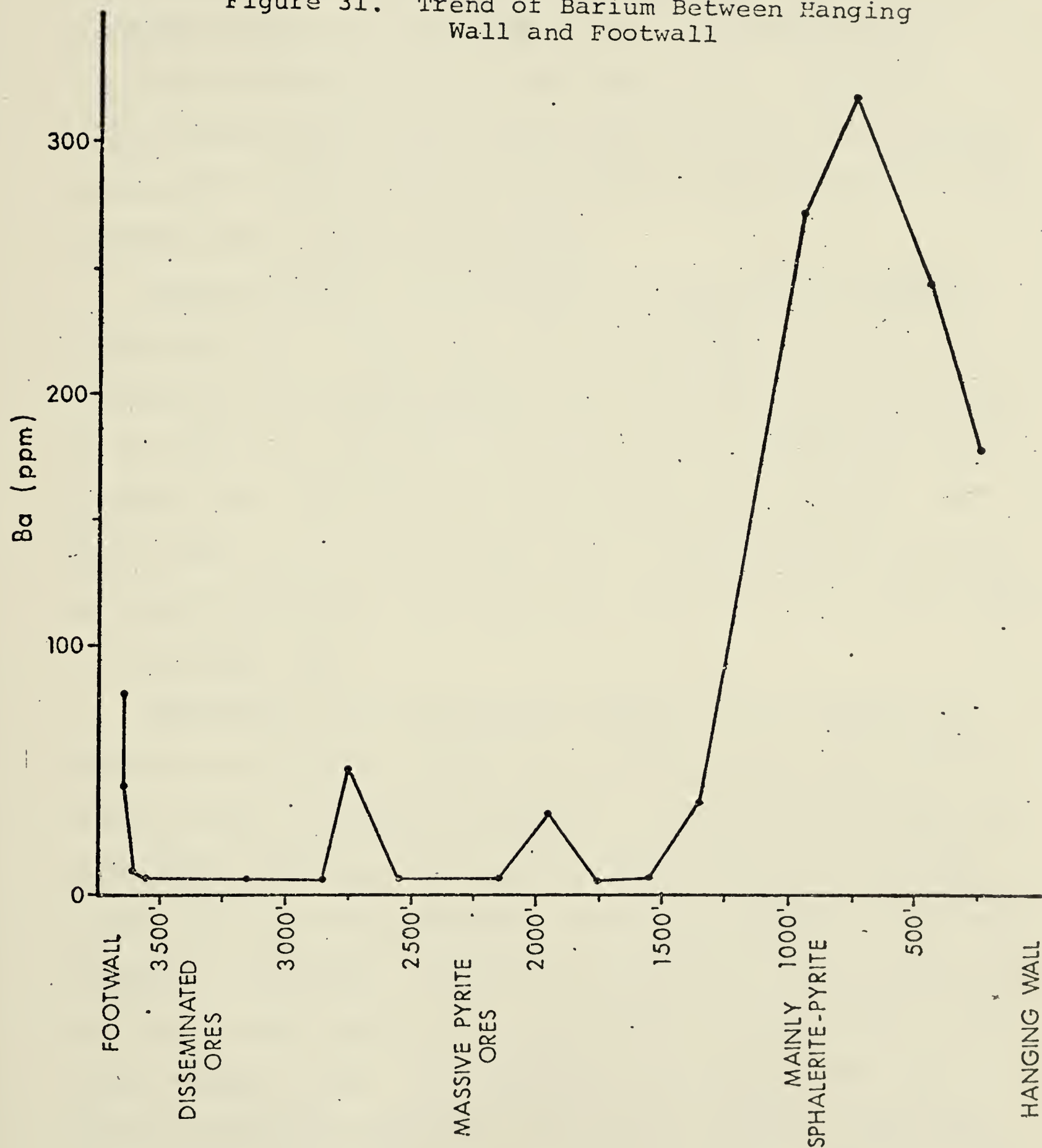


Figure 31. Trend of Barium Between Hanging Wall and Footwall



Hence manganese is relatively sensitive to a change of environment from one of predominantly carbonate deposition to one of predominantly sulphide deposition. Whitehead (1973) also proposed that variations in Fe and Mn concentrations can be attributed to environment differences that were present during time of deposition.

From the Ruttan Lake study the Fe/Mn ratios increase with depth (see Figure 30). It is unlikely that this variation is due to metamorphism since the metamorphism appears to be only of a regional nature and hence temperatures were probably not sufficient to redistribute the elements. If this trend is real then there was an accumulation of Mn and a general decrease in Fe from the lower parts of the ore body to the upper part.

Whitehead (1973) proposed a model for the genesis of massive ore deposits believed to be from basin-like depressions within a marine environment. During initial stages of fumarolic activity, the Mn was reduced within the sediment associated with the fumaroles or sulphide deposition and was removed in solution. The Mn was carried to the periphery of the basin where there was a preferential accumulation of Mn with respect to Fe. The increase in Mn towards the top of the stratigraphic sequence could be the result of the fractionation of Mn in the late stages of volcanic activity, the reduction of Mn and its subsequent migration during ore dia-

genesis, and a reducing environment which maintains Mn in a soluble state until there is an environment conducive to the precipitation of Mn.

The vertical and lateral variations shown in the Ba and Fe/Mn ratios in the Ruttan ores appear to be consistent with marine basin deposition and support the general hypothesis of volcanic-sedimentary deposition for massive sulphides, but from the sulphur isotope study the influence of seawater to ore deposition was very small.

CHAPTER V SUMMARY AND CONCLUSIONS

Geological mapping, core logging and optical studies revealed that the ore of the Ruttan Lake deposit are pre-metamorphic in age. The deposit contains pitching and swelling masses of ore whose orientation and shape seem to be due to the deformation and metamorphism that have affected the rocks of the region. Since the metals forming the ores were emplaced in their enclosing rocks prior to regional metamorphism and deformation that affected the host rocks, this could then explain the metamorphic grade of the host rocks, the degree of deformation by transposition and the grain size of the sulphides.

To draw some conclusions as to the origin and physiochemical conditions of ore emplacement of a highly metamorphosed deposit such as Ruttan Lake, one must be able to 'see' through this metamorphism. By studying the chemistry of the ores, i.e. sulphur isotopes, Fe content in sphalerite, trace element and Pb isotopes, it was hoped to accomplish this.

The data obtained from the sulphur isotope studies shows a comparatively narrow δS^{34} spread of the sulphides in the Ruttan Lake ore body. The geological evidence from the area indicates high-rank metamorphism and the narrow spread in δS^{34} values suggest homogenization or redistri-

bution of δS^{34} values. An isotopic temperature derived from this data would have an average greater than 450°C which appears to reflect the temperature of metamorphism rather than the temperature at time of ore emplacement.

The sulfur isotopic composition of the sulphides shows them to be slightly heavier at the top of the ore body and lighter towards the base which would indicate an increased oxidation of sulphur and perhaps a slight assimilation with seawater sulphur. If Rye and Ohmoto (1974) are correct, then this trend is real as the metamorphism can redistribute the sulphur isotope ratios but will not change the trend.

The narrow range of sulphur isotopic composition (with a near magmatic mean value) of the Ruttan Lake sulphides indicates a magmatic (volcanic) source of the sulphur rather than an homogenized product (later modified by metamorphism) of contemporaneous seawater sulphates and ascending volcanic H_2S sulphur. That there is some contamination of seawater is evident from the trace element study but it was not sufficient to affect the sulphur isotope composition to any extent.

Since the iron content in sphalerite is generally believed to be resistant to post mineral changes, it is possible to make some conclusions as to physiochemical conditions at time of ore deposition. Hence assuming equilibrium

deposition of pyrite, pyrrhotite and sphalerite, the results can be compared with experimental work in the Fe-Zn-S system done by Scott (1974) below 300°C. Temperature of ore deposition would be 160°-210°C and pressure range would be approximately 6 kilobars. The pressure of 6 Kb is probably the finally established pressure.

Lead isotope data of the Ruttan Lake mineralization is not concordant with growth curves for large stratabound ore bodies determined by Cooper et al. (1969). The data support a three or higher stage development of lead isotopes and suggests an Archean parentage with a maximum upper limit on t_1 of 2850 m.y. with mineralization occurring sometime between 1900 m.y. and 1140 m.y. ago.

The non-uniformity of the Pb isotope ratios suggests that the Ruttan Lake leads were extracted from the immediate basement through which ore solution passed, which would probably consist of all types of rocks and therefore various lead isotopic compositions. However, it seems more probable that the leads were derived from a certain deep-seated source and were well-mixed followed by at least two major events subsequent to ore deposition.

The trace element study shows evidence that the Ruttan Lake ores appear to be consistent with marine basin deposition and support the general hypothesis of volcanic-sedimentary deposition for massive sulphides. If so, the sulphides

of the deposit were supplied by hydrothermal emanations (possibly related to volcanism or some unknown source) and emplaced roughly in their present concentrations in the intercalated volcanic and sedimentary rocks at essentially the same time as these rocks were laid down.

BIBLIOGRAPHY

- AKISHIN, P.A., NIKITIN, O.T., PANCHENKOV, G.M. Geochemistry (U.S.S.R.), No. 5: 500, 1957.
- ARMSTRONG, R.L. A model for the evolution of strontium and lead isotopes in a dynamic earth. Rev. Geophysics 6, No. 2: 175-199, 1968.
- ARMSTRONG, R.L., COOPER, J.A. Lead isotopes in island arcs. Bull. Volcanol. 35: 27-63, 1971.
- AULT, W.U., KULP, J.L. Sulphur isotopes and ore deposits. Econ. Geol. 55: 73-100, 1960.
- BARNES, H.L. (Ed.) Geochemistry of hydrothermal ore deposits. 1967.
- BARTON, P.B.Jr., TOULMIN, P. Phase relations involving sphalerite in the Fe-Zn-S system. Econ. Geol. 61: 815-849, 1966.
- BATEMAN, J.D. McVeigh Lake area, Manitoba. Geological Survey of Canada, Paper 45-14: 1945.
- BOORMAN, R.S. Subsolidus studies in the ZnS-FeS-FeS₂ system. Econ. Geol. 62: 614-631, 1967.
- BOORMAN, R.S., SUTHERLAND, J.K., CHERNYSHEV, L.V. New data on the sphalerite-pyrrhotite-pyrite solvus. Econ. Geol. 66: 670-673, 1971.
- BRISTOL, C.C. Geology of the Issett Lake area (west half), Manitoba. Man. Mines Br., Publ. 63-4: 1966.
- BROWN, J.S. Oceanic lead isotopes and ore genesis. Econ. Geol. 60: 47-68, 1965.
- BURWASH, R.A. Geology of the Rusty Lake area (east half), Manitoba. Man. Mines Br., Publ. 60-3: 1962.
- CAHEN, L., EBERHARDT, P., GEISS, J., HOUTERMANS, F.G., JEDWAB, J., SIGNER, P. On a correlation between the common lead model age and the trace element content of galenas. Geochim. et Cosmoch. Acta. 14: 134, 1958.

- CAMERON, A.E., SMITH, D.H., WALKER, R.L. Mass spectrometry of nanogram-size samples of lead. *Analytical Chemistry*, March: 1969.
- CLARK, A.H. Stability field of monoclinic pyrrhotite. *Inst. Min. Metal. Trans.* 75B: 232-235, 1966.
- COOPER, J.A., REYNOLDS, P.H., RICHARDS, J.R. Double-spike calibration of the Broken Hill lead. *Earth Planet. Sci. Letters* 6: 467-478, 1969.
- CZAMANSKE, G.K., RYE, R.O. Experimentally determined sulphur isotope fractionations between sphalerite and galena in the temperature range 600°C to 275°C. *Econ. Geol.* 69: 17-25, 1974.
- DOE, B.R., HEDGE, C.E., WHITE, D.E. Preliminary investigation of the source of lead and strontium in deep geothermal brines underlying the Salton Sea geothermal area. *Econ. Geol.* 61: 462-483, 1966.
- DOE, B.R., STACEY, J.S. The application of lead isotopes to the problems of ore genesis and ore prospect evaluation: a review. *Econ. Geol.* 69: 757-776, 1974.
- EBERHARDT, P., GEISS, J., HOUTERMANS, F.G. Isotopic ratios of ordinary leads and their significance. *Z. Physics* 141: 91, 1955.
- FOLINSBEE, R.E., BAADSGAARD, H., CUMMING, G.L., GREEN, D.C. A very ancient island arc. In: The Crust and Upper Mantle of the Pacific Area. Edited by L. Knopoff, C.L. Drake and P.J. Hart. *Amer. Geophys. Union Geophys. Mon.* 12: 441-448, 1968.
- GOODWIN, A.M. Archean protocontinental growth and early crustal history of the Canadian Shield. *XXIII International Geological Congress* 1: 69-89, 1968.
- GOODWIN, A.M. Geochemical studies at the Helen iron range. *Econ. Geol.* 59: 684-718, 1964.
- HELGESON, H.C. Thermodynamics of hydrothermal systems at elevated temperatures and pressures. *Amer. J. Sci.* 267: 729-804, 1969.
- HENDERSON, J.F., NORMAN, G.W.H., DOWNIE, D.L. Granville Lake area (east half), Manitoba. *Geological Survey of Canada, Map* 344A: 1936.

- HUTCHINSON, R.W. Mineral potential in greenstone belts of northwestern Ontario. Paper presented to Lake Superior Inst. Conf., Thunder Bay, Ontario. May, 1970.
- HUTCHINSON, R.W. Volcanogenic sulphide deposits and their metallogenic significance. *Econ. Geol.* 68, No. 8: 1223-1246, 1973.
- IRVINE, T.N., BARAGAR, W.R.A. A guide to the chemical classification of the common volcanic rocks. *Can. Jour. Earth Sci.* 8: 523-548, 1971.
- JAFFEY, A.H., FLYNN, K.F., GLENDERIN, L.E., BENTLEY, W.C., ESSLING, A.M. Precision Measurement of half-lives and Specific Activities of ^{235}U and ^{238}U . *Phys. Rev. C4*: 1889-1906, 1971.
- JENSEN, M.L. Sulphur isotopes and hydrothermal mineral deposits. *Econ. Geol.* 54: 374-394, 1959.
- JONES, J.G. Pillow lavas as depth indicators. *Amer. J. of Sci.* 267: 181-195, 1969.
- KAJIWARA, Y. Sulphur isotope study of the Kuroko-ores of the Shakanai No. 1 deposits, Akita Prefecture, Japan. *Geochem J.* 4: 157-181, 1971.
- KAJIWARA, Y., KROUSE, H.R. Sulphur isotope partitioning in metallic sulphide systems. *Can. Jour. Earth Sci.* 8: 1401-1408, 1971.
- KAJIWARA, Y., SASAKI, A. Experimental study of sulphur isotopic fractionation between coexistent sulphide minerals. *Earth Planet. Sci. Letters* 7: 271-277, 1969.
- KANASEWICH, E.R. Approximate age of tectonic activity using anomalous lead isotopes. *Royal Astron. Soc. Geophys. Jour.* 7: 158-168, 1962.
- KANASEWICH, E.R., SLAWSON, W.F. Precision intercomparisons of lead isotope ratios. Ivigtut, Greenland: *Geochim. et Cosmochim. Acta* 28: 541-549, 1964.
- KANASEWICH, E.R., FARQUHAR, R.M. Lead isotope ratios from the Cobalt-Noranda area, Canada. *Can. Jour. Earth Sci.* 2: 1965.

- KULLERUD, G. The FeS-ZnS system, a geological thermometer. Norsk Geol. Tiddsskr. 32: 61-147, 1953.
- KULP, J.L., AULT, W.U., FEEBY, H.W. Sulphur isotope abundances in sulphide minerals. Econ. Geol. 51: 139-149, 1956.
- KUNO, H. High-alumina basalt. Journal Petrology 1: 121-145, 1960.
- KUNO, H. Differentiation of basaltic magmas. In: Basalts: The Poldervaart Treatise on Rocks of Basaltic Composition, 2: 623-688. Edited by H.H. Hess and A. Poldervaart. Interscience Publishers, John Wiley & Sons, New York: 1968.
- KUO, S.L., FOLINSBEE, R.E. Lead isotope geology of mineral deposits spatially related to the Tintina Trench, Yukon Territory. Econ. Geol. 69: 806-813, 1974.
- MATSUKUMA, T., HORIKOSHI, E. Kuroko deposits in Japan: a review, 153-180. In: Volcanism and Ore Genesis. Edited by T. Tatsumi. Univ. of Tokyo Press, Tokyo, 1970: 448, 1970.
- McMILLAN, R.H. A comparison of the geological environments of the base metal sulphide deposits of the "B" zone and "North Boundary Zone" at the Heath Steele Mine, New Brunswick. Unpublished M.Sc. Thesis, Univ. of Western Ontario, London, Ontario: 1969.
- MILLIGAN, G.C. Geology of the Lynn Lake district, Manitoba. Manitoba Mines Br., Publ. 57-1: 1960.
- MILLIGAN, G.C. Geology of the Earp Lake area (west half), Manitoba. Man. Mines Br., Publ. 61-2: 1964.
- MIYASHIRO, A. Volcanic rock series in island arcs and active continental margins. Amer. Jour. of Science 274: 321-355, 1974.
- OHMOTO, H. Influence of pH and fO_2 of hydrothermal fluids on the isotopic composition of sulphur species. Geol. Soc. Amer. Ann. Mtg. (Milwaukee), Abst.: 640, 1970.
- OHMOTO, H. Systematics of sulphur and carbon isotopes in hydrothermal ore deposits. Econ. Geol. 67: 551-578, 1972.

- PEARCE, G. Geology of the Pemichigamau Lake area (east half), Manitoba. Man. Mines Br., Publ. 61-3: 1964.
- PEARCE, T.H., GORMAN, B.E., BIRKETT, T.C. The $\text{TiO}_2\text{-K}_2\text{O-P}_2\text{O}_5$ diagram: a method of discriminating between oceanic and non-oceanic basalts. Earth Planet. Sci. Letters 24: 419-426, 1975.
- RUCKLIDGE, J.C., GASPERRINI, E. EMPADR VII specifications of a computer program for processing electron microprobe data. Dept. of Geology, University of Toronto, Publication: 1969.
- RUSSEL, R.D., FARQUHAR, R.M., CUMMING, G.L., WILSON, J.T. Dating galenas by means of their isotopic constitutions. Trans. Amer. Geophys. Union 35: 301, 1954.
- RUSSEL, R.D., FARQUHAR, R.M., HAWLEY, J.E. Isotopic analyses of leads from Broken Hill, Australia, with spectrographic analyses. Trans. Amer. Geophys. Union 38: 557, 1957.
- RUSSEL, R.D., FARQUHAR, R.M. Lead Isotopes in Geology: 1960.
- RUSSEL, R.D., KANASEWICH, E.R., OZARD, J.M. Isotopic abundances of Pb from a "frequently mixed" source. Earth Planet Sci. Letters 1: 85-88, 1966.
- RUSSEL, R.D., SLAWSON, W.F., ULRYCH, T.J., REYNOLDS, P.H. Further Applications of Concordia Plots to Rock Lead Isotope Abundances. Earth and Planet Sci. Letters 3: 284-288, 1967.
- RYE, R.O., CZAMANSKE, G.K. Experimental determination of sphalerite - galena sulphur isotope fractionation and application to the ores at Providencia, Mexico (Abstract). Geol. Soc. Amer., Abstracts with Programs for 1969: 195, 1969.
- RYE, R.O., OHMOTO, H. Sulphur and carbon isotopes and ore genesis: a review. Econ. Geol. 69: 826-842,
- RYE, D.M., RYE, R.O. Homestake gold mine, South Dakota: I. Stable isotope studies. Econ. Geol. 69: 293-317, 1974.

- SAKAI, H. Isotopic properties of sulphur compounds in hydrothermal processes. *Geochem. Jour.* 2: 29-49, 1968.
- SANGSTER, D.F. Relative sulphur isotope abundances of ancient seas and stratabound sulphide deposits. *Geol. Assoc. Canada, Proc.* 19: 79-91, 1968.
- SANGSTER, D.F. Precambrian volcanogenic massive sulphide deposits in Canada: a review. *Geol. Surv. of Canada, Paper* 72-22: 1972.
- SASAKI, A. Seawater sulphate as a possible determinant of sulphur isotopic compositions of some stratabound sulphide ores. *Geochem. Jour.* 4: 41-51, 1970.
- SATO, T. Physiochemical environments of Kuroko mineralization at Uchinotai deposit of Kosaka Mine, Akita prefecture. *Soc. Mining Geol. Japan, Special Issue* 2: 137-144, 1971.
- SCOTT, S.D. Experimental calibration of the sphalerite geobarometer. *Econ. Geol.* 68: 466-474, 1973.
- SCOTT, S.D. Sulphide mineralogy. Mineralogical Society of America, short course notes 1: November, 1974.
- SCOTT, S.D., BARNES, H.L. Sphalerite geothermometry and geobarometry. *Econ. Geol.* 66: 653-669, 1971.
- SCOTT, S.D., KISSIN, S.A. Sphalerite composition in the Zn-Fe-S system below 300°C. *Econ. Geol.* 68: 475-479, 1973.
- SHERRITT GORDON MINES LTD. Annual Report - 1972.
- SINCLAIR, W.D. A volcanic origin for the No. 5 zone of the Horne Mine, Noranda, Quebec. *Econ. Geol.* 66: 1225-1231, 1971.
- STACEY, J.S., DELEVAUX, M.H., ULRYCH, T.J. Some triple-filament lead isotope ratio measurements and an absolute growth curve for single-stage leads. *Earth Planet. Sci. Letters* 6: 15-25, 1969.
- STACEY, J.S., KRAMERS, J.D. Approximation of terrestrial lead isotope evolution by a two-stage model. *Earth Planet. Sci. Letters* 26: 207-221, 1975.

- STANTON, R.L. The application of sulphur isotope studies in ore genesis theory - a suggested model. N.Z. Jour. Geol. and Geophys. 3: 375-389, 1960.
- STANTON, R.L., RUSSEL, R.D. Anomalous leads and the emplacement of lead sulphide ores. Econ. Geol. 54: 588-607, 1959.
- STEEVES, M.A., LAMB, C.F. Geology of the Issett-Opachuanau-Pemichigamau-Earp Lakes area, Manitoba. Manitoba Mines Br., Publ. 71-2F: 1972.
- TATSUMOTO, M. Time differences in the formation of meteorites as determined from the ratio of lead-207 to lead-206. Science 180: 1279-1283, 1973.
- THODE, H.G. Sulphur isotope geochemistry. In: Studies in Analytical Geochemistry. Edited by D.M. Shaw. Roy. Soc. Can. Special Publ. No. 6: 25-41, 1963.
- TILTON, G.R. Isotopic lead ages of chondritic meteorites. Earth Planet. Sci. Letters 19: 321-329, 1973.
- TUPPER, W.M. Sulphur isotopes and the origin of the sulphide deposits of the Bathurst-Newcastle area of northern New Brunswick. Econ. Geol. 55: 1676-1707, 1960.
- ULRYCH, T.J. The anomalous nature of Ivigtut lead. Geochim. et Cosmochim. Acta 28: 1389-1396, 1964.
- VINOGRADOV, A.P., CHUPAKHIN, M.S., GRINENKO, V.A. Isotope ratios S^{32}/S^{34} in sulphides. Geochemistry 4: 331-338, 1956.
- WHITE, A.J.R., JAKES, P., CHRISTIE, D.M. Composition of greenstones and the hypothesis of seafloor spreading in the Archean. Geol. Soc. Australia, Spec. Publ. 3: 47-56, 1971.
- WHITEHEAD, R.E. Environment of stratiform sulphide deposition; variation in Mn:Fe ratio in host rocks at Heath Steele Mine, New Brunswick, Canada. Mineral Deposita (Berl.) 8: 148-160, 1973.
- WILSON, H.D.B., ANDREWS, P., MAXHAM, R.L., RAMLAL, K. Archean volcanism in the Canadian Shield. Can. Jour. Earth Sci. 2: 161-175, 1965.

APPENDIX A

Recipe for Magnetic Colloid

(from Scott, 1974, p. 5-18)

1. Dissolve 2 grams $\text{FeCl}_2 \cdot 4\text{H}_2\text{O}$ and 5.4 grams $\text{FeCl}_3 \cdot 6\text{H}_2\text{O}$ in 300 cc of distilled water at 70°C .
2. Dissolve 5 grams NaOH in 50 cc distilled water.
3. Mix solutions 1 and 2 and stir vigorously. Filter black precipitate and rinse several times with distilled water and finally with 0.01N HCl. Place the black precipitate in 500 cc 0.05% sodium oleate solution and boil for a short time to mix the soap solution and precipitate. The resulting colloid is stable for many months.

APPENDIX B

Extraction of Lead from Sulfide Minerals

(from S.L. Kuo, personal communication, 1974)

Metallic sulfides such as pyrites, pyrrhotites, chalcopyrites, sphalerites, etc. nearly always contain at least microgram traces of lead. The relatively large amount of iron present can be chemically separated from the lead by employment of an ion-exchange resin column stripping procedure.

1. Place 0.5 - 1 gm of sulfide in a vycor crucible. Add 15 cc of 6N HNO_3 and a few cc of 6N HCl . Gently evaporate to dryness on a hot plate (this may take 10 - 12 hours!).
2. Add 4 cc of 6N HCl , evaporate to dryness. Repeat this step with 2 cc of 6N HCl .
3. Add 20 cc of 1N HCl to dissolve the evaporate.
4. Centrifuge or filter the sample solution, then pour this solution into an ion-exchange column which is packed with DOWEX 1-x8 resin settled in 1N HCl . The particular columns used are approximately 1 cm x 30 cm with a 100 cc capacity reservoir.
5. Pass the 1N solution through the column. Discard the eluate. Wash the reservoir twice with 15 cc of 1N HCl , allowing the HCl to pass through the column. This will remove traces of solution adhering by capillary action.
6. Elute the columns with 70 cc of 1N HCl .
7. Strip Pb from the resin by adding 60 cc of 3N H_2O . The first 10 cc of the eluate can be discarded.

APPENDIX B (cont'd)

8. Evaporate the solution to dryness.
9. Convert the evaporate to nitrate form by adding 2 cc of concentrated HNO_3 and again evaporate to dryness. Repeat this procedure once more. Take up the evaporate with 10 cc of dilute (2%) HNO_3 .

The above procedure will yield relatively clean lead.

However, a dithizone extraction of this lead is required to give a good run on the mass spectrometer.

APPENDIX C

Procedure for Loading Samples on Re-Filament

(Modified by Tatsumoto, 1973)

1. Load 1 drop of Silica-gel on filament and evaporate to dryness with overhead heat lamp. Should turn a definite white color.
2. Put 1 drop of Phosphoric Acid (.75 pure) into Pb sample and concentrate by evaporating.
3. Place 1 drop (small amount only) on silica-gel and again evaporate. Should be able to see it fuse with the silica-gel.
4. Turn up current to .7 or .8 amp and hold there for 15 to 20 minutes.
5. Turn current up until phosphate starts to fume off.
6. Once phosphate has fumed off turn current up till it glows red. Flick back and forth two or three times.
7. Turn current off. Loaded sample should be in centre of filament and appear a white color.

APPENDIX D

Lead Isotope Regression Formula

(from S.L. Kuo, personal communication, 1975)

$$R = \frac{1}{\frac{1}{\tan 2\theta} + \frac{1}{\tan^2 2\theta} + 1}$$

where R = slope

$$\tan 2\theta = \frac{2 \bar{x} \Sigma \mu v}{\Sigma (\mu^2 - v^2)}$$

$$\mu = x_i - \bar{x}$$

$$v = y_i - \bar{y}$$

$$\bar{x} = x \text{ centroid}$$

$$\bar{y} = y \text{ centroid}$$

Uncertainty of slope

$$\delta R = \frac{(1 + R^2) \Sigma (V - R\mu)^2}{(n - 2) [\Sigma (\mu^2) + \Sigma (v^2)]}$$

PLATE I MICROPHOTOGRAPHS

Photograph	Description
1.	Massive ore-pyrite, chalcopyrite and pyrrhotite; quartz gangue; sample no. R-105D; Mag. 4X
2.	Colloform Texture in Massive pyrite. Sample No. R-103D; Magnification 4X
3.	Exsolution of Chalcopyrite and Pyrrhotite in Sphalerite; Quartz and Biotite Gangue. Sample No. R-120; Magnification 4X

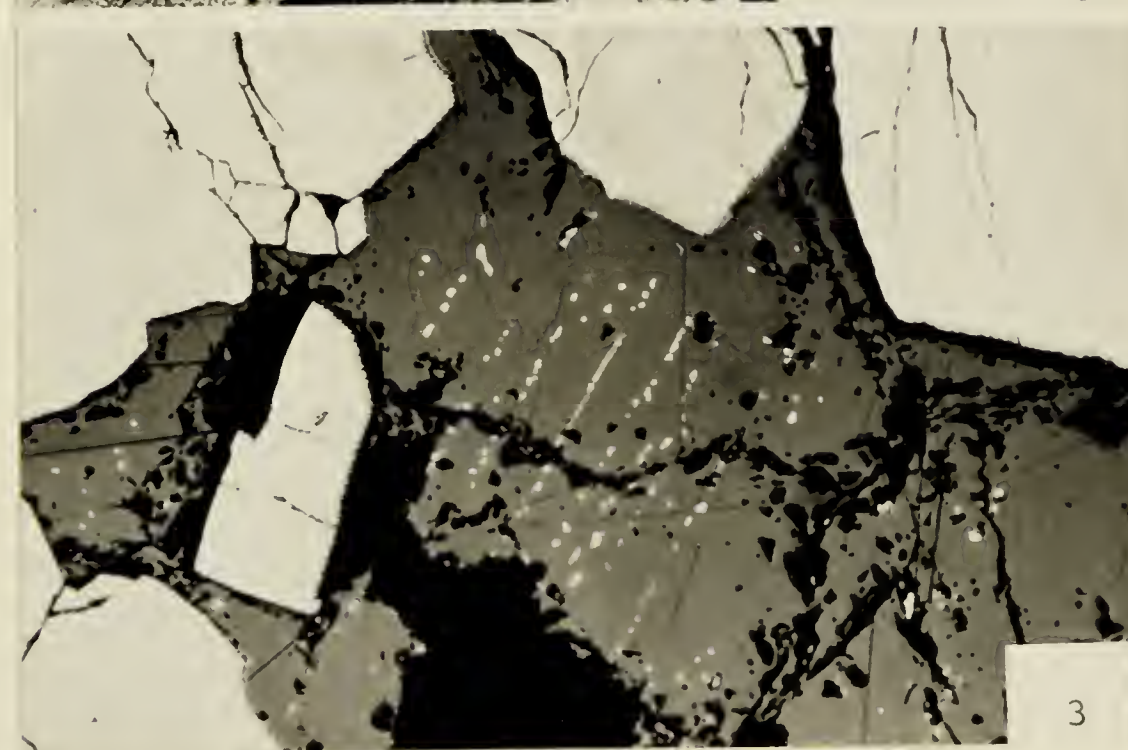
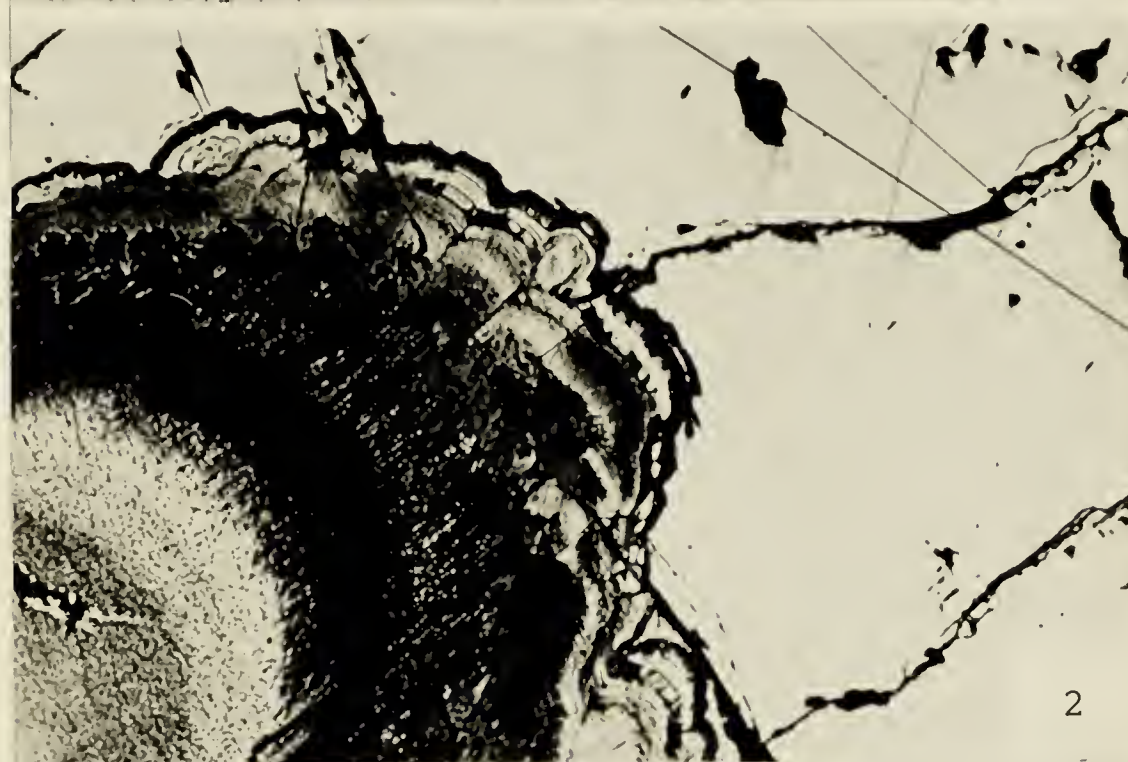
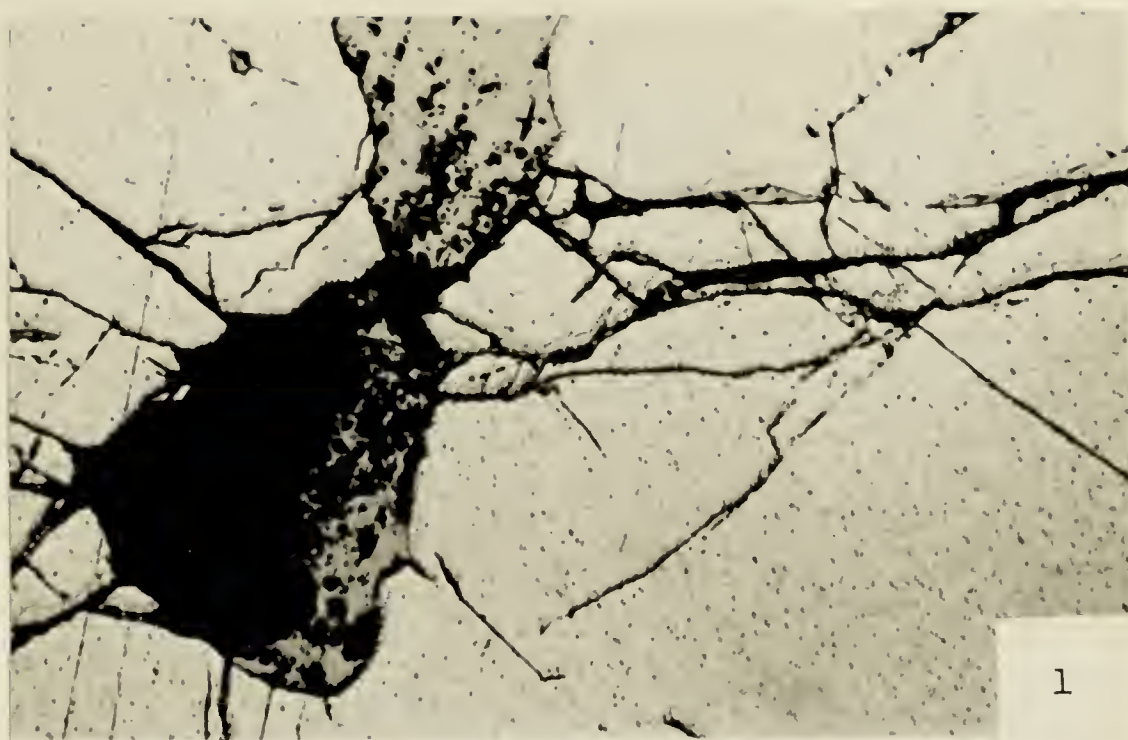
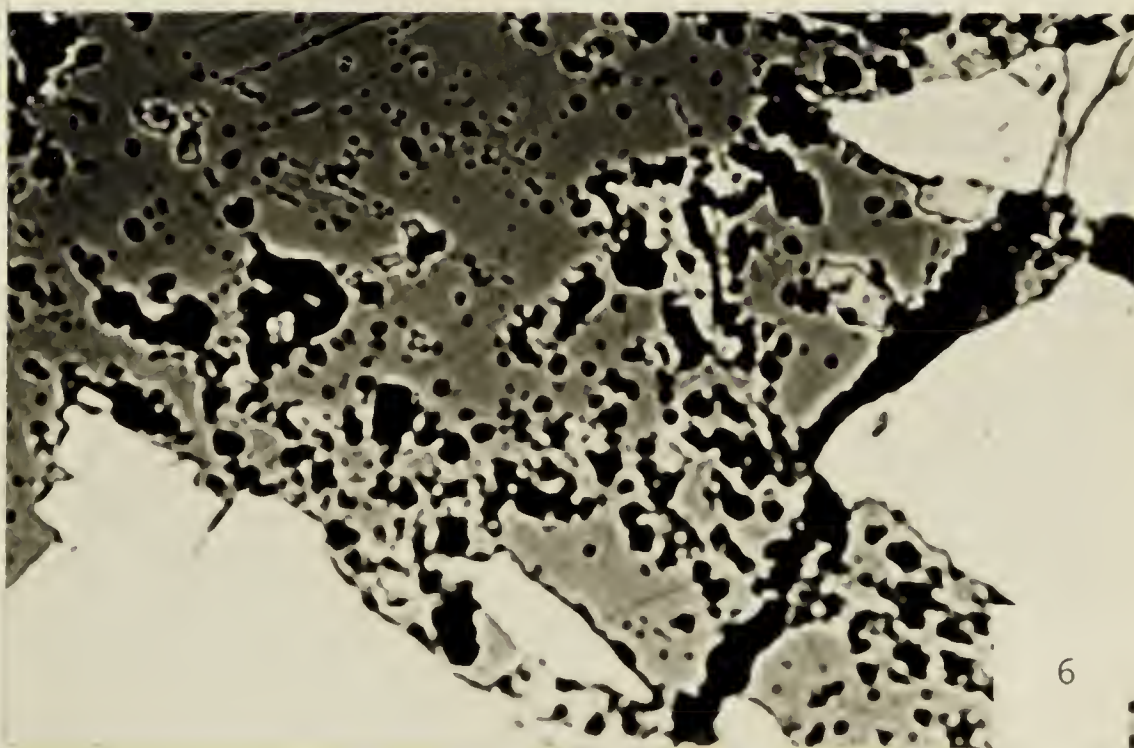
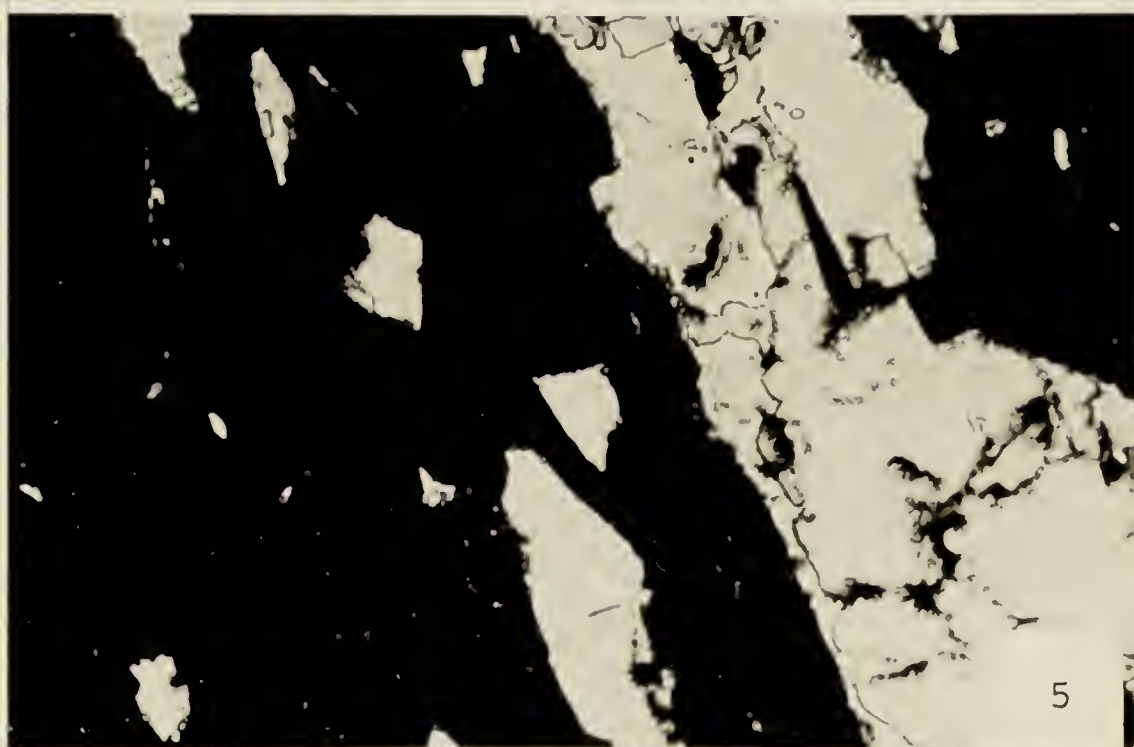




PLATE II MICROPHOTOGRAPHS

Photograph	Description
4.	Disseminated Pyrite, Chalcopyrite and Pyrrhotite in Chlorite-Biotite Schist. Sample No. R-100A; Magnification 4X
5.	Disseminated Pyrite and Pyrrhotite in chlorite, biotite schist. Sample No. R-100B; Mag. 4X
6.	Pyrite, Pyrrhotite and Chalcopyrite with film of magnetic colloid showing monoclinic pyrrhotite. Sample No. R-107D; Mag. 4X



B30142